ELECTROMAGNETIC SCATTERING FROM A HOMOGENEOUS BODY OF REVOLUTION

by

Joseph R. Mautz
Roger F. Harrington

TECHNICAL REPORT TR-77-10

November 1977

DEPARTMENT OF
ELECTRICAL AND COMPUTER ENGINEERING
SYRACUSE UNIVERSITY
SYRACUSE, NEW YORK 13210

(6) ELECTROMAGNETIC SCATTERING FROM A HOMOGENEOUS BODY OF REVOLUTION

(12) 88 (11) Nov 77

by

(10) Joseph R. Mautz
Roger F. Harrington

(9) TECHNICAL REPORT, TR-77-10
~~November 1977~~

(14) TR-77-10

This work was supported by the Rome Air Development Center through the Deputy of Electronic Technology under Contract No. F19628-76-C-0300, and through the Air Force Post Doctoral Program under Contract No. F30602-75-0121.

(15) F19628-76-C-0300, F30602-75-C-0121

DEPARTMENT OF
ELECTRICAL AND COMPUTER ENGINEERING
SYRACUSE UNIVERSITY
SYRACUSE, NEW YORK 13210

ABSTRACT

This report considers plane-wave scattering by a homogeneous material body of revolution. The problem is formulated in terms of equivalent electric and magnetic currents over the surface which defines the body. Application of the boundary conditions leads to four simultaneous surface integral equations to be satisfied by the two unknown equivalent currents, electric and magnetic. The set of four equations is reduced to a coupled pair of equations by taking linear combinations of the original four equations. Because many pairs of linear combinations are possible, there are many surface integral equation formulations for the problem. Two formulations commonly encountered in the literature are discussed and solved by the method of moments. A general computer program for material bodies of revolution is developed, listed, and documented. Examples of numerical computations are given for dielectric spheres and a finite dielectric cylinder. The computed results for the sphere are compared to the exact series solution obtained by separation of variables.

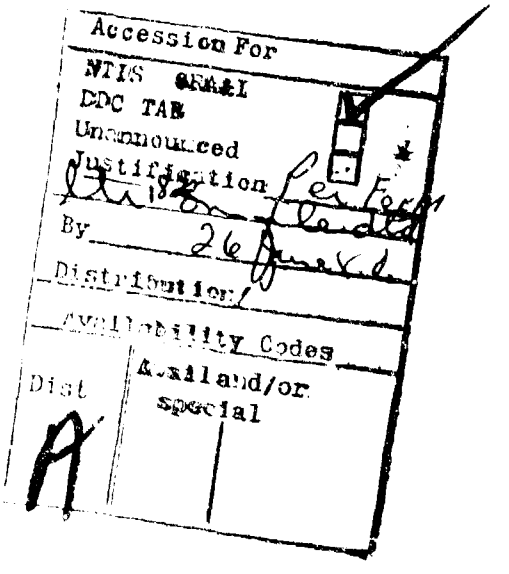

CONTENTS

PART ONE

ELECTROMAGNETIC SCATTERING FROM A HOMOGENEOUS MATERIAL BODY OF REVOLUTION

THEORY AND EXAMPLES

I. INTRODUCTION

The problem of plane-wave scattering by a homogeneous material body of revolution is formulated in terms of equivalent electric and magnetic currents over the body surface. Application of boundary conditions leads to a set of four integral equations to be satisfied. Linear combinations of these four equations lead to a coupled pair of equations to be solved. One choice of combination constants gives the formulation described by Poggio and Milier [1]. This formulation has been applied to material cylinders by Chang and Harrington [2], and to material bodies of revolution by Wu [3]. We will call this choice the PMCHW formulation (formed by the initials of the above cited investigators).

Another choice of combination constants gives the formulation obtained by Müller [4]. This formulation has been applied to dielectric cylinders by Solodukhov and Vasil'ev [5] and by Morita [6], and to bodies

---

[1] A. J. Poggio and E. K. Miller, "Integral Equation Solutions of Three-dimensional Scattering Problems," Chap. 4 of Computer Techniques for Electromagnetics, edited by R. Mittra, Pergamon Press, 1973, Equation (4.17).

[2] Yu Chang and R. F. Harrington, "A Surface Formulation for Characteristic Modes of Material Bodies," Report TR-74-7, Dept. of Electrical and Computer Engineering, Syracuse University, Syracuse, N.Y., October 1974.

[3] T. K. Wu, "Electromagnetic Scattering from Arbitrarily-Shaped Lossy Dielectric Bodies," Ph.D. Dissertation, University of Mississippi, 1976.

[4] C. Müller, Foundations of the Mathematical Theory of Electromagnetic Waves, Springer-Verlag, 1969, p. 301, Equations (40)-(41). (There are some sign errors in these equations.)

[5] V. V. Solodukhov and E. N. Vasil'ev, "Diffraction of a Plane Electromagnetic Wave by a Dielectric Cylinder of Arbitrary Cross Section," Soviet Physics - Technical Physics, vol. 15, No. 1, July 1970, pp. 32-36.

[6] N. Morita, "Analysis of Scattering by a Dielectric Rectangular Cylinder by Means of Integral Equation Formulation," Electronics and Communications in Japan, vol. 57-B, No. 10, October 1974, pp. 72-80.

of revolution by Vasil'ev and Materikova [7]. We will call this choice the Müller formulation. Conditions for the uniqueness of solutions are established in terms of the combination constants. It is found that solutions to both the PMCHW formulation and to Müller's formulation are unique at all frequencies.

Numerical solutions to the coupled pair of equations are obtained by the method of moments [8]. It is relatively easy to obtain numerical solutions to these equations because the required operators are the same as those evaluated in earlier reports [9, 10]. An exemplary computer program capable of obtaining the solution to both the PMCHW formulation and the Müller formulation is described and listed. This is a main program which uses subroutines similar to those in [10] to compute the equivalent electric and magnetic currents and the two principal plane scattering patterns for a loss-free homogeneous body of revolution excited by an axially incident electromagnetic plane wave. Computed results for the equivalent currents and principal plane scattering patterns of a dielectric sphere whose relative dielectric constant is four show reasonable agreement between our solution to the PMCHW formulation, our solution to the Müller formulation, and the "exact" series [11] solution in the resonance region. Computer program subroutines which calculate the "exact" series solution for perfectly conducting spheres as well as for loss-free homogeneous spheres will be described and listed in a subsequent report.

---

[7] E. N. Vasil'ev and L. B. Materikova, "Excitation of Dielectric Bodies of Revolution," Soviet Physics - Technical Physics, vol. 10, No. 10, April 1966, pp. 1401-1406.

[8] R. F. Harrington, Field Computation by Moment Methods, Macmillan Co., New York, 1968.

[9] J. R. Mautz and R. F. Harrington, "H-Field, E-Field, and Combined Field Solutions for Bodies of Revolution," Interim Technical Report RADC-TR-77-109, Rome Air Development Center, Griffiss Air Force Base, New York, March 1977.

[10] J. R. Mautz and R. F. Harrington, "Computer Programs for H-Field, E-Field, and Combined Field Solutions for Bodies of Revolution," Interim Technical Report RADC-TR-77-215, Rome Air Development Center, Griffiss Air Force Base, New York, June 1977.

[11] R. F. Harrington, Time-Harmonic Electromagnetic Fields, McGraw-Hill Book, Co., 1961. Section 6-9.

II. SURFACE INTEGRAL EQUATION FORMULATION

An electromagnetic field propagating in a homogeneous medium of permeability μ_e and permittivity ϵ_e is incident on the surface S of a homogeneous obstacle of permeability μ_d and permittivity ϵ_d. The subscript e denotes exterior medium and the subscript d denotes diffracting medium. We wish to calculate the scattered electromagnetic field $\underset{\sim}{E}^s$, $\underset{\sim}{H}^s$ outside S and the diffracted electromagnetic field $\underset{\sim}{E}$, $\underset{\sim}{H}$ inside S in terms of the electromagnetic field $\underset{\sim}{E}^i$, $\underset{\sim}{H}^i$ which would exist on S in the absence of the obstacle. This original problem is shown in Fig. 1 where $\underset{\sim}{J}^i$, $\underset{\sim}{M}^i$ are the electric and magnetic sources of $\underset{\sim}{E}^i$, $\underset{\sim}{H}^i$ and $\underset{\sim}{n}$ is the unit normal vector which points outward from S.

The equivalence principle (stated in Appendix A) is used to piece together an outside situation consisting of medium μ_e, ϵ_e and field $\underset{\sim}{E}^s$, $\underset{\sim}{H}^s$ outside S and an inside situation consisting of medium μ_e, ϵ_e and field $-\underset{\sim}{E}^i$, $-\underset{\sim}{H}^i$ inside S. This composite situation is shown in Fig. 2. Since $\underset{\sim}{E}^s$, $\underset{\sim}{H}^s$ is source-free outside S and $\underset{\sim}{E}^i$, $\underset{\sim}{H}^i$ is source-free inside S, the only sources in Fig. 2 are the equivalent electric surface current $\underset{\sim}{J}$ and the equivalent magnetic surface current $\underset{\sim}{M}$ on S.

As a second application of the equivalence principle, we combine an outside situation consisting of medium μ_d, ϵ_d and zero field with an inside situation consisting of medium μ_d, ϵ_d and field $\underset{\sim}{E}$, $\underset{\sim}{H}$. This combination of situations is shown in Fig. 3. Since $\underset{\sim}{E}$, $\underset{\sim}{H}$ is source-free inside S, the only sources in Fig. 3 are the equivalent electric surface current $-\underset{\sim}{J}$ and the equivalent magnetic surface current $-\underset{\sim}{M}$ on S. By using (A-1) and (A-2) to express the surface currents in terms of the discontinuities of the tangential fields across S and by using

$$\underset{\sim}{n} \times \underset{\sim}{E} = \underset{\sim}{n} \times (\underset{\sim}{E}^s + \underset{\sim}{E}^i) \tag{1}$$

$$\underset{\sim}{n} \times \underset{\sim}{H} = \underset{\sim}{n} \times (\underset{\sim}{H}^s + \underset{\sim}{H}^i) \tag{2}$$

on S, the interested reader can verify that the surface currents in Fig. 3 are indeed the negatives of those in Fig. 2. Equations (1) and (2) are the boundary conditions that the tangential components of the fields in the

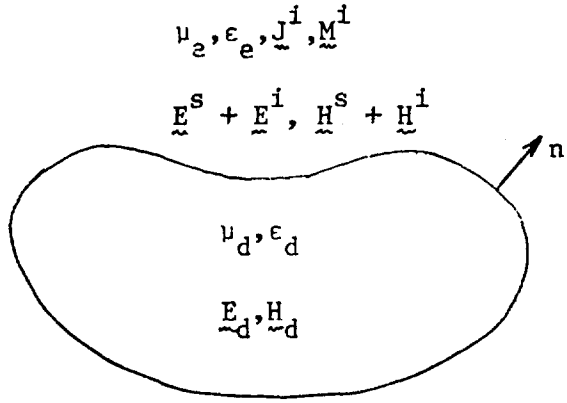

Fig. 1. Original problem.

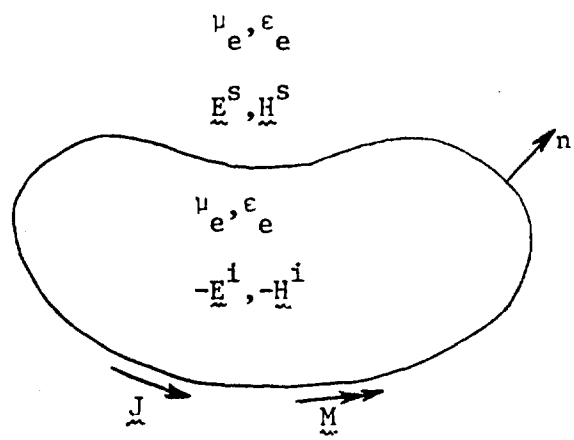

Fig. 2. Outside equivalence.

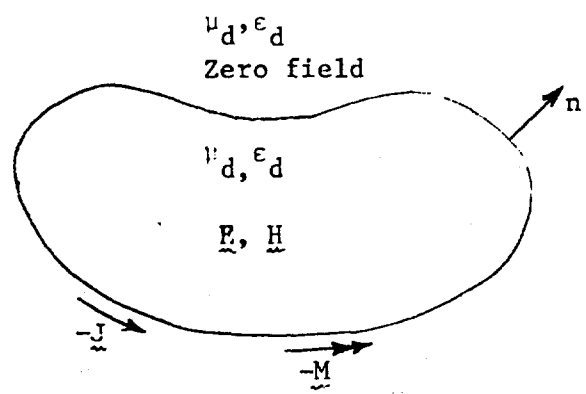

Fig. 3. Inside equivalence.

original problem as shown in Fig. 1 are continuous across S.

The scattered field $\underset{\sim}{E}^s$, $\underset{\sim}{H}^s$ outside S and the diffracted field $\underset{\sim}{E}$, $\underset{\sim}{H}$ inside S could easily be calculated if $\underset{\sim}{J}$ and $\underset{\sim}{M}$ were known because the media into which $\underset{\sim}{J}$ and $\underset{\sim}{M}$ radiate is homogeneous in Figs. 2 and 3. We have to determine $\underset{\sim}{J}$ and $\underset{\sim}{M}$. The equivalence principle states that there exist $\underset{\sim}{J}$ and $\underset{\sim}{M}$ which radiate the fields in Figs. 2 and 3, but the equivalence principle does not tell what $\underset{\sim}{J}$ and $\underset{\sim}{M}$ are. The equivalence principle does state that

$$\underset{\sim}{J} = \underset{\sim}{n} \times \underset{\sim}{H} \tag{3}$$

$$\underset{\sim}{M} = \underset{\sim}{E} \times \underset{\sim}{n} \tag{4}$$

but this is not very useful because $\underset{\sim}{E}$ and $\underset{\sim}{H}$ are unknown.

From Figs. 2 and 3,

$$-\underset{\sim}{n} \times \underset{\sim}{E}_e^- = \underset{\sim}{n} \times \underset{\sim}{E}^i \tag{5}$$

$$-\underset{\sim}{n} \times \underset{\sim}{H}_e^- = \underset{\sim}{n} \times \underset{\sim}{H}^i \tag{6}$$

$$-\underset{\sim}{n} \times \underset{\sim}{E}_d^+ = 0 \tag{7}$$

$$-\underset{\sim}{n} \times \underset{\sim}{H}_d^+ = 0 \tag{8}$$

where

$\underset{\sim}{E}_e^-$ is the electric field just inside S due to $\underset{\sim}{J}$, $\underset{\sim}{M}$, radiating in μ_e, ε_e

$\underset{\sim}{H}_e^-$ is the magnetic field just inside S due to $\underset{\sim}{J}$, $\underset{\sim}{M}$, radiating in μ_e, ε_e

$\underset{\sim}{E}_d^+$ is the electric field just outside S due to $\underset{\sim}{J}$, $\underset{\sim}{M}$, radiating in μ_d, ε_d

$\underset{\sim}{H}_d^+$ is the magnetic field just outside S due to $\underset{\sim}{J}$, $\underset{\sim}{M}$, radiating in μ_d, ε_d

The equivalent currents $\underset{\sim}{J}$, $\underset{\sim}{M}$ which appear in Figs. 2 and 3 satisfy (5)-(8) because (5)-(8) were obtained from Figs. 2 and 3. It is shown in Appendix B that the solution to (5)-(8) is unique. Therefore, (5)-(8) uniquely determine the equivalent currents $\underset{\sim}{J}$, $\underset{\sim}{M}$ of Figs. 2 and 3.

Equations (5)-(8) form a set of four equations in the two unknowns $\underset{\sim}{J}$ and $\underset{\sim}{M}$. The usual methods of equation solving apply only when the number of equations is equal to the number of unknowns. We want to reduce the set of four equations (5)-(8) to two equations. One way to do this is to form the linear combination

$$-\underset{\sim}{n} \times (\underset{\sim}{E}_e^- + \alpha \underset{\sim}{E}_d^+) = \underset{\sim}{n} \times \underset{\sim}{E}^i \tag{9}$$

of (5) and (7) and the linear combination

$$-\underset{\sim}{n} \times (\underset{\sim}{H}_e^- + \beta \underset{\sim}{H}_d^+) = \underset{\sim}{n} \times \underset{\sim}{H}^i \tag{10}$$

of (6) and (8) where α and β are complex constants.

The solution $\underset{\sim}{J}$, $\underset{\sim}{M}$ to (5)-(8) satisfies (9) and (10). This $\underset{\sim}{J}$, $\underset{\sim}{M}$ will be the only solution to the pair of equations (9) and (10) if

$$-\underset{\sim}{n} \times (\underset{\sim}{E}_e^- + \alpha \underset{\sim}{E}_d^+) = 0 \tag{11}$$

$$-\underset{\sim}{n} \times (\underset{\sim}{H}_e^- + \beta \underset{\sim}{H}_d^+) = 0 \tag{12}$$

have only the trivial solution $\underset{\sim}{J} = \underset{\sim}{M} = 0$. From (11) and (12),

$$P_e = -\alpha\beta^* P_d \tag{13}$$

where P_e is the complex power flow of $\underset{\sim}{E}_e^-$, $\underset{\sim}{H}_e^-$ inside S and P_d is the complex power flow of $\underset{\sim}{E}_d^+$, $\underset{\sim}{H}_d^+$ outside S. The asterisk in (13) denotes complex conjugate. If $\alpha\beta^*$ is real, then the real part of (13) reduces to

$$\text{Real}(P_e) = -\alpha\beta^* \text{Real}(P_d) \tag{14}$$

If $\alpha\beta^*$ is not only real but also positive, then

$$\text{Real}(P_d) = 0 \tag{15}$$

because both $\text{Real}(P_e)$ and $\text{Real}(P_d)$ are greater than or equal to zero. Equation (15) implies that

$$\underset{\sim}{n} \times \underset{\sim}{E}_d^+ = \underset{\sim}{n} \times \underset{\sim}{H}_d^+ = 0 \tag{16}$$

Substitution of (16) into (11) and (12) yields

$$\underset{\sim}{n} \times \underset{\sim}{E}_e^- = \underset{\sim}{n} \times \underset{\sim}{H}_e^- = 0 \tag{17}$$

The system of equations (16) and (17) is precisely the homogeneous system of equations associated with (5)-(8). It was shown in Appendix B that this homogeneous system of equations has only the trivial solution $\underset{\sim}{J} = \underset{\sim}{M} = 0$. Therefore, if $\alpha\beta^*$ is real and positive, then the coupled pair of equations (11) and (12) has only the trivial solution $\underset{\sim}{J} = \underset{\sim}{M} = 0$ so that the solution $\underset{\sim}{J}$, $\underset{\sim}{M}$ to (5)-(8) is the only solution to the coupled pair of equations (9) and (10).

If $\alpha = \beta = 1$, then (9) and (10) become

$$-\underset{\sim}{n} \times (\underset{\sim}{E}_e^- + \underset{\sim}{E}_d^+) = \underset{\sim}{n} \times \underset{\sim}{E}^i \tag{18}$$

$$-\underset{\sim}{n} \times (\underset{\sim}{H}_e^- + \underset{\sim}{H}_d^+) = \underset{\sim}{n} \times \underset{\sim}{H}^i \tag{19}$$

The set of equations (18) and (19) is the coupled pair of surface integral equations transcribed by Poggio and Miller [1]. We call these equations the PMCHW equations. Since $\alpha = \beta = 1$ implies that $\alpha\beta^*$ is real and positive, the argument consisting of (11)-(17) and involving real power flow shows that (18) and (19) uniquely determine the desired $\underset{\sim}{J}$, $\underset{\sim}{M}$ of Figs. 2 and 3.

That (18) and (19) uniquely determine $\underset{\sim}{J}$, $\underset{\sim}{M}$ of Figs. 2 and 3 can also be shown as follows. The desired $\underset{\sim}{J}$, $\underset{\sim}{M}$ of Figs. 2 and 3 satisfies (18) and (19) because (18) and (19) were obtained from Figs. 2 and 3. This desired $\underset{\sim}{J}$, $\underset{\sim}{M}$ will be the only solution to (18) and (19) if the associated set of homogeneous equations

$$-\underset{\sim}{n} \times (\underset{\sim}{E}_e^- + \underset{\sim}{E}_d^+) = 0 \tag{20}$$

$$-\underset{\sim}{n} \times (\underset{\sim}{H}_e^- + \underset{\sim}{H}_d^+) = 0 \tag{21}$$

has only the trivial solution $\underset{\sim}{J} = \underset{\sim}{M} = 0$.

The following argument shows that (20) and (21) have only the trivial solution $\underset{\sim}{J} = \underset{\sim}{M} = 0$. Let $\underset{\sim}{E}_d$, $\underset{\sim}{H}_d$ be the electromagnetic field outside S due to $\underset{\sim}{J}$, $\underset{\sim}{M}$ radiating in μ_d, ε_d. Let $\underset{\sim}{E}_e$, $\underset{\sim}{H}_e$ be the electromagnetic field inside S due to $\underset{\sim}{J}$, $\underset{\sim}{M}$ radiating in μ_e, ε_e. Use the equivalence principle to form the composite situation consisting of medium μ_d, ε_d and field $\underset{\sim}{E}_d$, $\underset{\sim}{H}_d$ outside S and medium μ_e, ε_e and field $-\underset{\sim}{E}_e$, $-\underset{\sim}{H}_e$ inside S as shown in Fig. 4. In Fig. 4, $\underset{\sim}{E}_d$, $\underset{\sim}{H}_d$ is a source-free Maxwellian field outside S. Since $\underset{\sim}{E}_e$, $\underset{\sim}{H}_e$ is

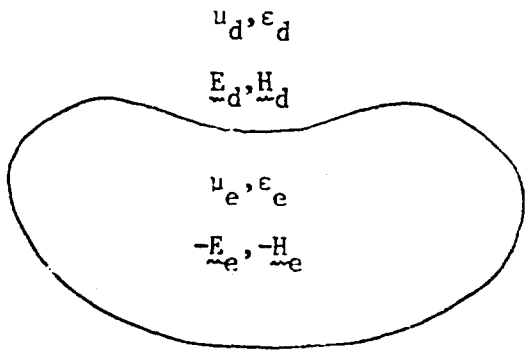

Fig. 4. Composite situation used to prove that (20) and (21) have only the trivial solution $\underset{\sim}{J} = \underset{\sim}{M} = 0$.

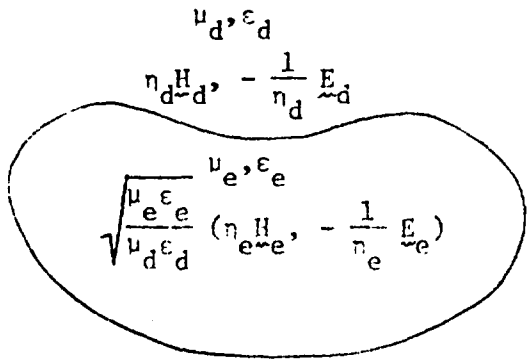

Fig. 5. Composite situation used to prove that (26) and (27) have only the trivial solution $\underset{\sim}{J} = \underset{\sim}{M} = 0$.

a source-free Maxwellian field inside S, the field $-\underset{\sim}{E}_e$, $-\underset{\sim}{H}_e$ appearing in Fig. 4 is also a source-free Maxwellian field inside S. Now, (20) and (21) state that the tangential components of the field in Fig. 4 are continuous across S. Thus, Fig. 4 is entirely source-free so that the field in Fig. 4 is zero everywhere in which case (B-1)-(B-4) are satisfied. But, as shown in Appendix B, (B-1)-(B-4) have only the trivial solution $\underset{\sim}{J} = \underset{\sim}{M} = 0$. Hence, (20) and (21) have only the trivial solution $\underset{\sim}{J} = \underset{\sim}{M} = 0$.

If

$$\alpha = -\frac{\varepsilon_d}{\varepsilon_e} \tag{22}$$

$$\beta = -\frac{\mu_d}{\mu_e} \tag{23}$$

then (9) and (10) become

$$-\underset{\sim}{n} \times (\underset{\sim}{E}_e^- - \frac{\varepsilon_d}{\varepsilon_e} \underset{\sim}{E}_d^+) = \underset{\sim}{n} \times \underset{\sim}{E}^i \tag{24}$$

$$-\underset{\sim}{n} \times (\underset{\sim}{H}_e^- - \frac{\mu_d}{\mu_e} \underset{\sim}{H}_d^+) = \underset{\sim}{n} \times \underset{\sim}{H}^i \tag{25}$$

The set of equations (24) and (25) is the coupled pair of surface integral equations obtained by Müller [4]. We call these equations the Müller equations. The singularity that the kernels of the integral equations (24) and (25) exhibit as the source point passes through the field point is not as pronounced as the singularity of the kernels of (18) and (19). If μ_e, ε_e, μ_d, and ε_d are real in (22)-(25), then $\alpha\beta^*$ is real and positive. In this case, the argument consisting of (11)-(17) shows that (24) and (25) uniquely determine the desired $\underset{\sim}{J}$, $\underset{\sim}{M}$ of Figs. 2 and 3.

An alternate proof, valid for lossy media, that (24) and (25) uniquely determine the desired $\underset{\sim}{J}$, $\underset{\sim}{M}$ is presented. This proof is similar to the argument which used Fig. 4 to show that (18) and (19) uniquely determine the desired $\underset{\sim}{J}$, $\underset{\sim}{M}$ and is as follows. The desired $\underset{\sim}{J}$, $\underset{\sim}{M}$ of Figs. 2 and 3 satisfies (24) and (25) because (24) and (25) were obtained from Figs. 2 and 3. This desired $\underset{\sim}{J}$, $\underset{\sim}{M}$ will be the only solution to (24) and (25) if the associated set of homogeneous equations

$$-\underset{\sim}{n} \times (\underset{\sim}{E}_e^- - \frac{\varepsilon_d}{\varepsilon_e} \underset{\sim}{E}_d^+) = 0 \tag{26}$$

$$-\underset{\sim}{n} \times (\underset{\sim}{H}_e^- - \frac{\mu_d}{\mu_e} \underset{\sim}{H}_d^+) = 0 \tag{27}$$

has only the trivial solution $\underset{\sim}{J} = \underset{\sim}{M} = 0$.

The following argument shows that (26) and (27) have only the trivial solution $\underset{\sim}{J} = \underset{\sim}{M} = 0$. Let $\underset{\sim}{E}_d$, $\underset{\sim}{H}_d$ be the electromagnetic field outside S due to $\underset{\sim}{J}$, $\underset{\sim}{M}$ radiating in μ_d, ε_d. Because the electromagnetic field $\underset{\sim}{E}_d$, $\underset{\sim}{H}_d$ is a source-free Maxwellian field in μ_d, ε_d outside S, the dual electromagnetic field $\eta_d \underset{\sim}{H}_d$, $-\frac{1}{\eta_d} \underset{\sim}{E}_d$ where

$$\eta_d = \sqrt{\frac{\mu_d}{\varepsilon_d}} \tag{28}$$

is also a source-free Maxwellian field outside S. Let $\underset{\sim}{E}_e$, $\underset{\sim}{H}_e$ be the electromagnetic field inside S due to $\underset{\sim}{J}$, $\underset{\sim}{M}$ radiating in μ_e, ε_e. Because the electromagnetic field $\underset{\sim}{E}_e$, $\underset{\sim}{H}_e$ is a source-free Maxwellian field inside S, the dual electromagnetic field $\eta_e \underset{\sim}{H}_e$, $-\frac{1}{\eta_e} \underset{\sim}{E}_e$ where

$$\eta_e = \sqrt{\frac{\mu_e}{\varepsilon_e}} \tag{29}$$

is also a source-free Maxwellian field inside S. Use the equivalence principle to form the composite situation consisting of medium μ_d, ε_d and field $\eta_d \underset{\sim}{H}_d$, $-\frac{1}{\eta_d} \underset{\sim}{E}_d$ outside S and medium μ_e, ε_e and field $\sqrt{\frac{\mu_e \varepsilon_e}{\mu_d \varepsilon_d}} (\eta_e \underset{\sim}{H}_e, -\frac{1}{\eta_e} \underset{\sim}{E}_e)$ inside S as shown in Fig. 5. Now, (26) and (27) state that the tangential components of the field in Fig. 5 are continuous across S. Thus, Fig. 5 is entirely source-free so that the field in Fig. 5 is zero everywhere in which case (B-1)-(B-4) are satisfied. But, as shown in Appendix B, (B-1)-(B-4) have only the trivial solution $\underset{\sim}{J} = \underset{\sim}{M} = 0$. Hence, (26) and (27) have only the trivial solution $\underset{\sim}{J} = \underset{\sim}{M} = 0$.

III. METHOD OF MOMENTS SOLUTION FOR A BODY OF REVOLUTION

In this section, a method of moments solution to (9) and (10) is developed for a homogeneous loss-free body of revolution. Special cases of (9) and (10) are the PMCHW equations (18) and (19) and the Müller equations (24) and (25).

For compatibility with equation (40) on page 14 of [9], we rewrite (9) as

$$-\frac{1}{\eta_e}\left(\underset{\sim}{E}_e^- + \alpha \underset{\sim}{E}_d^+\right)_{tan} = \frac{1}{\eta_e}\underset{\sim}{E}_{tan}^i \tag{30}$$

where tan denotes tangential components on S and η_e is given by (29). The fields on the left-hand sides of (30) and (10) are written as the sum of fields due to $\underset{\sim}{J}$ and fields due to $\underset{\sim}{M}$. Advantage is taken of the fact that the operator which gives the electric field due to a magnetic current is the negative of the operator which gives the magnetic field due to an electric current and that the operator which gives the magnetic field due to a magnetic current is the square of the reciprocal of the intrinsic impedance times the operator which gives the electric field due to an electric current. In view of the above considerations, (30) and (10) become

$$\left(-\frac{1}{\eta_e}\underset{\sim}{E}_e(\underset{\sim}{J}) + \frac{1}{\eta_e}\underset{\sim}{H}_e^-(\underset{\sim}{M}) - \frac{\alpha}{\eta_e}\underset{\sim}{E}_d(\underset{\sim}{J}) + \frac{\alpha}{\eta_e}\underset{\sim}{H}_d^+(\underset{\sim}{M})\right)_{tan} = \frac{1}{\eta_e}\underset{\sim}{E}_{tan}^i \tag{31}$$

$$-\underset{\sim}{n} \times \left(\underset{\sim}{H}_e^-(\underset{\sim}{J}) + \frac{1}{\eta_e^2}\underset{\sim}{E}_e(\underset{\sim}{M}) + \beta\underset{\sim}{H}_d^+(\underset{\sim}{J}) + \frac{\beta}{\eta_d^2}\underset{\sim}{E}_d(\underset{\sim}{M})\right) = \underset{\sim}{n} \times \underset{\sim}{H}^i \tag{32}$$

where $\underset{\sim}{E}$ denotes the operator which gives the electric field due to an electric current. The subscript e or d on $\underset{\sim}{E}$ denotes radiation in either μ_e, ε_e or μ_d, ε_d. The superscript + or −, if present on $\underset{\sim}{E}$, denotes field evaluation either just outside S or just inside S. The $\underset{\sim}{H}$'s in (31) and (32) are the corresponding magnetic field due to electric current operators. We stress that all $\underset{\sim}{E}$'s and $\underset{\sim}{H}$'s in (31) and (32) are, by definition, operators which give electric and magnetic fields due to electric currents, even though these operators act on both electric and magnetic currents $\underset{\sim}{J}$ and $\underset{\sim}{M}$ in (31) and (32).

Let

$$\underset{\sim}{J} = \sum_{n=-\infty}^{\infty} \sum_{j=1}^{N} (I_{nj}^{t} \underset{\sim}{J}_{nj}^{t} + I_{nj}^{\phi} \underset{\sim}{J}_{nj}^{\phi}) \tag{33}$$

$$\underset{\sim}{M} = \eta_e \sum_{n=-\infty}^{\infty} \sum_{j=1}^{N} (V_{nj}^{t} \underset{\sim}{J}_{nj}^{t} + V_{nj}^{\phi} \underset{\sim}{J}_{nj}^{\phi}) \tag{34}$$

where I_{nj}^{t}, I_{nj}^{ϕ}, V_{nj}^{t}, and V_{nj}^{ϕ} are coefficients to be determined and

$$\underset{\sim}{J}_{nj}^{t} = \underset{\sim}{u}_t f_j(t) e^{jn\phi} \tag{35}$$

$$\underset{\sim}{J}_{nj}^{\phi} = \underset{\sim}{u}_{\phi} f_j(t) e^{jn\phi} \tag{36}$$

In (35) and (36), t is the arc length along the generating curve of the body body of revolution and ϕ is the longitudinal angle. $\underset{\sim}{u}_t$ and $\underset{\sim}{u}_{\phi}$ are unit vectors in the t and ϕ directions respectively such that $\underset{\sim}{u}_{\phi} \times \underset{\sim}{u}_t = \underset{\sim}{n}$ and $f_j(t)$ is the scalar function of t defined on page 10 of [9]. The body of revolution and coordinate system are shown in Fig. 6. Substitution of (33) and (34) into (31) and (32) yields

$$\sum_{n=-\infty}^{\infty} \sum_{j=1}^{N} \left\{ (\underset{\sim}{H}_e^{-}(\underset{\sim}{J}_{nj}^{t}) + \alpha \underset{\sim}{H}_d^{+}(\underset{\sim}{J}_{nj}^{t}))_{\tan} V_{nj}^{t} + (\underset{\sim}{H}_e^{-}(\underset{\sim}{J}_{nj}^{\phi}) + \alpha \underset{\sim}{H}_d^{+}(\underset{\sim}{J}_{nj}^{\phi}))_{\tan} V_{nj}^{\phi} + \right.$$

$$\left. (-\frac{\underset{\sim}{E}_e(\underset{\sim}{J}_{nj}^{t})}{\eta_e} - \frac{\alpha\eta_d}{\eta_e} \frac{\underset{\sim}{E}_d(\underset{\sim}{J}_{nj}^{t})}{\eta_d})_{\tan} I_{nj}^{t} + (-\frac{\underset{\sim}{E}_e(\underset{\sim}{J}_{nj}^{\phi})}{\eta_e} - \frac{\alpha\eta_d}{\eta_e} \frac{\underset{\sim}{E}_d(\underset{\sim}{J}_{nj}^{\phi})}{\eta_d})_{\tan} I_{nj}^{\phi} \right\} = \frac{1}{\eta_e} \underset{\sim}{E}_{\tan}^{i} \tag{37}$$

$$-\underset{\sim}{n} \times \sum_{n=-\infty}^{\infty} \sum_{j=1}^{N} \left\{ (\frac{\underset{\sim}{E}_e(\underset{\sim}{J}_{nj}^{t})}{\eta_e} + \frac{\beta\eta_e}{\eta_d} \frac{\underset{\sim}{E}_d(\underset{\sim}{J}_{nj}^{t})}{\eta_d}) V_{nj}^{t} + (\frac{\underset{\sim}{E}_e(\underset{\sim}{J}_{nj}^{\phi})}{\eta_e} + \frac{\beta\eta_e}{\eta_d} \frac{\underset{\sim}{E}_d(\underset{\sim}{J}_{nj}^{\phi})}{\eta_d}) V_{nj}^{\phi} + \right.$$

$$\left. (\underset{\sim}{H}_e^{-}(\underset{\sim}{J}_{nj}^{t}) + \beta \underset{\sim}{H}_d^{+}(\underset{\sim}{J}_{nj}^{t})) I_{nj}^{t} + (\underset{\sim}{H}_e^{-}(\underset{\sim}{J}_{nj}^{\phi}) + \beta \underset{\sim}{H}_d^{+}(\underset{\sim}{J}_{nj}^{\phi})) I_{nj}^{\phi} \right\} = \underset{\sim}{n} \times \underset{\sim}{H}^{i} \tag{38}$$

Define the inner product of two vector functions on S to be the integral over S of the dot product of these two vector functions. Because the field operators in (37) and (38) are the same as those considered in [9],

only the nth term of the sum (37) or (38) contributes to the inner product of (37) or (38) with either $\underset{\sim}{J}^{t}_{\sim ni}$ or $\underset{\sim}{J}^{\phi}_{\sim ni}$. Hence, the inner product of (37) with $\underset{\sim}{J}^{t}_{\sim ni}$, i=1,2,...N, and $\underset{\sim}{J}^{\phi}_{\sim ni}$, i=1,2,...N, successively and the inner product of (38) with $\underset{\sim}{J}^{t}_{\sim ni}$, i=1,2,...N, and $\underset{\sim}{J}^{\phi}_{\sim ni}$, i=1,2,...N, successively gives the matrix equation

$$\begin{bmatrix} (Y^{\phi t}_{ne} + \alpha Y^{\phi t}_{nd}) & (Y^{\phi\phi}_{ne} + \alpha \hat{Y}^{\phi\phi}_{nd}) & (Z^{tt}_{ne} + \frac{\alpha\eta_d}{\eta_e} Z^{tt}_{nd}) & (Z^{t\phi}_{ne} + \frac{\alpha\eta_d}{\eta_e} Z^{t\phi}_{nd}) \\ (-Y^{tt}_{ne} - \alpha \hat{Y}^{tt}_{nd}) & (-Y^{t\phi}_{ne} - \alpha Y^{t\phi}_{nd}) & (Z^{\phi t}_{ne} + \frac{\alpha\eta_d}{\eta_e} Z^{\phi t}_{nd}) & (Z^{\phi\phi}_{ne} + \frac{\alpha\eta_d}{\eta_e} Z^{\phi\phi}_{nd}) \\ (Z^{\phi t}_{ne} + \frac{\beta\eta_e}{\eta_d} Z^{\phi t}_{nd}) & (Z^{\phi\phi}_{ne} + \frac{\beta\eta_e}{\eta_d} Z^{\phi\phi}_{nd}) & (Y^{tt}_{ne} + \beta \hat{Y}^{tt}_{nd}) & (Y^{t\phi}_{ne} + \beta Y^{t\phi}_{nd}) \\ (-Z^{tt}_{ne} - \frac{\beta\eta_e}{\eta_d} Z^{tt}_{nd}) & (-Z^{t\phi}_{ne} - \frac{\beta\eta_e}{\eta_d} Z^{t\phi}_{nd}) & (Y^{\phi t}_{ne} + \beta Y^{\phi t}_{nd}) & (Y^{\phi\phi}_{ne} + \beta \hat{Y}^{\phi\phi}_{nd}) \end{bmatrix} \begin{bmatrix} \vec{V}^{t}_{n} \\ \vec{V}^{\phi}_{n} \\ \vec{I}^{t}_{n} \\ \vec{I}^{\phi}_{n} \end{bmatrix} = \begin{bmatrix} \vec{\hat{V}}^{t}_{n} \\ \vec{\hat{V}}^{\phi}_{n} \\ \vec{\hat{I}}^{t}_{n} \\ \vec{\hat{I}}^{\phi}_{n} \end{bmatrix} \tag{39}$$

for $n = 0, \pm 1, \pm 2, \ldots\ldots$. In (39), $\vec{V}^{t}_{n}$, $\vec{V}^{\phi}_{n}$, $\vec{I}^{t}_{n}$, and $\vec{I}^{\phi}_{n}$ are column vectors of the coefficients appearing in (33) and (34). Also,

$$(Y^{pq}_{nf})_{ij} = -\iint_{S} \underset{\sim}{J}^{p}_{\sim ni} \cdot \underset{\sim}{n} \times \underset{\sim}{H}_{f}(\underset{\sim}{J}^{q}_{\sim nj}) ds \tag{40}$$

$$(Z^{pq}_{nf})_{ij} = -\frac{1}{\eta_f} \iint_{S} \underset{\sim}{J}^{p}_{\sim ni} \cdot \underset{\sim}{E}_{f}(\underset{\sim}{J}^{q}_{\sim nj}) ds \tag{41}$$

$$\hat{V}^{p}_{ni} = \frac{1}{\eta_e} \iint_{S} \underset{\sim}{J}^{p}_{\sim ni} \cdot \underset{\sim}{E}^{i} ds \tag{42}$$

$$\hat{I}^{p}_{ni} = \iint_{S} \underset{\sim}{J}^{p}_{\sim ni} \cdot \underset{\sim}{n} \times \underset{\sim}{H}^{i} ds \tag{43}$$

where p may be either t or ϕ, q may be either t or ϕ, and f may be either e or d. If p=q in (40), it matters whether the magnetic field $\underset{\sim}{H}_{f}(\underset{\sim}{J}^{q}_{\sim nj})$ is evaluated just outside or just inside S. The Y's without

carets in (39) are given by the right-hand side of (40) in which the magnetic field is evaluated just inside S. The Y's with carets in (39) are given by the right-hand side of (40) with magnetic field evaluation just outside S.

The Y and Z submatrices on the left-hand side of (39) are the same as in equation (88) on page 24 of [9] with the reservations that the caret on Y denotes magnetic field evaluation just outside S, and the extra subscript e or d denotes radiation in either μ_e, ε_e or μ_d, ε_d. The $\hat{I}$ column vectors on the right-hand side of (39) are the same as in equation (88) on page 24 of [9] whereas the $\hat{V}$ column vectors in (39) are the same as the V's without carets in equation (88) on page 24 of [9].

The solution $\vec{V}_n^t$, $\vec{V}_n^\phi$, $\vec{I}_n^t$, and $\vec{I}_n^\phi$ to the matrix equation (39) determines the equivalent electric and magnetic currents $\underset{\sim}{J}$ and $\underset{\sim}{M}$ according to (33) and (34). From Fig. 2, these currents radiate in μ_e, ε_e to produce the scattered field outside S.

IV. FAR FIELD MEASUREMENT AND PLANE WAVE EXCITATION

In this section, measurement vectors are used to obtain the far field of the equivalent surface currents $\underset{\sim}{J}$ and $\underset{\sim}{M}$ radiating in μ_e, ε_e. This far field is the far field scattered by the homogeneous body of revolution. For plane wave excitation, the composite vector on the right-hand side of (39) is expressed in terms of these measurement vectors.

By reciprocity,

$$\underset{\sim}{E}^s \cdot I\underset{\sim}{\ell}_r = \iint_S (\underset{\sim}{J}(\underset{\sim}{r}) \cdot \underset{\sim}{E}(I\underset{\sim}{\ell}_r) - \underset{\sim}{M}(\underset{\sim}{r}) \cdot \underset{\sim}{H}(I\underset{\sim}{\ell}_r))ds \qquad (44)$$

where $\underset{\sim}{E}^s$ is the far electric field due to $\underset{\sim}{J}$ and $\underset{\sim}{M}$, $I\underset{\sim}{\ell}_r$ is a receiving electric dipole at the far field measurement point, $\underset{\sim}{E}(I\underset{\sim}{\ell}_r)$ is the electric field due to $I\underset{\sim}{\ell}_r$, and $\underset{\sim}{H}(I\underset{\sim}{\ell}_r)$ is the magnetic field due to $I\underset{\sim}{\ell}_r$. Both $\underset{\sim}{E}(I\underset{\sim}{\ell}_r)$ and $\underset{\sim}{H}(I\underset{\sim}{\ell}_r)$ are evaluated at point $\underset{\sim}{r}$ on S where $\underset{\sim}{r}$ is the point at which the differential portion of surface ds is located. If $\underset{\sim}{\ell}_r$ is tangent to the radiation sphere,

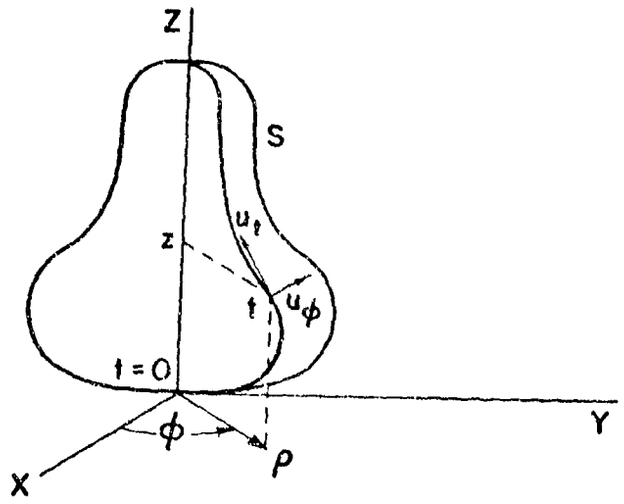

Fig. 6. Body of revolution and coordinate system.

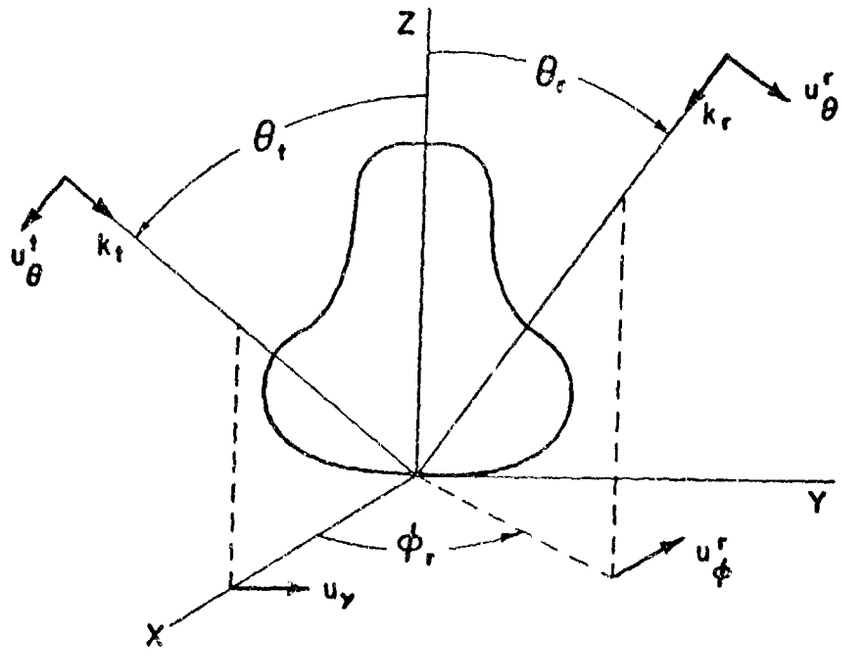

Fig. 7. Plane wave scattering by a dielectric body of revolution.

$$\underset{\sim}{E}(I\ell_{\underset{\sim}{r}}) = \frac{-jk\eta\, e^{-jkr_r}}{4\pi r_r} I\ell_{\underset{\sim}{r}}\, e^{-jk_{\underset{\sim}{r}} \cdot \underset{\sim}{r}} \tag{45}$$

$$\underset{\sim}{H}(I\ell_{\underset{\sim}{r}}) = \frac{-j\, e^{-jkr_r}}{4\pi r_r} (k_{\underset{\sim}{r}} \times I\ell_{\underset{\sim}{r}}) e^{-jk_{\underset{\sim}{r}} \cdot \underset{\sim}{r}} \tag{46}$$

where r_r is the distance between the measurement point and the origin in the vicinity of S. Also, $k_{\underset{\sim}{r}}$ is the propagation vector of the plane wave coming from $I\ell_{\underset{\sim}{r}}$, k is the propagation constant and η is the intrinsic impedance of the medium outside S. To simplify the notation in this section, we have omitted the subscript e from all parameters dependent on the medium. It is understood that all far field measurement vectors and plane wave excitation vectors depend only on the external medium μ_e, ε_e.

Substitution of (33), (34), (45), and (46) into (44) gives

$$E_\theta^s = \frac{-j\eta\, e^{-jkr_r}}{4\pi r_r} \sum_{n=-\infty}^{\infty} (\tilde{R}_n^{t\phi} \vec{V}_n^t + \tilde{R}_n^{\phi\phi} \vec{V}_n^\phi + \tilde{R}_n^{t\theta} \vec{I}_n^t + \tilde{R}_n^{\phi\theta} \vec{I}_n^\phi) e^{jn\phi_r} \tag{47}$$

for $I\ell_{\underset{\sim}{r}} = \underset{\sim}{u}_\theta^r$ and

$$E_\phi^s = \frac{-jn e^{-jkr_r}}{4\pi r_r} \sum_{n=-\infty}^{\infty} (-\tilde{R}_n^{t\theta} \vec{V}_n^t - \tilde{R}_n^{\phi\theta} \vec{V}_n^\phi + \tilde{R}_n^{t\phi} \vec{I}_n^t + \tilde{R}_n^{\phi\phi} \vec{I}_n^\phi) e^{jn\phi_r} \tag{48}$$

for $I\ell_{\underset{\sim}{r}} = \underset{\sim}{u}_\phi^r$ where $\underset{\sim}{u}_\theta^r$ and $\underset{\sim}{u}_\phi^r$ are unit vectors in the θ_r and ϕ_r directions respectively. As shown in Fig. 7, θ_r and ϕ_r are the angular coordinates of the receiver location at which $I\ell_{\underset{\sim}{r}}$ is placed. In (47) and (48), E_θ^s and E_ϕ^s are the θ_r and ϕ_r components of $\underset{\sim}{E}^s$. Also, $\vec{V}_n^t$, $\vec{V}_n^\phi$, $\vec{I}_n^t$, and $\vec{I}_n^\phi$ are column vectors of the coefficients appearing in (33) and (34). Furthermore, $\tilde{R}_n^{pq}$ is a row vector whose jth element is given by

$$R_{nj}^{pq} = k\, e^{-jn\phi_r} \iint_S J_{nj}^p \cdot \underset{\sim}{u}_q^r\, e^{-jk_{\underset{\sim}{r}} \cdot \underset{\sim}{r}} ds \tag{49}$$

where p may be either t or ϕ and q may be either θ or ϕ. In view of (35) and (36), (49) is the same as equation (92) on page 26 of [9]. It is shown in [9] that the right-hand side of (49) does not depend on ϕ_r.

For plane wave incidence and expansion functions $\underset{\sim}{J}^{t}_{nj}$ and $\underset{\sim}{J}^{\phi}_{nj}$ given by (35) and (36), the equivalent currents (33) and (34) and the fields (47) and (48) have special forms. To obtain these forms, assume that the incident electromagnetic field $\underset{\sim}{E}^{i}$, $\underset{\sim}{H}^{i}$ is either a θ polarized field defined by

$$\underset{\sim}{E}^{i} = k\eta \, \underset{\sim}{u}^{t}_{\theta} \, e^{-j\underset{\sim}{k}_{t} \cdot \underset{\sim}{r}} \tag{50}$$

$$\underset{\sim}{H}^{i} = - k \, \underset{\sim}{u}_{y} \, e^{-j\underset{\sim}{k}_{t} \cdot \underset{\sim}{r}} \tag{51}$$

or a ϕ polarized field defined by

$$\underset{\sim}{E}^{i} = k\eta \, \underset{\sim}{u}_{y} \, e^{-j\underset{\sim}{k}_{t} \cdot \underset{\sim}{r}} \tag{52}$$

$$\underset{\sim}{H}^{i} = k \, \underset{\sim}{u}^{t}_{\theta} \, e^{-j\underset{\sim}{k}_{t} \cdot \underset{\sim}{r}} \tag{53}$$

where $\underset{\sim}{k}_{t}$ is the propagation vector and, as shown in Fig. 7, $\underset{\sim}{u}^{t}_{\theta}$ and $\underset{\sim}{u}_{y}$ are unit vectors in the θ_t and y directions respectively. Here, θ_t is the colatitude of the direction from which the incident wave comes. $\underset{\sim}{k}_{t}$ is in the xz plane. No generality is lost by putting $\underset{\sim}{k}_{t}$ in the xz plane because if $\underset{\sim}{k}_{t}$ were shifted out of the xz plane by an angle ϕ_t, the response would also be shifted by the same angle ϕ_t.

Substituting (50) and (51) into (42) and (43), then substituting (52) and (53) into (42) and (43), next taking advantage of the relationships

$$\underset{\sim}{J}^{t}_{-ni} \times \underset{\sim}{n} = \underset{\sim}{J}^{\phi}_{-ni} \tag{54}$$

$$\underset{\sim}{J}^{\phi}_{-ni} \times \underset{\sim}{n} = - \underset{\sim}{J}^{t}_{ni} \tag{55}$$

which are apparent from (35), (36) and Fig. 6, then comparing the results with (49), and finally using equation (104) on page 29 of [9], we obtain

$$\begin{bmatrix} \vec{V}{}^{t\theta}_n & \vec{V}{}^{t\phi}_n \\ \vec{V}{}^{\phi\theta}_n & \vec{V}{}^{\phi\phi}_n \\ \vec{I}{}^{t\theta}_n & \vec{I}{}^{t\phi}_n \\ \vec{I}{}^{\phi\theta}_n & \vec{I}{}^{\phi\phi}_n \end{bmatrix} = \begin{bmatrix} \vec{R}{}^{t\theta}_n & -\vec{R}{}^{t\phi}_n \\ -\vec{R}{}^{\phi\theta}_n & \vec{R}{}^{\phi\phi}_n \\ -\vec{R}{}^{\phi\phi}_n & -\vec{R}{}^{\phi\theta}_n \\ -\vec{R}{}^{t\phi}_n & -\vec{R}{}^{t\theta}_n \end{bmatrix} \tag{56}$$

The first superscript on $\vec{V}_n$ and $\vec{I}_n$ in (56) is the superscript which appears on the right-hand side of (39). The second superscript on $\vec{V}_n$ and $\vec{I}_n$ in (56) denotes the polarization of the incident plane wave. If this second superscript is θ, the θ polarized field given by (50) and (51) is incident. If this second subscript is ϕ, the ϕ polarized field given by (52) and (53) is incident. The jth element of the column vector $\vec{R}{}^{pq}_n$ on the right-hand side of (56) is given by (49) with θ_r replaced by θ_t. Conceding that θ_r does not appear explicitly in (49), we really mean that θ_r is replaced by θ_t after the surface integral in (49) is evaluated. In other words, θ_r is replaced by θ_t in equation (95) on page 27 of [9].

For plane wave incidence, the +n and -n terms in formulas (33) and (34) for the equivalent currents can be combined as follows. According to equations (102) and (103) of [9], the Y and Z submatrices in (39) are either even or odd in n. The even-odd properties in n of the submatrices of the square matrix on the left-hand side of (39) are tabulated as

$$\begin{bmatrix} - & + & + & - \\ + & - & - & + \\ - & + & + & - \\ + & - & - & + \end{bmatrix}$$

where + denotes an even submatrix and - denotes an odd submatrix. It follows that the submatrices of the inverse of the square matrix on the left-hand side of (39) have even-odd properties in n given by

$$\begin{bmatrix} - & + & - & + \\ + & - & + & - \\ + & - & + & - \\ - & + & - & + \end{bmatrix}$$

From (56) and the even-odd properties of $\overset{\pm}{R}{}^{pq}_{n}$ given by equation (104) on page 29 of [9], the column vectors $\overset{\pm}{V}_n$ and $\overset{\pm}{I}_n$ on the right-hand side of (39) are either even or odd in n. The even-odd properties of the sub-matrices on the left-hand side of (56) are tabulated as

$$\begin{bmatrix} + & - \\ - & + \\ + & - \\ - & + \end{bmatrix}$$

Because of the above even-odd properties of the square matrix on the left-hand side of (39) and the column vector on the right-hand side of (39), the solutions to (39) satisfy

$$\begin{bmatrix} \overset{\pm}{V}{}^{t\theta}_{-n} & \overset{\pm}{V}{}^{t\phi}_{-n} \\ \overset{\pm}{V}{}^{\phi\theta}_{-n} & \overset{\pm}{V}{}^{\phi\phi}_{-n} \\ \overset{\pm}{I}{}^{t\theta}_{-n} & \overset{\pm}{I}{}^{t\phi}_{-n} \\ \overset{\pm}{I}{}^{\phi\theta}_{-n} & \overset{\pm}{I}{}^{\phi\phi}_{-n} \end{bmatrix} = \begin{bmatrix} -\overset{\pm}{V}{}^{t\theta}_{n} & \overset{\pm}{V}{}^{t\phi}_{n} \\ \overset{\pm}{V}{}^{\phi\theta}_{n} & -\overset{\pm}{V}{}^{\phi\phi}_{n} \\ \overset{\pm}{I}{}^{t\theta}_{n} & -\overset{\pm}{I}{}^{t\phi}_{n} \\ -\overset{\pm}{I}{}^{\phi\theta}_{n} & \overset{\pm}{I}{}^{\phi\phi}_{n} \end{bmatrix} \tag{57}$$

The first superscript on the column vectors $\overset{\pm}{V}_{+n}$ and $\overset{\pm}{I}_{+n}$ in (57) is that which appears on the column vectors $\overset{\pm}{V}_n$ and $\overset{\pm}{I}_n$ on the left-hand side of (39). The second superscript on the column vectors in (57) denotes either the θ or the ϕ polarized incident plane wave. Substitution of (57), (35), and (36) into (33) and (34) yields

$$\underset{\sim}{J}^{\theta} = (\tilde{f}\vec{I}_o^{t\theta})\underset{\sim}{u}_t + \sum_{n=1}^{\infty} 2(\tilde{f}\vec{I}_n^{t\theta})\underset{\sim}{u}_t\cos(n\phi) + 2j(\tilde{f}\vec{I}_n^{\phi\theta})\underset{\sim}{u}_\phi\sin(n\phi) \tag{58}$$

$$\frac{1}{\eta}\underset{\sim}{M}^{\theta} = (\tilde{f}\vec{V}_o^{\phi\theta})\underset{\sim}{u}_\phi + \sum_{n=1}^{\infty} 2j(\tilde{f}\vec{V}_n^{t\theta})\underset{\sim}{u}_t\sin(n\phi) + 2(\tilde{f}\vec{V}_n^{\phi\theta})\underset{\sim}{u}_\phi\cos(n\phi) \tag{59}$$

for the θ polarized incident wave and

$$\underset{\sim}{J}^{\phi} = (\tilde{f}\vec{I}_o^{\phi\phi})\underset{\sim}{u}_\phi + \sum_{n=1}^{\infty} 2j(\tilde{f}\vec{I}_n^{t\phi})\underset{\sim}{u}_t\sin(n\phi) + 2(\tilde{f}\vec{I}_n^{\phi\phi})\underset{\sim}{u}_\phi\cos(n\phi) \tag{60}$$

$$\frac{1}{\eta}\underset{\sim}{M}^{\phi} = (\tilde{f}\vec{V}_o^{t\phi})\underset{\sim}{u}_t + \sum_{n=1}^{\infty} 2(\tilde{f}\vec{V}_n^{t\phi})\underset{\sim}{u}_t\cos(n\phi) + 2j(\tilde{f}\vec{V}_n^{\phi\phi})\underset{\sim}{u}_\phi\sin(n\phi) \tag{61}$$

for the ϕ polarized incident wave. In (58)-(61), $\tilde{f}$ is a row vector of the $f_j(t)$. The superscript θ or ϕ on $\underset{\sim}{J}$ or $\underset{\sim}{M}$ in (58)-(61) differentiates the equivalent currents for the θ polarized incident wave from those for the ϕ polarized incident wave.

The far scattered fields (47) and (48) are specialized to the θ polarized incident plane wave by apperding the additional subscript θ to E^s on the left-hand sides of (47) and (48) and the additional superscript θ to $\vec{V}_n^t$, $\vec{V}_n^\phi$, $\vec{I}_n^t$, and $\vec{I}_n^\phi$ on the right-hand sides of (47) and (48). Moreover, in view of equation (104) on page 29 of [9] and (57), the +n and -n terms in (47) and (48) can be combined. As a result, (47) and (48) become

$$E_{\theta\theta}^s = \frac{-jne^{-jkr_r}}{4\pi r_r}\left\{\tilde{R}_o^{\phi\phi}\vec{V}_o^{\phi\theta} + \tilde{R}_o^{t\theta}\vec{I}_o^{t\theta} + 2\sum_{n=1}^{\infty}(\tilde{R}_n^{t\phi}\vec{V}_n^{t\theta} + \tilde{R}_n^{\phi\phi}\vec{V}_n^{\phi\theta} + \right.$$

$$\left. + \tilde{R}_n^{t\theta}\vec{I}_n^{t\theta} + \tilde{R}_n^{\phi\theta}\vec{I}_n^{\phi\theta})\cos(n\phi_r)\right\} \tag{62}$$

$$E_{\phi\theta}^s = \frac{ne^{-jkr_r}}{2\pi r_r}\sum_{n=1}^{\infty}(-\tilde{R}_n^{t\theta}\vec{V}_n^{t\theta} - \tilde{R}_n^{\phi\theta}\vec{V}_n^{\phi\theta} + \tilde{R}_n^{t\phi}\vec{I}_n^{t\theta} +$$

$$+ \tilde{R}_n^{\phi\phi}\vec{I}_n^{\phi\theta})\sin(n\phi_r) \tag{63}$$

for the θ polarized incident plane wave. Similarly, (47) and (48) become

$$E^s_{\theta\phi} = \frac{ne^{-jkr_r}}{2\pi r_r} \sum_{n=1}^{\infty} (\tilde{R}^{t\phi\to t\phi}_n V^{t\phi}_n + \tilde{R}^{\phi\phi\to\phi\phi}_n V^{\phi\phi}_n + \tilde{R}^{t\theta\to t\phi}_n I^{t\phi}_n + \tilde{R}^{\phi\theta\to\phi\phi}_n I^{\phi\phi}_n)\sin(n\phi_r) \tag{64}$$

$$E^s_{\phi\phi} = \frac{-jne^{-jkr_r}}{4\pi r_r} \left\{ - \tilde{R}^{t\theta\to t\phi}_o V^{t\phi}_o + \tilde{R}^{\phi\phi\to\phi\phi}_o I^{\phi\phi}_o + 2 \sum_{n=1}^{\infty} (-\tilde{R}^{t\theta\to t\phi}_n V^{t\phi}_n - \tilde{R}^{\phi\theta\to\phi\phi}_n V^{\phi\phi}_n + \right.$$

$$\left. + \tilde{R}^{t\phi\to t\phi}_n I^{t\phi}_n + \tilde{R}^{\phi\phi\to\phi\phi}_n I^{\phi\phi}_n)\cos(n\phi_r) \right\} \tag{65}$$

for the ϕ polarized incident plane wave. The first subscript on E^s on the left-hand sides of (62)-(65) denotes the receiver polarization and the second subscript on E^s denotes the transmitter polarization.

The scattering cross section σ_{pq} is defined by

$$\sigma_{pq} = \frac{4\pi r_r^2 |E^s_{pq}|^2}{|\underset{\sim}{E}^i|^2} \tag{66}$$

where p is either θ or ϕ and q is either θ or ϕ. In (66), E^s_{pq} is a component of the scattered field given by (62)-(65) and $|\underset{\sim}{E}^i|$ is the magnitude of the electric field of the incident plane wave. According to (50) and (52),

$$|\underset{\sim}{E}^i| = k\eta \tag{67}$$

for both polarizations so that

$$\sigma_{pq} = \frac{4\pi r_r^2 |E^s_{pq}|^2}{k^2\eta^2} \tag{68}$$

Normalized versions of (68) are

$$\frac{\sigma_{pq}}{\pi a^2} = \frac{4r_r^2 |E^s_{pq}|^2}{k^2 a^2 \eta^2} \tag{69}$$

$$\frac{\sigma_{pq}}{\lambda^2} = \frac{r_r^2 |E^s_{pq}|^2}{\pi\eta^2} \tag{70}$$

where a is some characteristic length associated with the scatterer and λ is the wavelength in the external medium.

V. EXAMPLES

A computer program has been written to calculate the equivalent currents and scattering patterns for a dielectric body of revolution excited by an axially incident plane wave. This program is described and listed in Part Two. Some computational results obtained with this program are given in this section.

Figures 8 and 9 show the magnitude and phase of the normalized equivalent currents $\frac{J_\theta}{H_y}$, $\frac{J_\phi}{H_y}$, $\frac{M_\theta}{E_x}$, and $\frac{M_\phi}{E_x}$ on the surface of a dielectric sphere for which $ka = 3$ and $\varepsilon_r = 4$. Here, k is the propagation constant in free space, a is the radius of the sphere and ε_r is the relative dielectric constant of the sphere. Figure 8 represents our solution of the PMCHW formulation. Figure 9 depicts our solution of the Müller formulation.

In Figs. 8 and 9, the incident field is a plane wave traveling in the positive z direction. THETA = 0° is the forward scattering direction and THETA = 180° is the backscattering direction. The incident field is given by (50) and (51) with $\theta_t = 180°$. The origin $\underset{\sim}{r} = 0$ is at the center of the sphere. In Figs. 8 and 9, J_θ is the $\underset{\sim}{u}_\theta = -\underset{\sim}{u}_t$ component of electric current (58) versus θ in the $\phi = 0$ plane, J_ϕ is the $\underset{\sim}{u}_\phi$ component of (58) versus θ in the $\phi = 90°$ plane, M_θ is the $\underset{\sim}{u}_\theta = -\underset{\sim}{u}_t$ component of magnetic current (59) versus θ in the $\phi = 90°$ plane, and M_ϕ is the $\underset{\sim}{u}_\phi$ component of (59) versus θ in the $\phi = 0°$ plane. For axial incidence, only the n=1 term is present in (58) and (59). The symbols × and + denote respectively magnitude and phase of the method of moments solution for the pertinent component of the electric or magnetic current. The solid curves are the exact equivalent currents obtained from the Mie series solution [11]. The normalizing constants E_x and H_y are defined in terms of the incident field (50) and (51) by

$$E_x = \underset{\sim}{u}_x \cdot \underset{\sim}{E}^i\Big|_{r=0} = -k\eta$$
$$H_y = \underset{\sim}{u}_y \cdot \underset{\sim}{H}^i\Big|_{r=0} = -k \qquad (71)$$

---

[11] R. F. Harrington, Time-Harmonic Electromagnetic Fields, McGraw-Hill Book Co., 1961. Section 6-9.

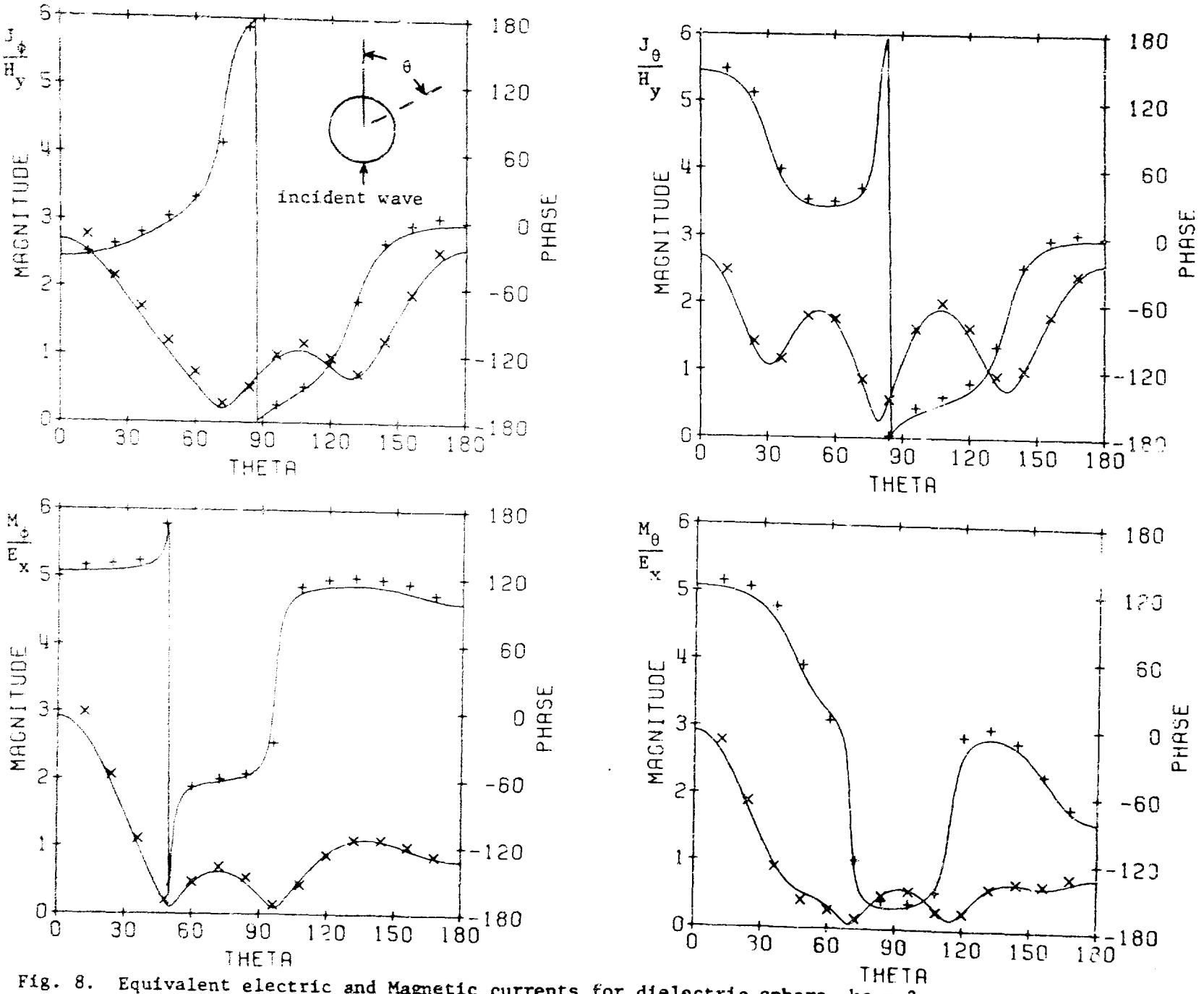

Fig. 8. Equivalent electric and Magnetic currents for dielectric sphere, ka = 3, ε_r = 4, PMCHW solution. Symbols × and + denote magnitude and phase respectively. Solid line denotes exact solution.

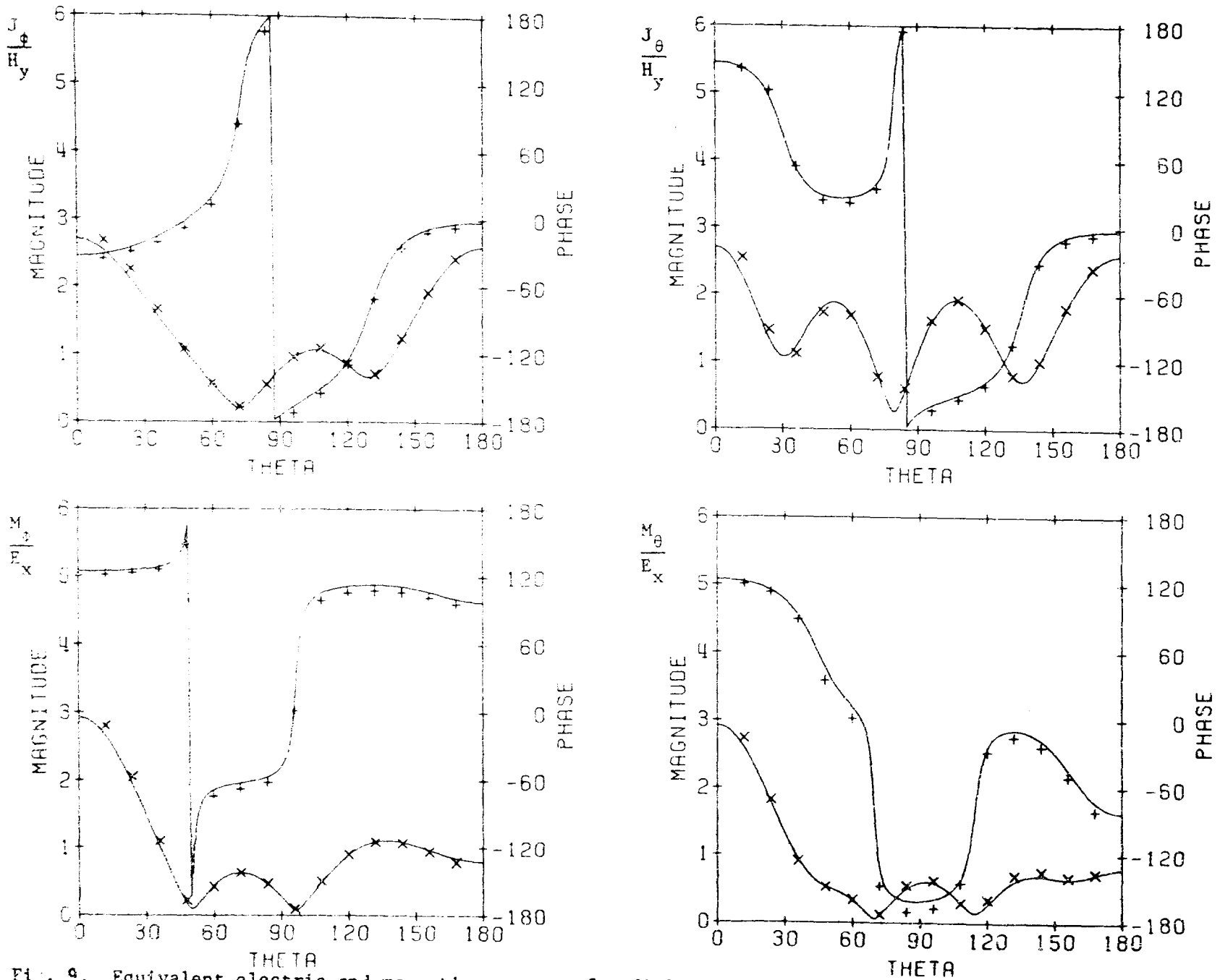

Fig. 9. Equivalent electric and magnetic currents for dielectric sphere, ka = 3, ϵ_r = 4, Müller solution. Symbols × and + denote magnitude and phase respectively. Solid line denotes exact solution.

where k and η are respectively the propagation constant of free space and the impedance of free space.

The currents of Figs. 8 and 9 were obtained by using a 20 point Gaussian quadrature formula for all integrations in ϕ. All integrations over the functions $\{f_j(t)\}$ in $t = a(\pi-\theta)$ were done by sampling each $f_j(t)$ four times. The $\{f_j(t)\}$ consisted of 14 overlapping triangle (divided by the cylindrical coordinate radius) functions equally spaced in θ. More precisely,

$$\begin{aligned} NP &= 31 \\ NPHI &= 20 \\ MT &= 2 \end{aligned} \tag{72}$$

where the above variables are input data for the computer program described and listed in Part Two, Section V.

Figures 10 and 11 show the scattering patterns radiated by the currents of Figs. 8 and 9 respectively. The symbols * and + denote $\frac{\sigma_{\theta\theta}}{\pi a^2}$ and $\frac{\sigma_{\phi\theta}}{\pi a^2}$ respectively. The solid curves are the exact patterns obtained from the Mie series solution [11]. The patterns $\sigma_{\theta\theta}$ and $\sigma_{\phi\theta}$ are given by (69), (62) and (63). Here $\sigma_{\theta\theta}$ is the θ polarized pattern versus θ_r in the $\phi = 0$ plane and $\sigma_{\phi\theta}$ is the ϕ polarized pattern versus θ_r in the $\phi = 90°$ plane. The THETA in Figs. 10 and 11 refers to θ_r. For axial incidence, only the n=1 terms are present in (62) and (63). Elsewhere [3, 12], the pattern $\sigma_{\theta\theta}$ is called the horizontal polarization because it is polarized parallel to the scattering plane. Similarly, the pattern $\sigma_{\phi\theta}$ is called the vertical polarization because it is polarized perpendicular to the scattering plane.

Figures 12-17 show the scattering patterns for three other dielectric spheres. Figures 12 and 13 are for relative dielectric constant $\epsilon_r = 1.1$, Figs. 14 and 15 for $\epsilon_r = 10.$, and Figs. 16 and 17 for $\epsilon_r = 20$. All other

---

[12] P. Barber and C. Yeh, "Scattering of Electromagnetic Waves by Arbitrarily Shaped Dielectric Bodies," Applied Optics, vol. 14, No. 12, December 1975, pp. 2864-2872.

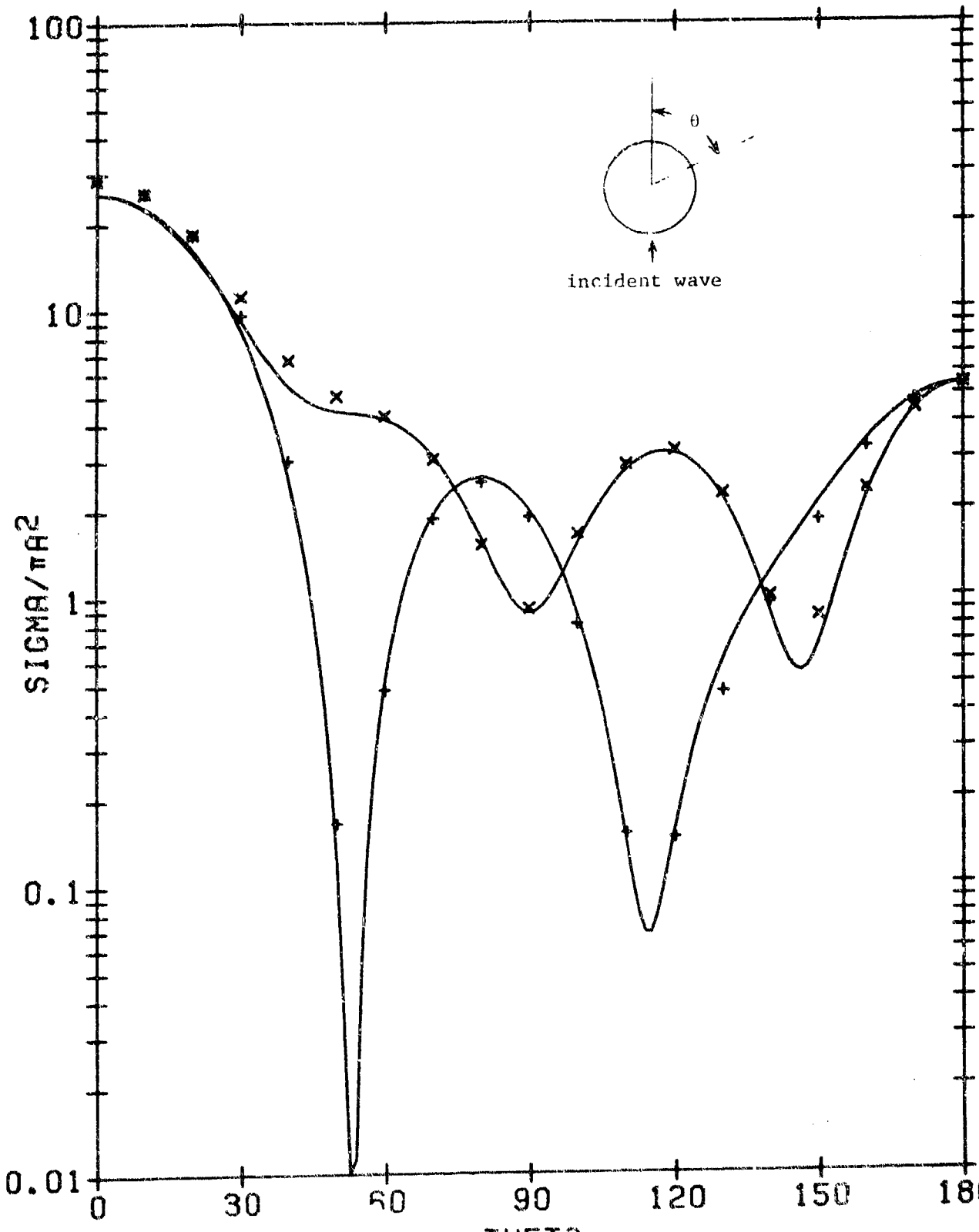

Fig. 10. Plane wave scattering patterns for dielectric sphere, ka = 3, ϵ_r = 4, PMCHW solution. Symbols × and + denote horizontal polarization and vertical polarization respectively. Solid line denotes exact solution.

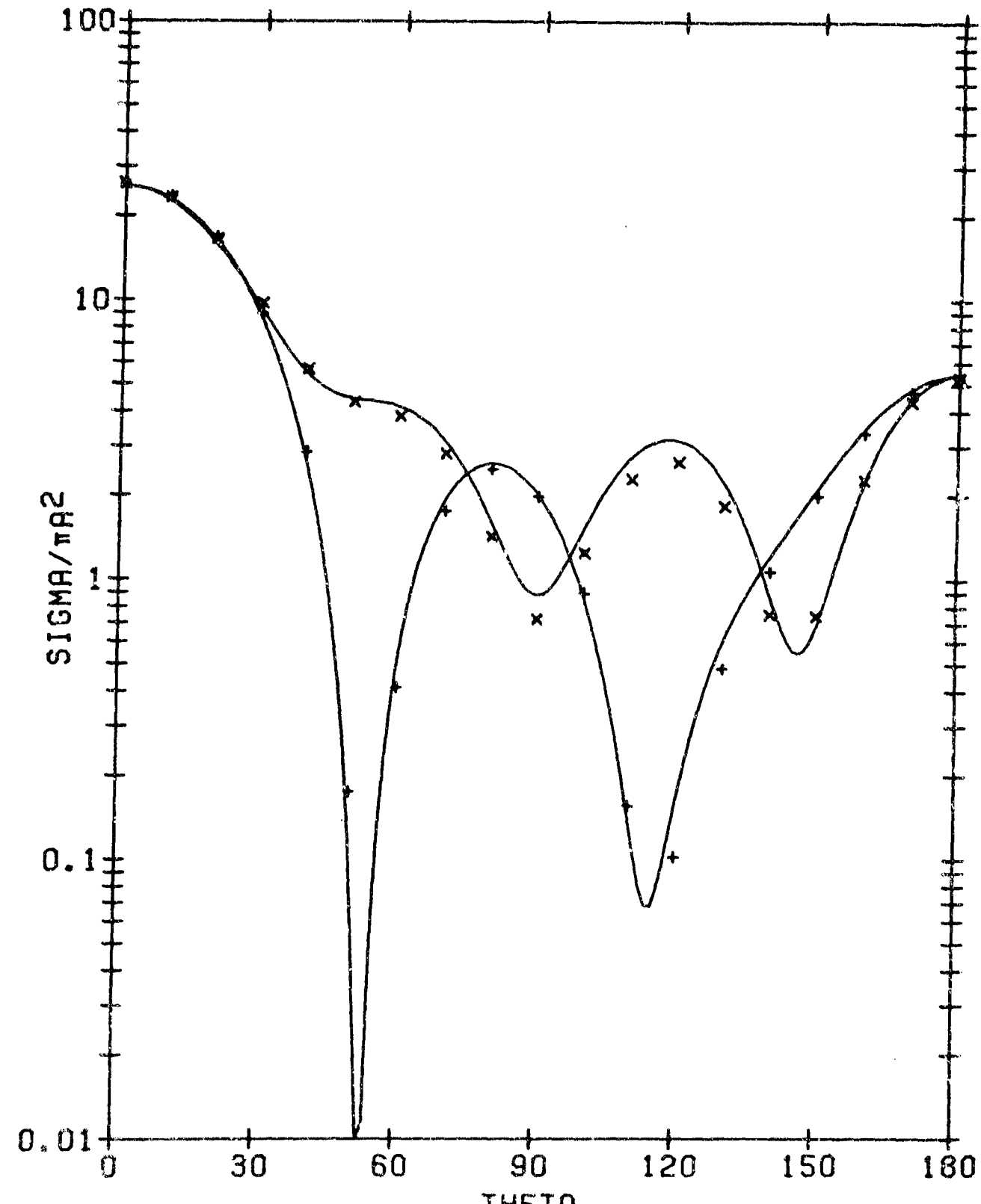

Fig. 11. Plane wave scattering patterns for dielectric sphere, ka = 3, ϵ_r = 4, Müller solution. Symbols × and + denote horizontal polarization and vertical polarization respectively. Solid line denotes exact solution.

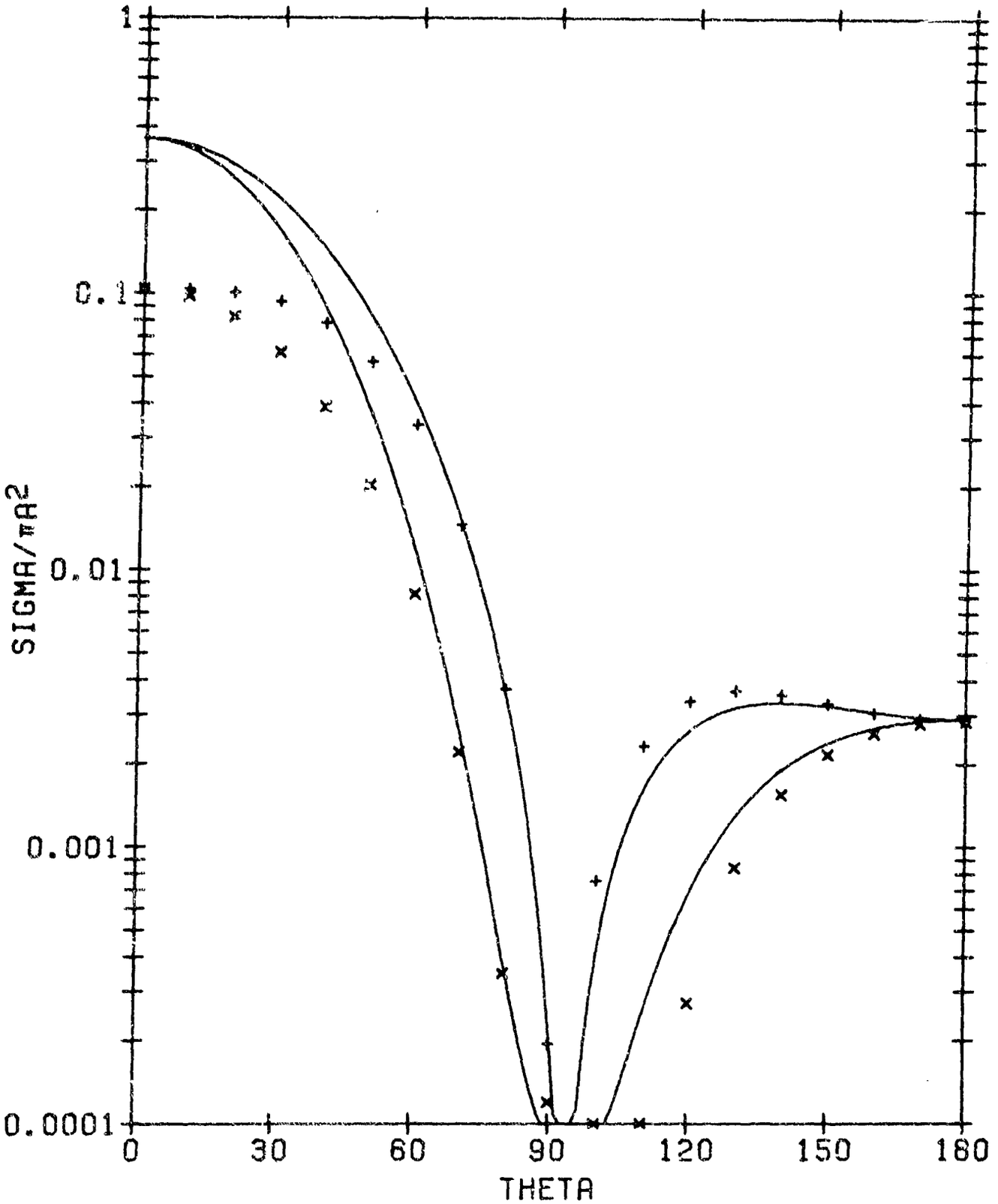

Fig. 12. Plane wave scattering patterns for dielectric sphere, ka = 3, ϵ_r = 1.1, PMCHW solution. Symbols × and + denote horizontal polarization and vertical polarization respectively. Solid line denotes exact solution.

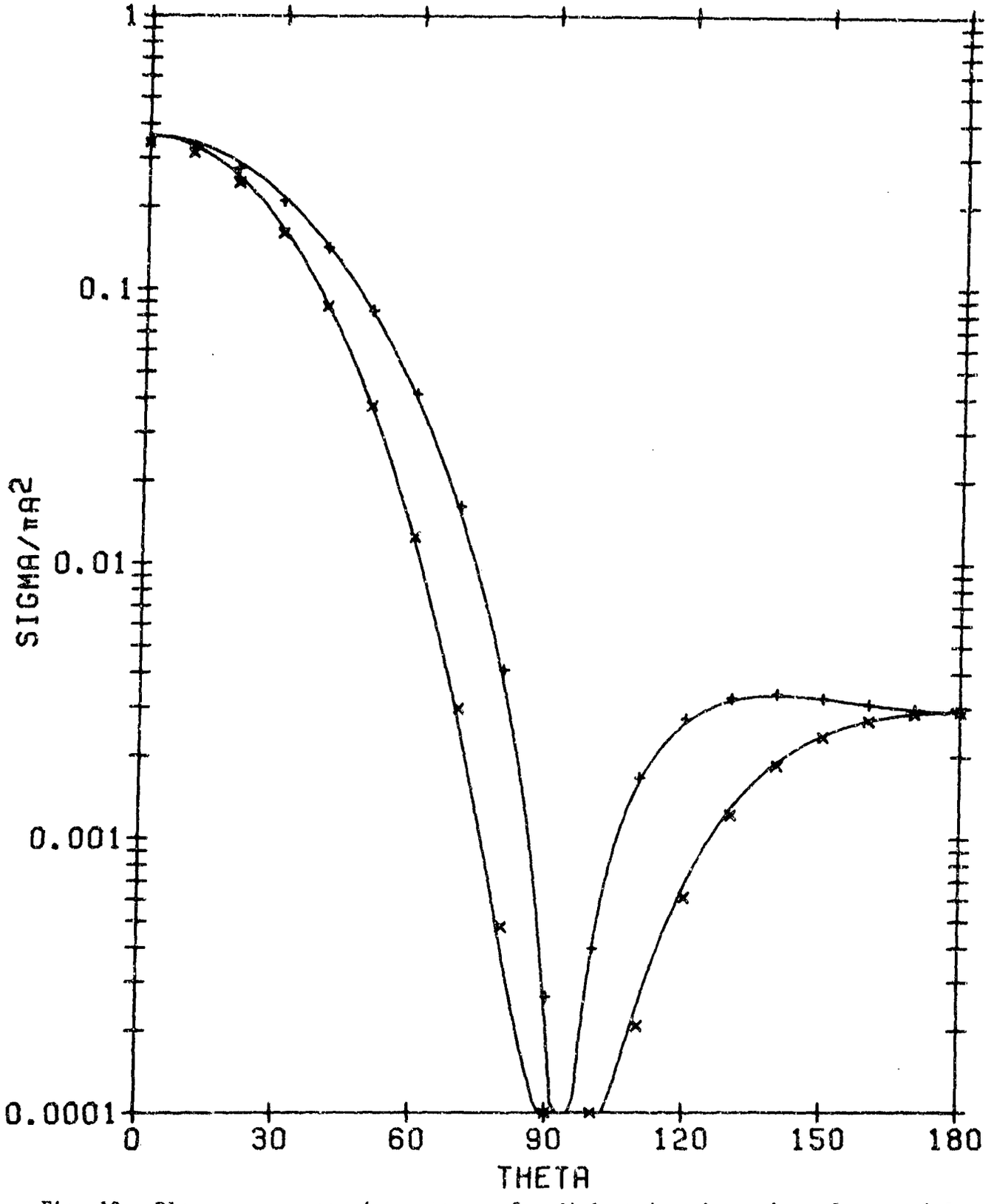

Fig. 13. Plane wave scattering patterns for dielectric sphere, ka = 3, ϵ_r = 1.1, Müller solution. Symbols × and + denote horizontal polarization and vertical polarization respectively. Solid line denotes exact solution.

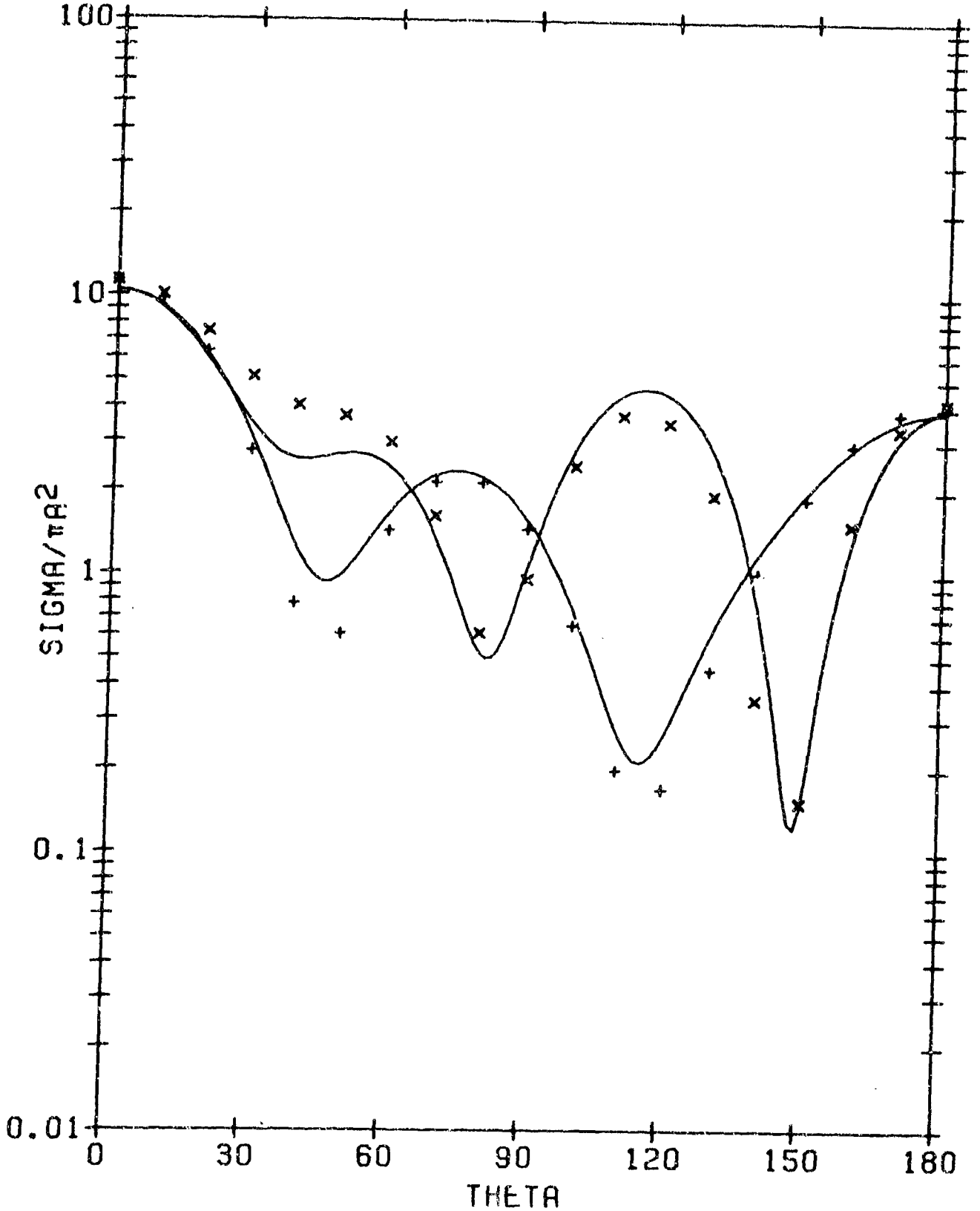

Fig. 14. Plane wave scattering patterns for dielectric sphere, ka = 3, ϵ_r = 10, PMCHW solution. Symbols × and + denote horizontal polarization and vertical polarization respectively. Solid line denotes exact solution.

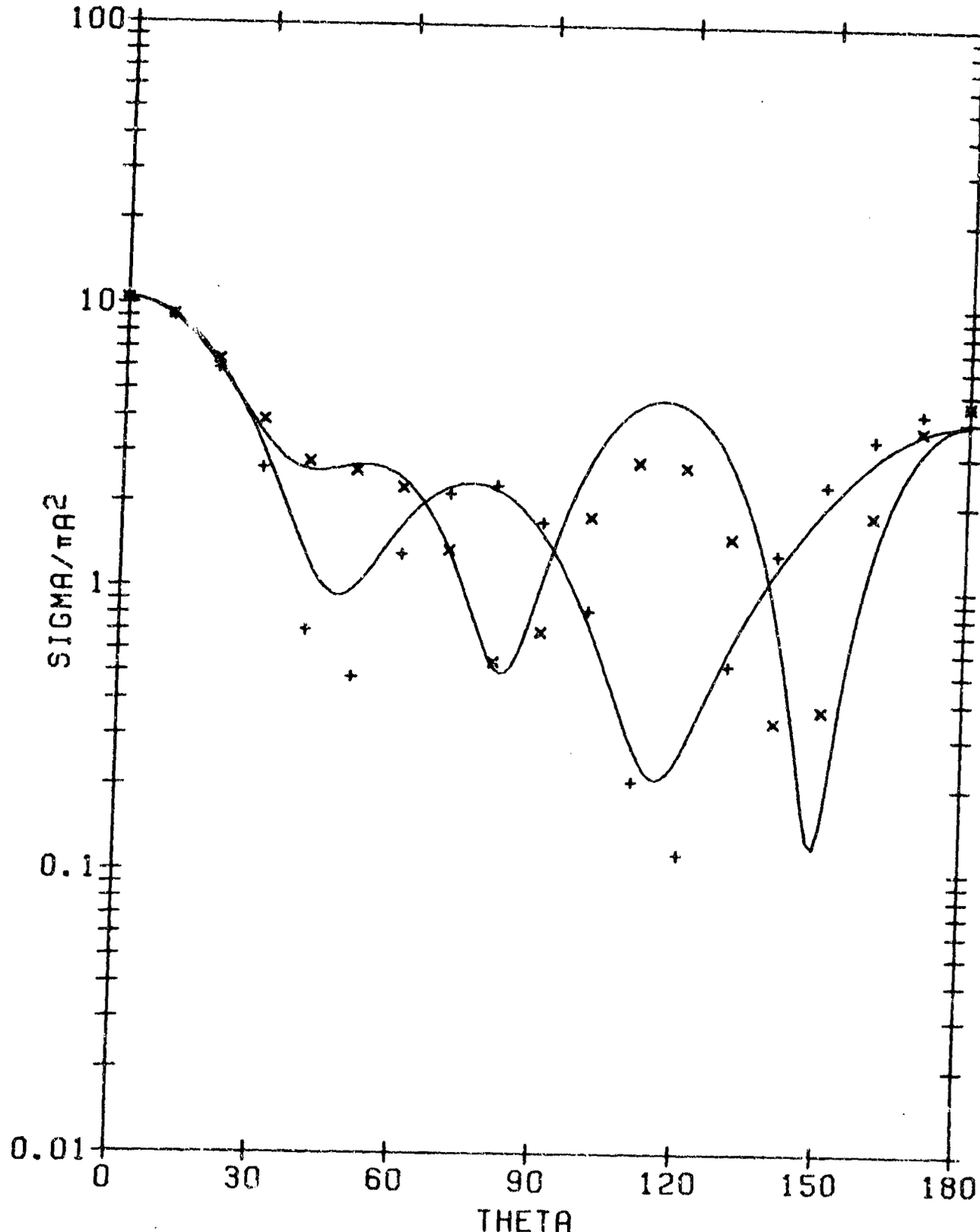

Fig. 15. Plane wave scattering patterns for dielectric sphere, ka = 3, ε_r = 10, Müller solution. Symbols × and + denote horizontal polarization and vertical polarization respectively. Solid line denotes exact solution.

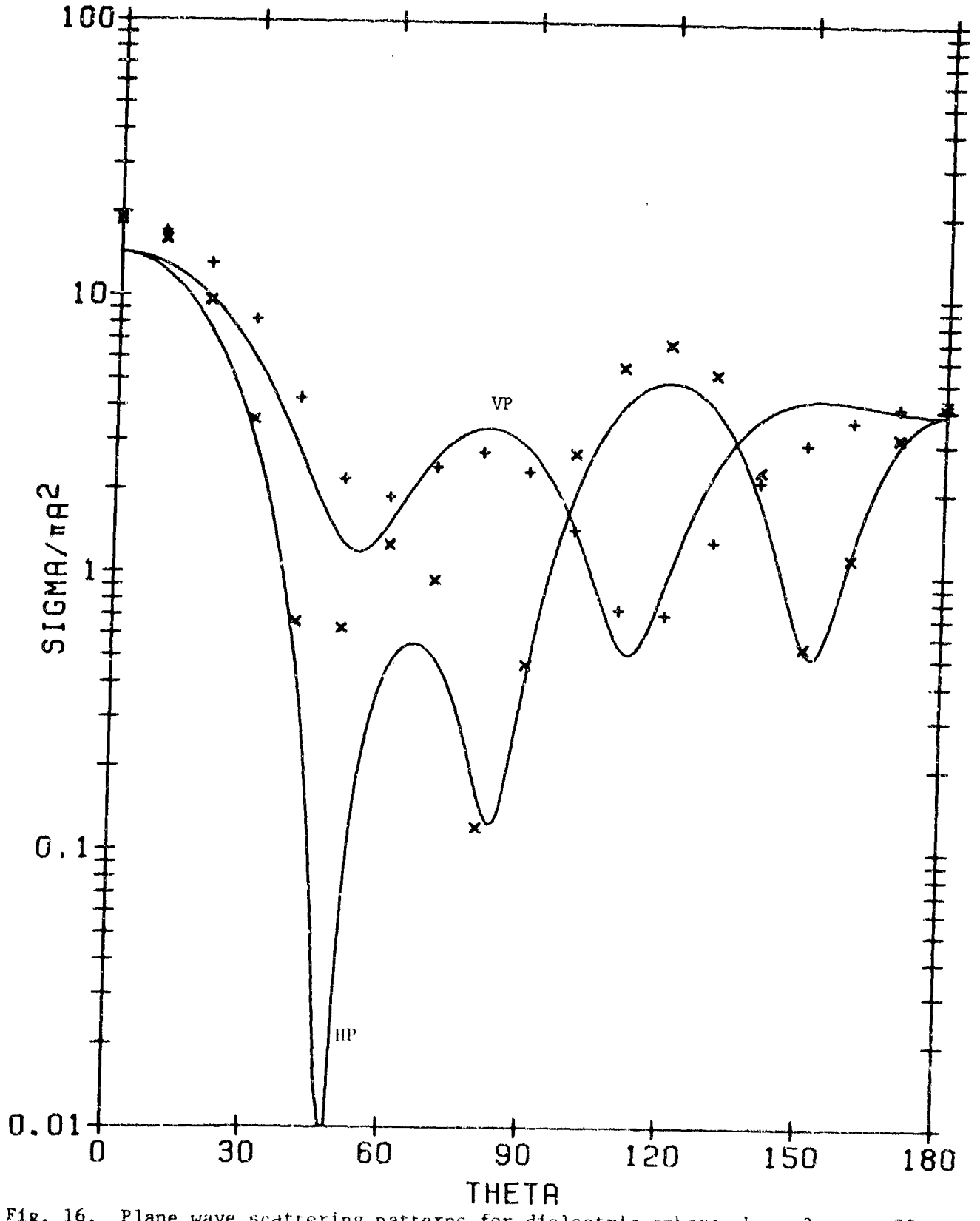

Fig. 16. Plane wave scattering patterns for dielectric sphere, ka = 3, ϵ_r = 20, PMCHW solution. Symbols × and + denote horizontal polarization and vertical polarization respectively. Solid line denotes exact solution.

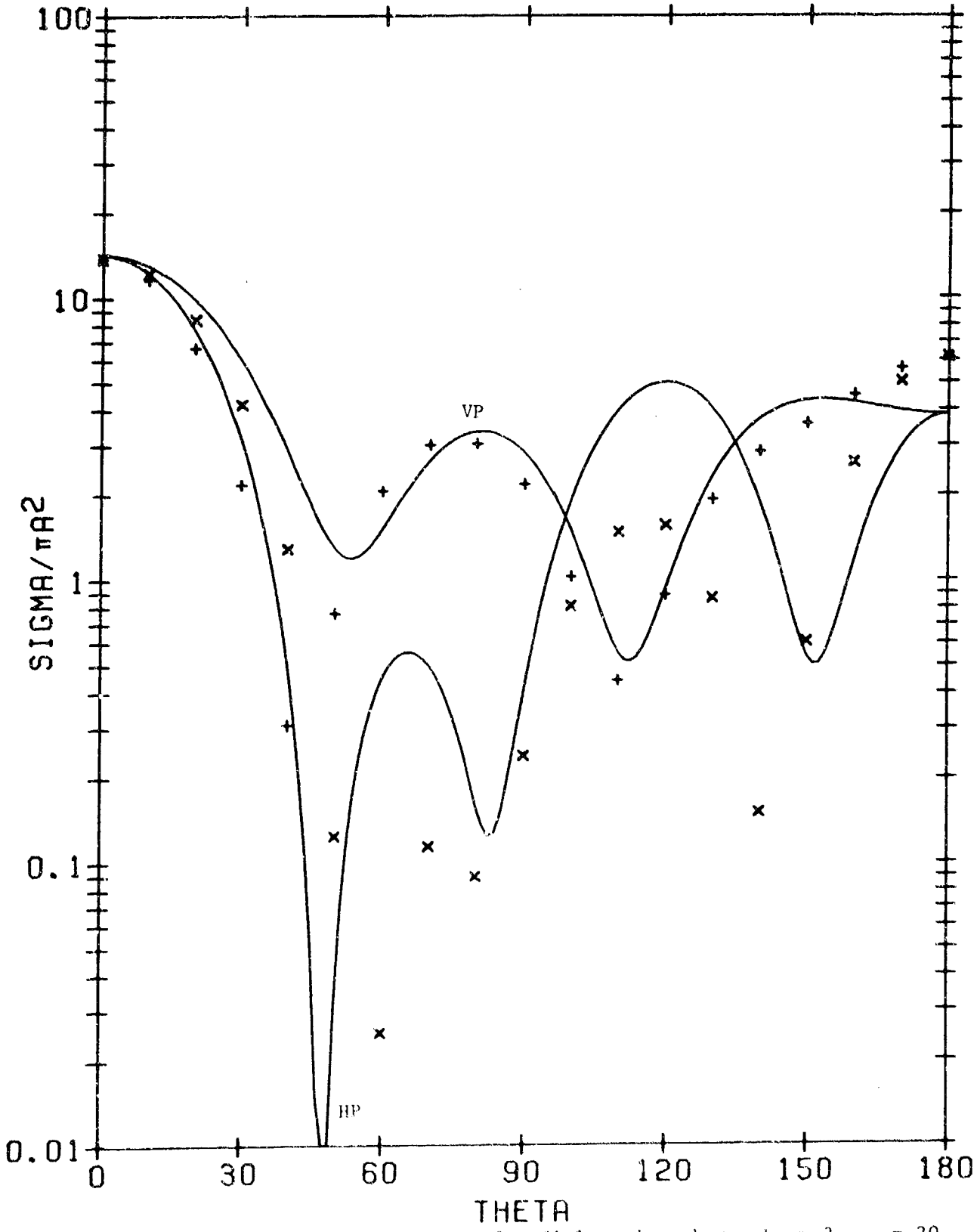

Fig. 17. Plane wave scattering patterns for dielectric sphere, ka = 3, ϵ_r = 20, Müller solution. Symbols · and + denote horizontal polarization and vertical polarization respectively. Solid line denotes exact solution.

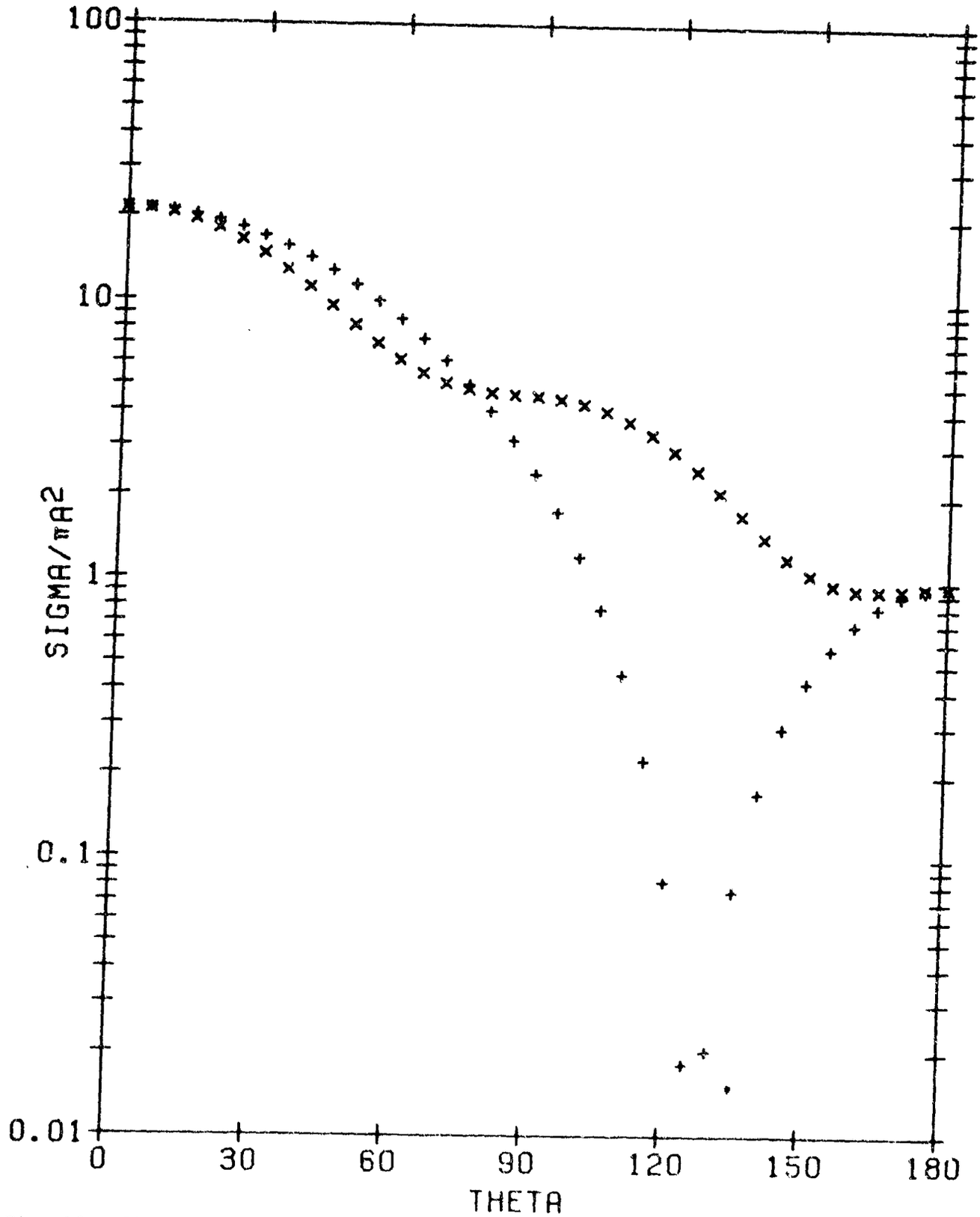

Fig. 18. Plane wave scattering patterns for finite dielectric cylinder of radius a and height 2a. a = 0.25 free space wavelengths, ϵ_r = 4, PMCHW solution. Symbols × and + denote horizontal polarization and vertical polarization respectively.

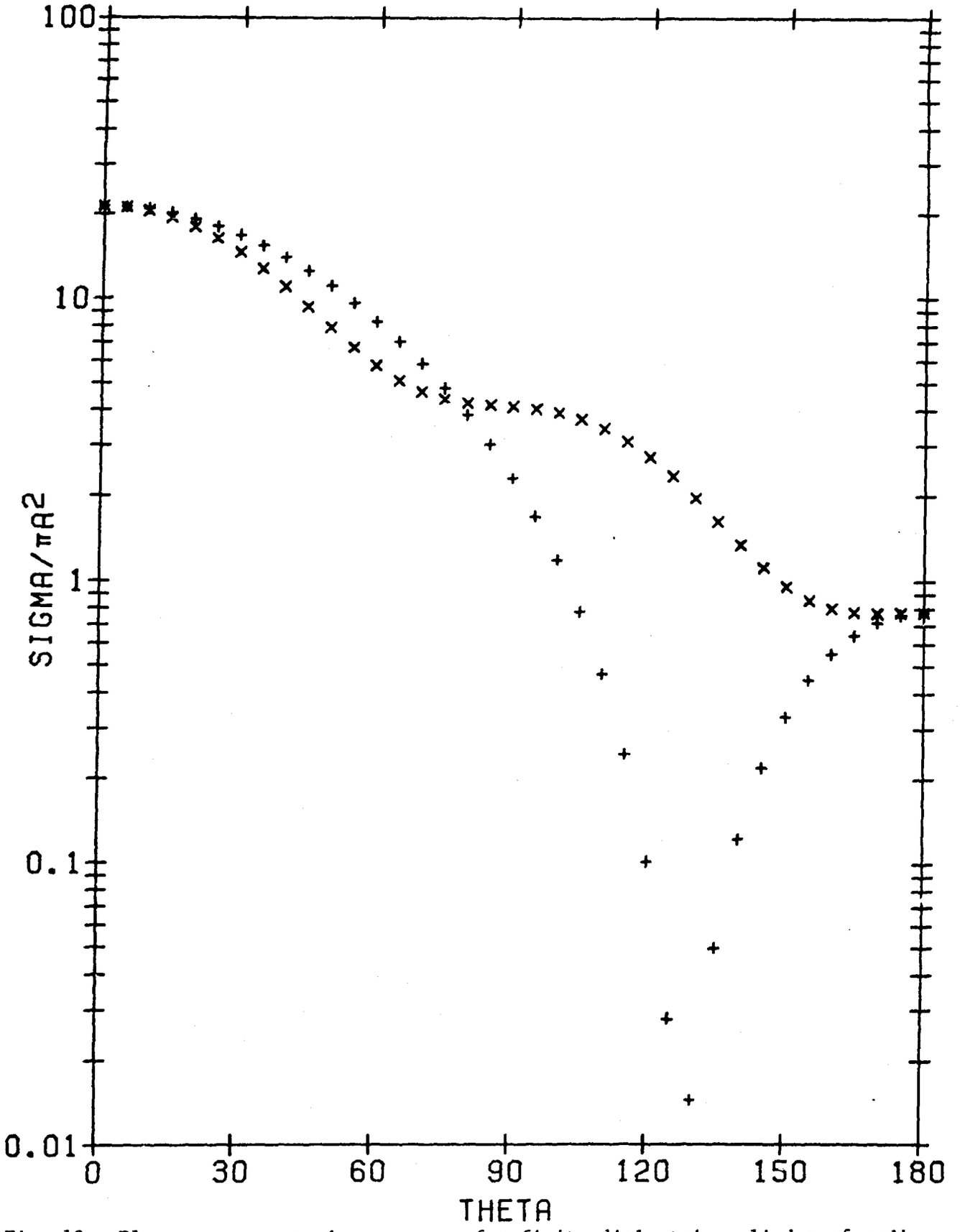

Fig. 19. Plane wave scattering patterns for finite dielectric cylinder of radius a and height 2a. a = 0.25 free space wavelengths, ε_r = 4, Müller solution. Symbols × and + denote horizontal polarization and vertical polarization respectively.

parameters in Figs. 12-17 are the same as in Figs. 10 and 11. In Figs. 12 and 13, values less than 0.0001 are plotted at 0.0001.

Figures 18 and 19 show the computed scattering patterns of a finite dielectric cylinder of radius a and height 2a when a is 0.25 free space wavelengths. The relative dielectric constant of the cylinder is $\varepsilon_r = 4$. The incident field is a plane wave traveling in the positive z direction, the same field which was incident upon the previous dielectric spheres. Figure 18 shows $\frac{\sigma_{\theta\theta}}{\pi a^2}$ and $\frac{\sigma_{\phi\theta}}{\pi a^2}$ as obtained from our solution of the PMCHW formulation. Figure 19 shows $\frac{\sigma_{\theta\theta}}{\pi a^2}$ and $\frac{\sigma_{\phi\theta}}{\pi a^2}$ as obtained from our solution of the Müller formulation. The patterns $\frac{\sigma_{\theta\theta}}{\pi a^2}$ and $\frac{\sigma_{\phi\theta}}{\pi a^2}$ are plotted with the symbols × and + respectively.

The equivalent currents which radiate the patterns of Figs. 18 and 19 were obtained by using a 48 point Gaussian quadrature formula for all integrations in ϕ. All integrations in t over the functions $\{f_j(t)\}$ were done by sampling each $f_j(t)$ four times. The $\{f_j(t)\}$ consisted of 11 overlapping triangle (divided by the cylindrical coordinate radius) functions equally spaced in t. More precisely,

$$\begin{aligned} NP &= 25 \\ NPHI &= 48 \\ MT &= 2 \end{aligned} \tag{73}$$

where the above variables are input data for the computer program described and listed in Part Two, Section V.

VI. DISCUSSION

According to Figs. 12 and 13, the scattering patterns obtained from our solution of the Müller formulation are more accurate than those obtained from our solution of the PMCHW formulation for the dielectric sphere with ka = 3 and $\varepsilon_r = 1.1$. From plots not included in this report, we observed that both our PMCHW solution and our Müller solution for the equivalent

Y 0

currents on the dielectric sphere were reasonably accurate. However, the following argument shows that when ε_r is near one, a slight inaccuracy in the equivalent currents could affect the scattering patterns drastically. As ε_r approaches one, the equivalent electric and magnetic currents approach $\underset{\sim}{n} \times \underset{\sim}{H}^i$ and $\underset{\sim}{E}^i \times \underset{\sim}{n}$ respectively whereas the scatterning patterns approach zero. This means that the equivalent electric and magnetic currents produce fields which nearly cancel each other. Hence, a slight inaccuracy in the equivalent currents could cause a large percentage inaccuracy in the scattering patterns.

We believe that our Müller solution is more accurate than our PMCHW solution whenever ε_r is close to one. When α and β are given by (22) and (23) as in the Müller formulation, the left-hand sides of (9) and (10) approach $-\underset{\sim}{M}$ and $\underset{\sim}{J}$ respectively as ε_r approaches one. In this case, the expected solution

$$\underset{\sim}{J} = \underset{\sim}{n} \times \underset{\sim}{H}^i$$

$$\underset{\sim}{M} = \underset{\sim}{E}^i \times \underset{\sim}{n}$$

can be obtained by inspection of (9) and (10). However, if $\alpha = \beta = 1$ as in the PMCHW formulation, the solution to (9) and (10) is not obvious when $\varepsilon_r = 1$ because the field operators on the left-hand sides of (9) and (10) are not diagonal. With our Müller solution, the matrix on the left-hand side of (39) would become tridiagonal for $\varepsilon_r = 1$ if its first two rows of submatrices were interchanged. With our PMCHW solution, no such simplification of this matrix is possible for $\varepsilon_r = 1$.

We recommend at least 10 expansion functions per wavelength per component along the generating curve of the dielectric body of revolution. For example, if the generating curve were one wavelength long, the order of the square matrix on the left-hand side of (39) should be at least 36. The number 36 is arrived at as follows. There should be at least 9 expansion functions per component of current. We say 9 expansion functions rather than 10 because we are using overlapping triangle functions with no peak of triangle function at either ends of the generating curve. There are two components of electric current and two components of magnetic current.

According to equations (20)-(23) of [9] and (58)-(61) of [9], each element of the square matrix in (39) is a triple integral consisting of one integration with respect to ϕ and two integrations with respect to t. The ϕ integral is evaluated by using a Gaussian quadrature formula. Each t integration is done by crude sampling akin to the trapezoid rule. In any case, there should be at least 10 sample points per wavelength in the media in question. For instance, if ρ_{max} is the largest cylindrical coordinate radius of the dielectric body of revolution and t_{max} is the length of the generating curve, then

$$\begin{aligned} NP &\geq \frac{10t_{max}}{\lambda} + 1 \\ NPHI &\geq \frac{10\pi\rho_{max}}{\lambda} \end{aligned} \tag{74}$$

where NP and NPHI are input arguments of the subroutine YZ described and listed in Part Two, Section II and λ is the wavelength in the media in question. If f = e in (40)-(41) then λ is the wavelength in the external media, but if f = d in (40)-(41) then λ is the wavelength inside the diffracting body of revolution. The main program in Part Two, Section V is oversimplified in that it uses the same values of NP and NPHI for both f = e and f = d.

Loss of accuracy in the computed patterns of Figs. 16 and 17 may be due to the fact that (74) was violated. According to (74), the values of NP and NPHI for f = d should be nearly 70 or greater instead of the low values appearing in (72). Unfortunately, increasing the values of the variables NP and NPHI increases the computer time required to solve the problem.

We have been trying to obtain accurate numerical results for the dielectric sphere for which a = 0.2 free space wavelengths and $\varepsilon_r = 80.$ from our general dielectric body of revolution program. We have not been able to obtain clear-cut convergence with respect to the variables on the left-hand sides of (72) because we could not afford to increase them as much as desired. Our PMCHW solution and our Müller solution for the equivalent currents and scattering patterns differ from each other and from the exact solution.

For the sphere, each element of the square matrix on the left-hand side of (39) can be written as a sum over the infinite set of spherical modes. So far, we have not been able to successfully implement this alternate evaluation of the matrix elements in terms of spherical modes. The major difficulty seems to be lack of agreement of a few matrix elements for which both expansion and testing functions are near one of the poles of the sphere.

Both the PMCHW solution and the Müller solution are obtained by taking a linear combination of (5) and (7) and a linear combination of (6) and (8). There are two other possibilities which are

(1) A linear combination of (5) and (6) and a linear combination of (7) and (8).

(2) A linear combination of (5) and (8) and a linear combination of (6) and (7).

These other two possibilities give rise to alternative numerical solutions which may compare favorably with the PMCHW solution and the Müller solution.

APPENDIX A

THE EQUIVALENCE PRINCIPLE

Let $\underset{\sim}{E}_e$, $\underset{\sim}{H}_e$ be an electromagnetic field defined outside a closed surface S. The permeability, permittivity, and electric and magnetic source currents outside S are μ_e, ϵ_e, $\underset{\sim}{J}_e$, and $\underset{\sim}{M}_e$ respectively. This outside situation where the subscript e stands for "exterior medium" is shown in Fig. A-1. In Fig. A-1, the media and sources inside S are undisclosed. Let $\underset{\sim}{E}_d$, $\underset{\sim}{H}_d$ be an electromagnetic field defined inside S where the permeability, permittivity, and electric and magnetic sources are μ_d, ϵ_d, $\underset{\sim}{J}_d$, and $\underset{\sim}{M}_d$ respectively. This inside situation where the subscript d stands for "diffracting medium" is shown in Fig. A-2. In Fig. A-2, the media and sources outside S are undisclosed. The equivalence principle states that the solution to the composite radiation problem consisting of medium μ_e, ϵ_e and sources $\underset{\sim}{J}_e$, $\underset{\sim}{M}_e$ outside S, medium μ_d, ϵ_d and sources $\underset{\sim}{J}_d$, $\underset{\sim}{M}_d$ inside S, and electric and magnetic surface currents $\underset{\sim}{J}$, $\underset{\sim}{M}$ on S given by

$$\underset{\sim}{J} = \underset{\sim}{n} \times (\underset{\sim}{H}_e - \underset{\sim}{H}_d) \tag{A-1}$$

$$\underset{\sim}{M} = (\underset{\sim}{E}_e - \underset{\sim}{E}_d) \times \underset{\sim}{n} \tag{A-2}$$

where $\underset{\sim}{n}$ is the exterior unit normal vector on S is the composite electromagnetic field $\underset{\sim}{E}$, $\underset{\sim}{H}$ defined by

$$\underset{\sim}{E}, \underset{\sim}{H} = \underset{\sim}{E}_e, \underset{\sim}{H}_e \quad \text{outside S} \tag{A-3}$$

$$\underset{\sim}{E}, \underset{\sim}{H} = \underset{\sim}{E}_d, \underset{\sim}{H}_d \quad \text{inside S} \tag{A-4}$$

The composite radiation problem is shown in Fig. A-3 which is entitled composite situation.

The equivalence principle is proved by showing that the configuration of media and sources in Fig. A-3 gives rise to the composite field $\underset{\sim}{E}$, $\underset{\sim}{H}$ defined by (A-3) and (A-4). Now, $\underset{\sim}{E}$, $\underset{\sim}{H}$ will be the field generated by the media and sources of Fig. A-3 if $\underset{\sim}{E}$, $\underset{\sim}{H}$ satisfies Maxwell's equations with source terms included and the radiation condition at infinity. $\underset{\sim}{E}$, $\underset{\sim}{H}$ satisfies Maxwell's equations outside S and inside S because $\underset{\sim}{E}_e$, $\underset{\sim}{H}_e$ and

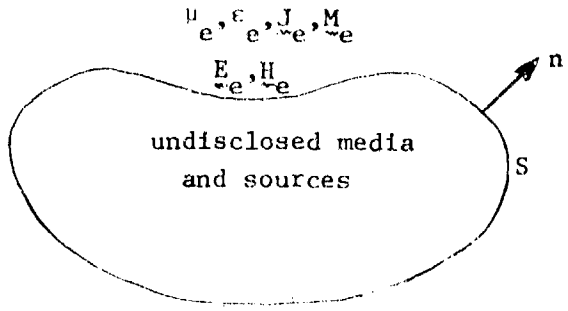

Fig. A-1. Outside Situation.

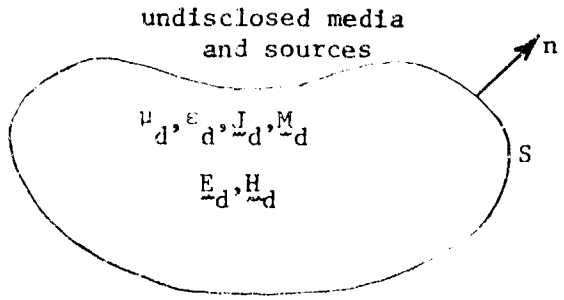

Fig. A-2. Inside Situation.

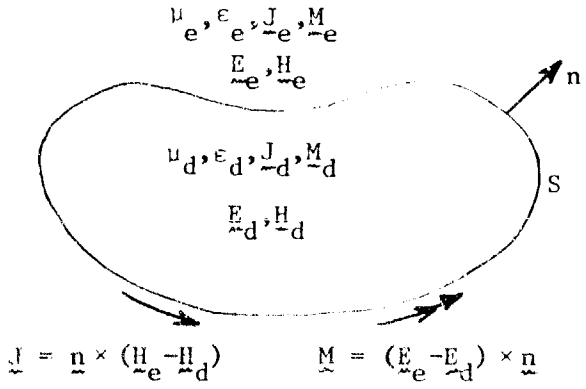

Fig. A-3. Composite Situation.

$\underset{\sim}{E}_d$, $\underset{\sim}{H}_d$ satisfy Maxwell's equations outside S and inside S respectively. $\underset{\sim}{E}$, $\underset{\sim}{H}$ also satisfies the radiation condition at infinity because $\underset{\sim}{E}_e$, $\underset{\sim}{H}_e$ satisfies the radiation condition at infinity. It remains to be shown that Maxwell's equations for $\underset{\sim}{E}$, $\underset{\sim}{H}$ exhibit the surface current sources $\underset{\sim}{J}$ and $\underset{\sim}{M}$ given by (A-1) and (A-2).

It is well known that a surface current source on S gives rise to a discontinuity across S of the tangential component of the field. The preceding statement is easily verified by means of an argument based on the integral forms of Maxwell's equations. Now, this same argument can be construed to imply that a discontinuity across S of the tangential component of the field gives rise to a surface current source on S. Hence Maxwell's equations for $\underset{\sim}{E}$, $\underset{\sim}{H}$ exhibit the electric and magnetic surface current sources $\underset{\sim}{J}$ and $\underset{\sim}{M}$ on S given by (A-1) and (A-2). Therefore, $\underset{\sim}{E}$, $\underset{\sim}{H}$ is the solution to the composite radiation problem shown in Fig. A-3 because $\underset{\sim}{E}$, $\underset{\sim}{H}$ satisfies Maxwell's equations with sources and the radiation condition at infinity.

APPENDIX B

PROOF THAT THE SOLUTION TO EQUATIONS (5)-(8) IS UNIQUE

The solution $\underset{\sim}{J}$, $\underset{\sim}{M}$ to (5)-(8) will be unique if the associated set of homogeneous equations

$$-\underset{\sim}{n} \times \underset{\sim}{E}_e^- = 0 \tag{B-1}$$

$$-\underset{\sim}{n} \times \underset{\sim}{H}_e^- = 0 \tag{B-2}$$

$$-\underset{\sim}{n} \times \underset{\sim}{E}_d^+ = 0 \tag{B-3}$$

$$-\underset{\sim}{n} \times \underset{\sim}{H}_d^+ = 0 \tag{B-4}$$

has only the trivial solution $\underset{\sim}{J} = \underset{\sim}{M} = 0$.

From (B-1) and (B-2), $\underset{\sim}{J}$, $\underset{\sim}{M}$ radiate in μ_e, ϵ_e to produce a field whose tangential components are zero just inside S. Hence, according to the relation between $\underset{\sim}{J}$, $\underset{\sim}{M}$ and the discontinuity of tangential field across S as exemplified by (A-1) and (A-2), the field $\underset{\sim}{E}_e$, $\underset{\sim}{H}_e$ radiated by $\underset{\sim}{J}$, $\underset{\sim}{M}$ in μ_e, ϵ_e outside S satisfies

$$\underset{\sim}{n} \times \underset{\sim}{H}_e = \underset{\sim}{J} \tag{B-5}$$

$$\underset{\sim}{E}_e \times \underset{\sim}{n} = \underset{\sim}{M} \tag{B-6}$$

just outside S. See Fig. B-1.

From (B-3) and (B-4) the electric and magnetic currents $-\underset{\sim}{J}$, $-\underset{\sim}{M}$ radiate in μ_d, ϵ_d to produce a field whose tangential components are zero just outside S. Hence, according to the relation between $-\underset{\sim}{J}$, $-\underset{\sim}{M}$ and the discontinuity of tangential field across S, the field $-\underset{\sim}{E}_d$, $-\underset{\sim}{H}_d$ radiated by $-\underset{\sim}{J}$, $-\underset{\sim}{M}$ in μ_d, ϵ_d satisfies

$$\underset{\sim}{n} \times (-\underset{\sim}{H}_d) = \underset{\sim}{J} \tag{B-7}$$

$$(-\underset{\sim}{E}_d) \times \underset{\sim}{n} = \underset{\sim}{M} \tag{B-8}$$

just inside S. See Fig. B-2.

The equivalence principle is used to combine the outside situation in Fig. B-1 with the inside situation in Fig. B-2 to obtain the composite situation shown in Fig. B-3. Because of (B-5)-(B-8), the composite

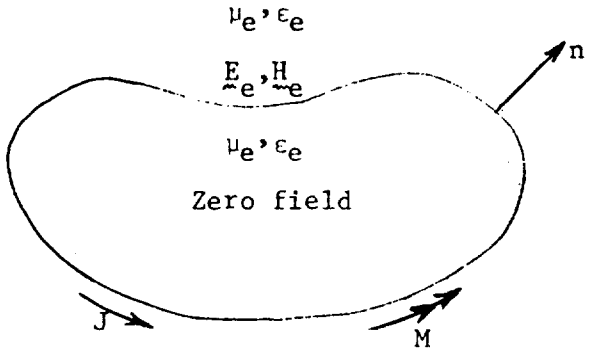

Fig. B-1. Radiation of $\underset{\sim}{J}, \underset{\sim}{M}$ according to (B-1) and (B-2).

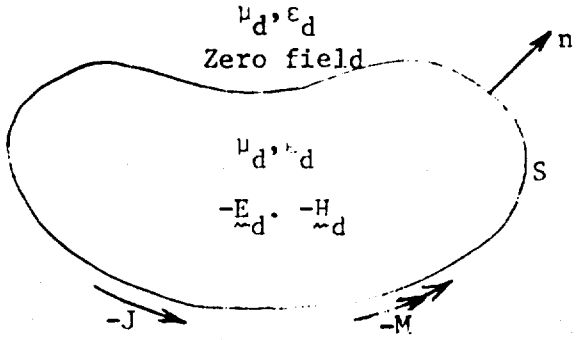

Fig. B-2. Radiation of $-\underset{\sim}{J}$, $-\underset{\sim}{M}$ according to (B-3) and (B-4).

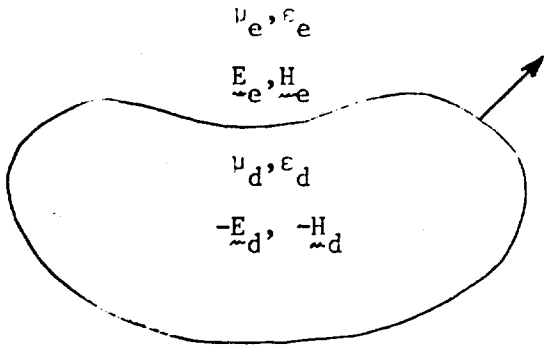

Fig. B-3. Composite Situation.

situation in Fig. B-3 is source-free. Therefore, the field in Fig. B-3 is zero everywhere. Hence, the fields in Figs. B-1 and B-2 are zero everywhere which implies that $\underset{\sim}{J} = \underset{\sim}{M} = 0$.

Thus, the solution to (5)-(8) is unique because the associated set (B-1)-(B-4) of homogeneous equations has only the trivial solution.

APPENDIX C

MORE EXAMPLES

The equivalent currents and scattering patterns for the dielectric spheres for which $\epsilon_r = 4$ and ka = 4, 5, and 6 are plotted in Appendix C. Figures C-1 to C-4 are for ka = 4, Figs. C-5 to C-8 are for ka = 5, and Figs. C-9 to C-12 are for ka = 6. All other parameters are the same as in Figs. 8-11 in Section V. In particular, the input data for the computer program which generated the method of moments results plotted in Figs. C-1 to C-12 is given by (72).

It is evident from Figs. 8-11 and Figs. C-1 to C-12 that the method of moments solutions for the equivalent currents and scattering patterns are not as accurate at ka = 4, 5, and 6 as at ka = 3. Loss of accuracy at the higher values of ka may be due to violation of (73).

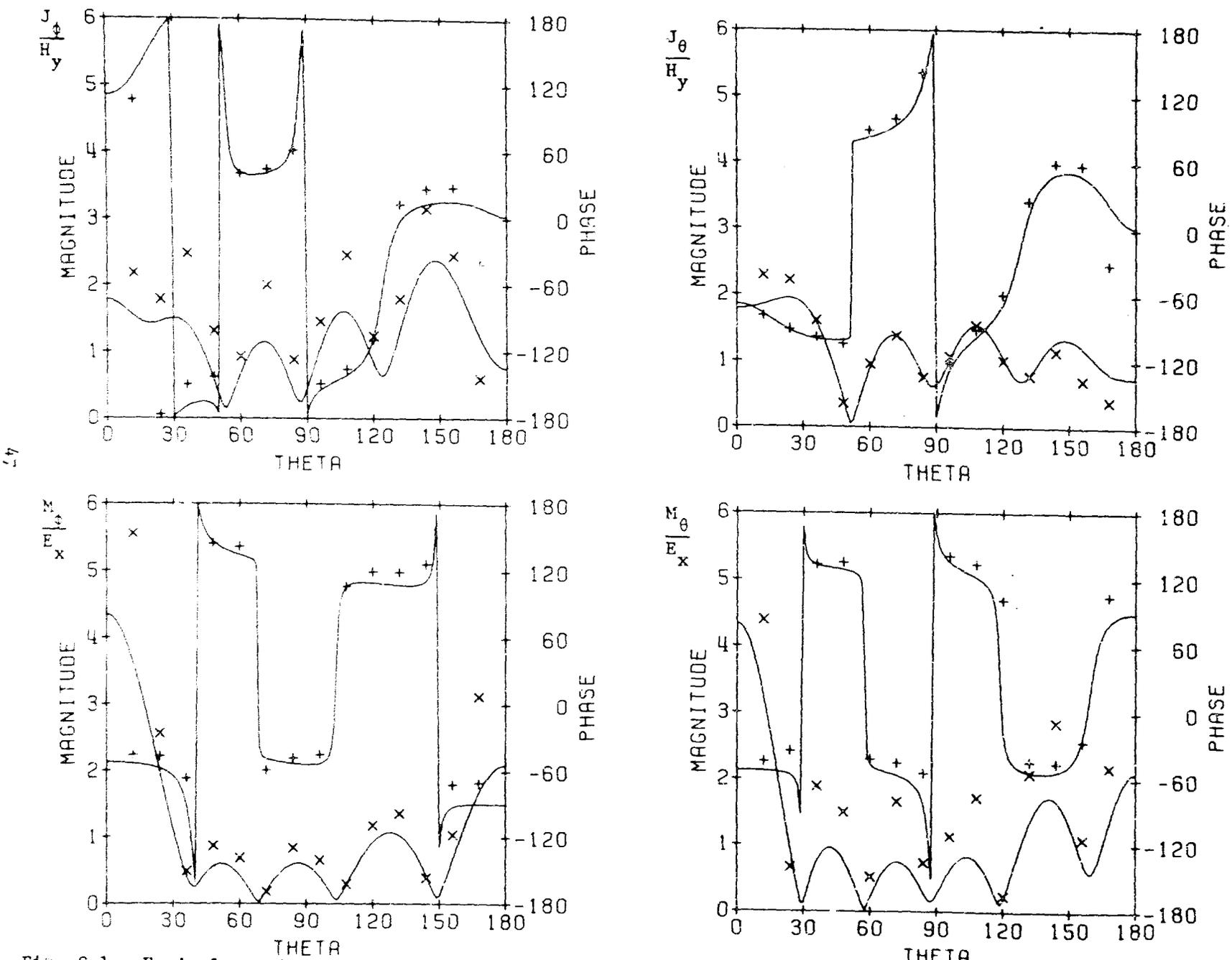

Fig. C-1. Equivalent electric and magnetic currents for dielectric sphere, ka = 4, ε_r = 4, PMCHW solution. Symbols × and + denote magnitude and phase respectively. Solid line denotes exact solution.

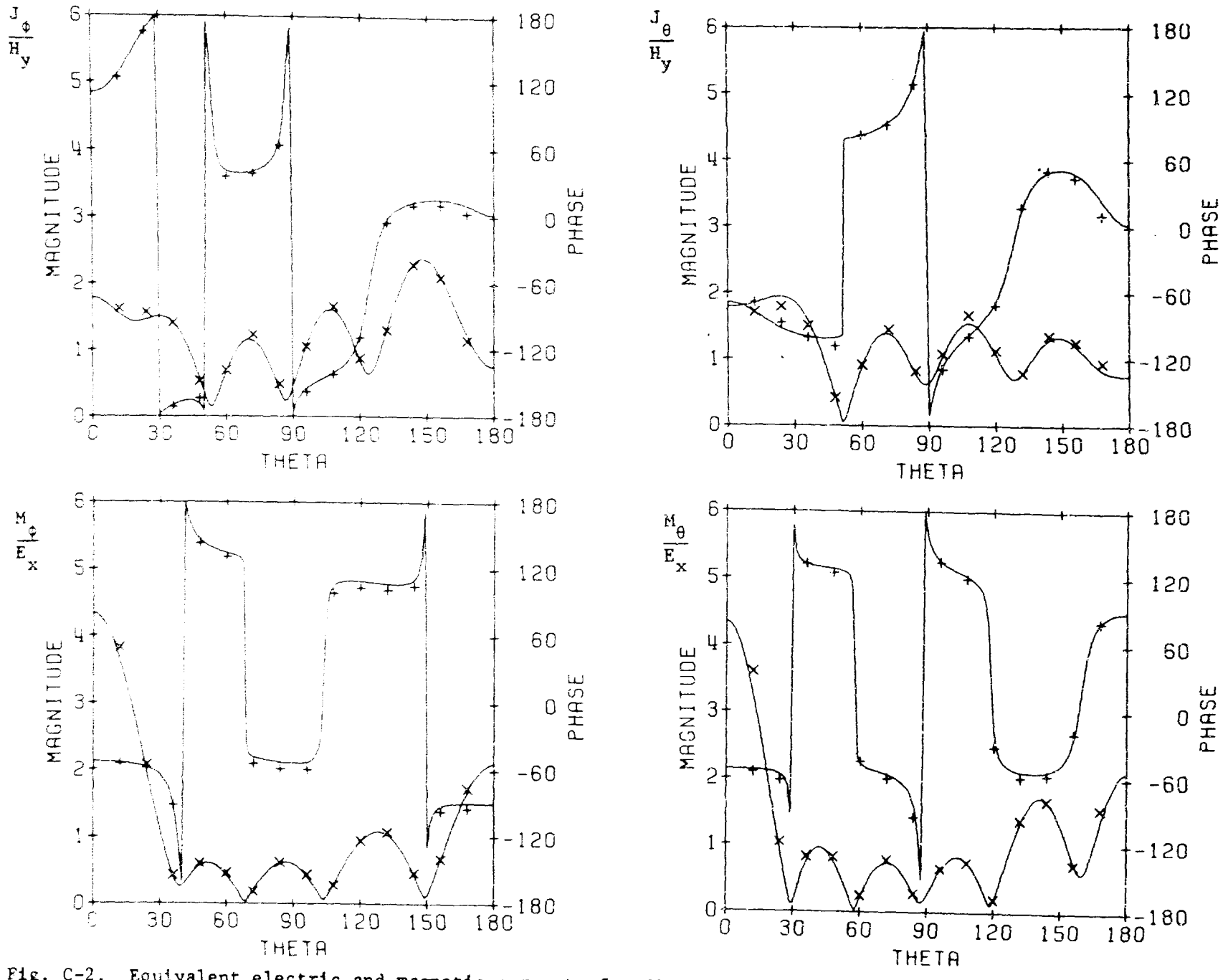

Fig. C-2. Equivalent electric and magnetic currents for dielectric sphere, ka = 4, ε_r = 4, Müller solution. Symbols × and + denote magnitude and phase respectively. Solid line denotes exact solution.

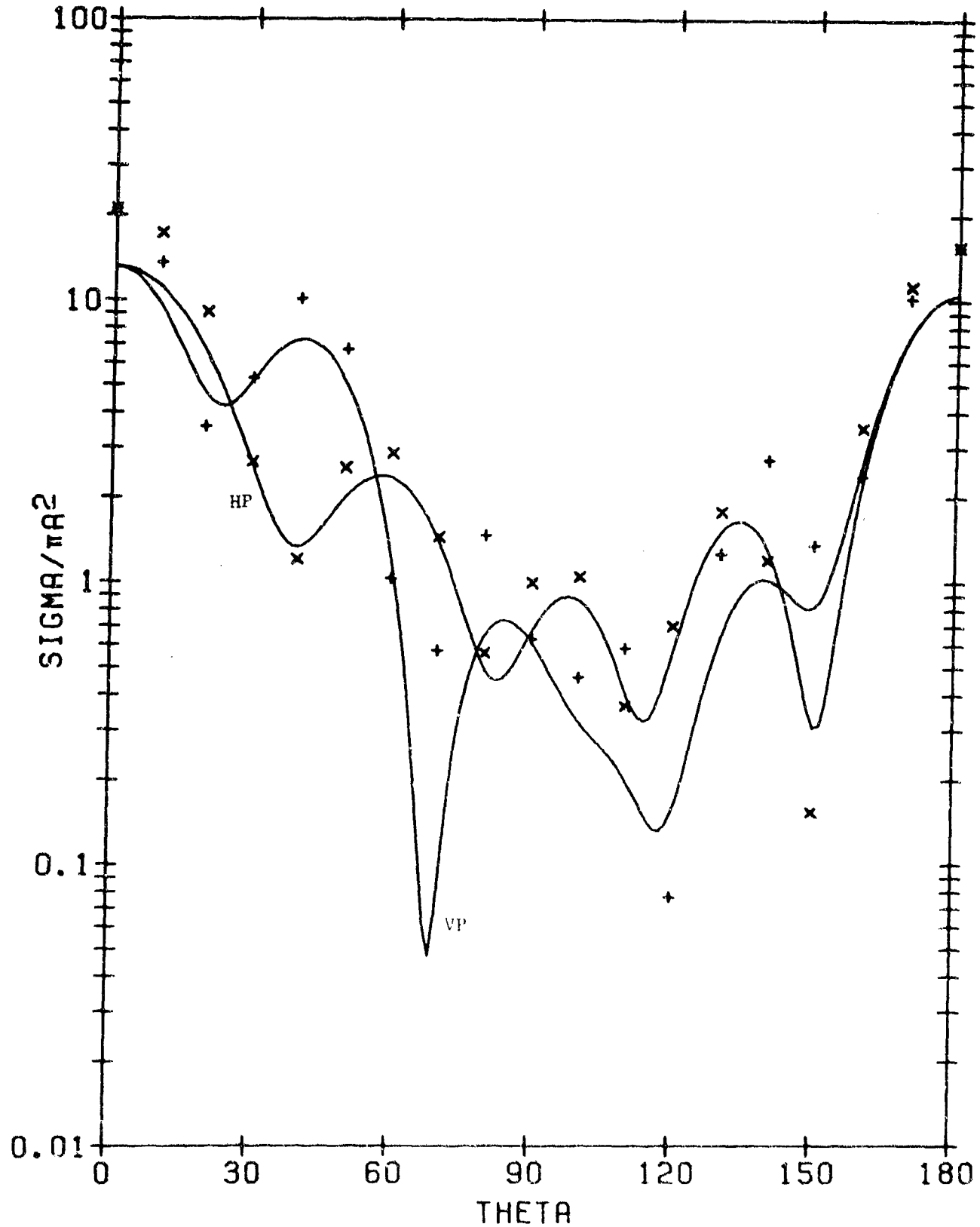

Fig. C-3. Plane wave scattering patterns for dielectric sphere, ka = 4, ϵ_r = 4, PMCHW solution. Symbols × and + denote horizontal polarization and vertical polarization respectively. Solid line denotes exact solution.

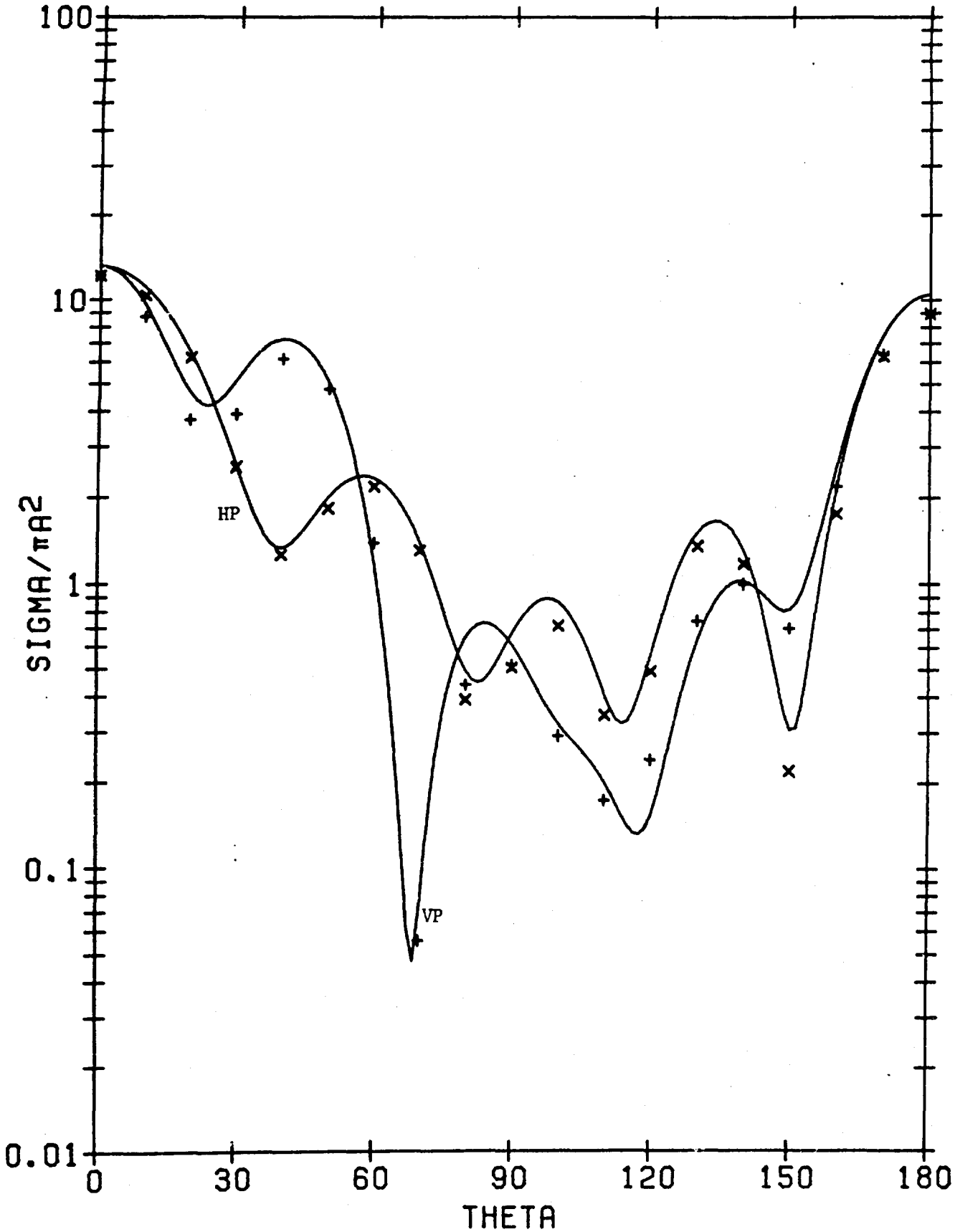

Fig. C-4. Plane wave scattering patterns for dielectric sphere, ka = 4, ε_r = 4, Müller solution. Symbols × and + denote horizontal polarization and vertical polarization respectively. Solid line denotes exact solution.

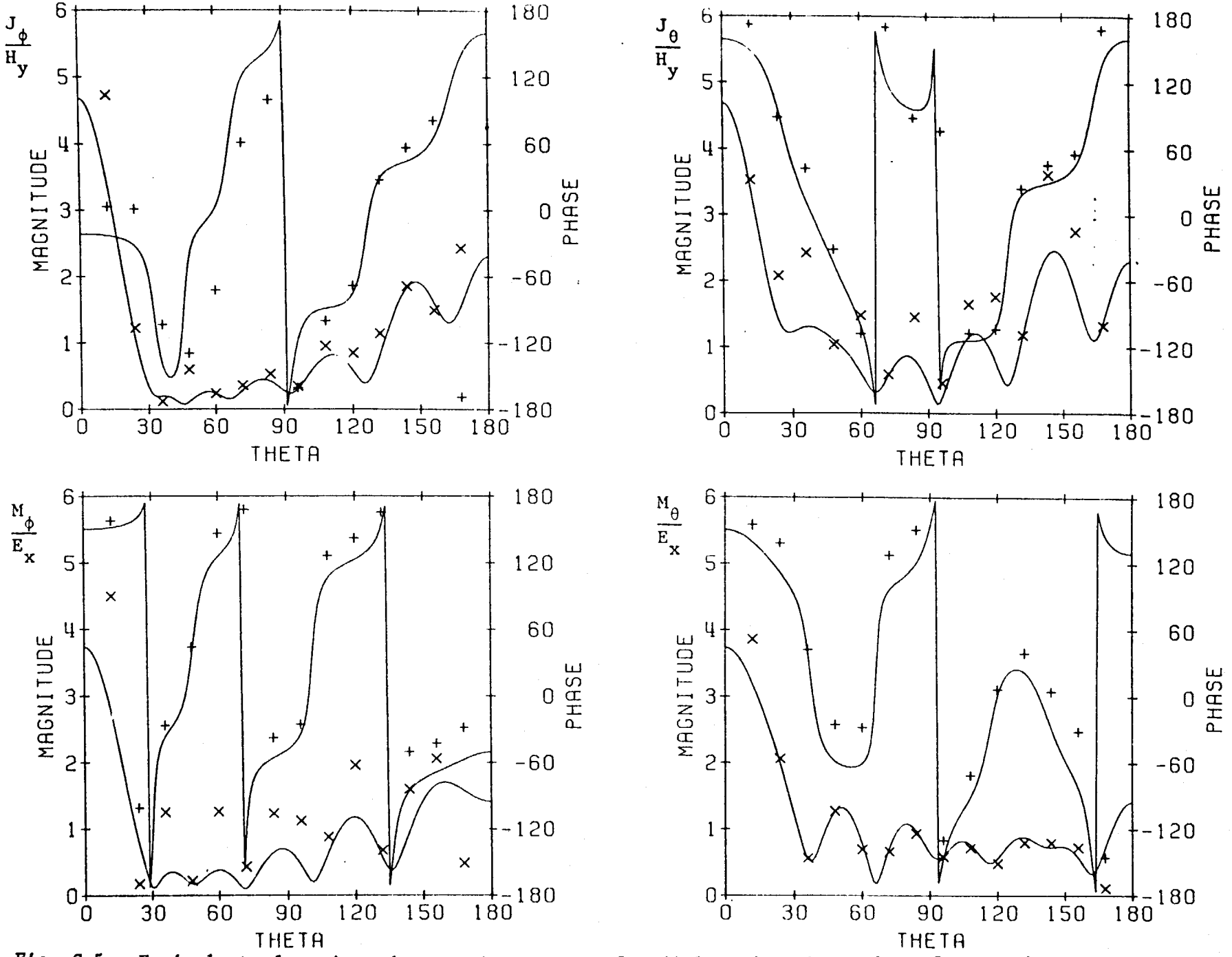

Fig. C-5. Equivalent electric and magnetic currents for dielectric sphere, ka = 5, ε_r = 4, PMCHW solution. Symbols × and + denote magnitude and phase respectively. Solid line denotes exact solution.

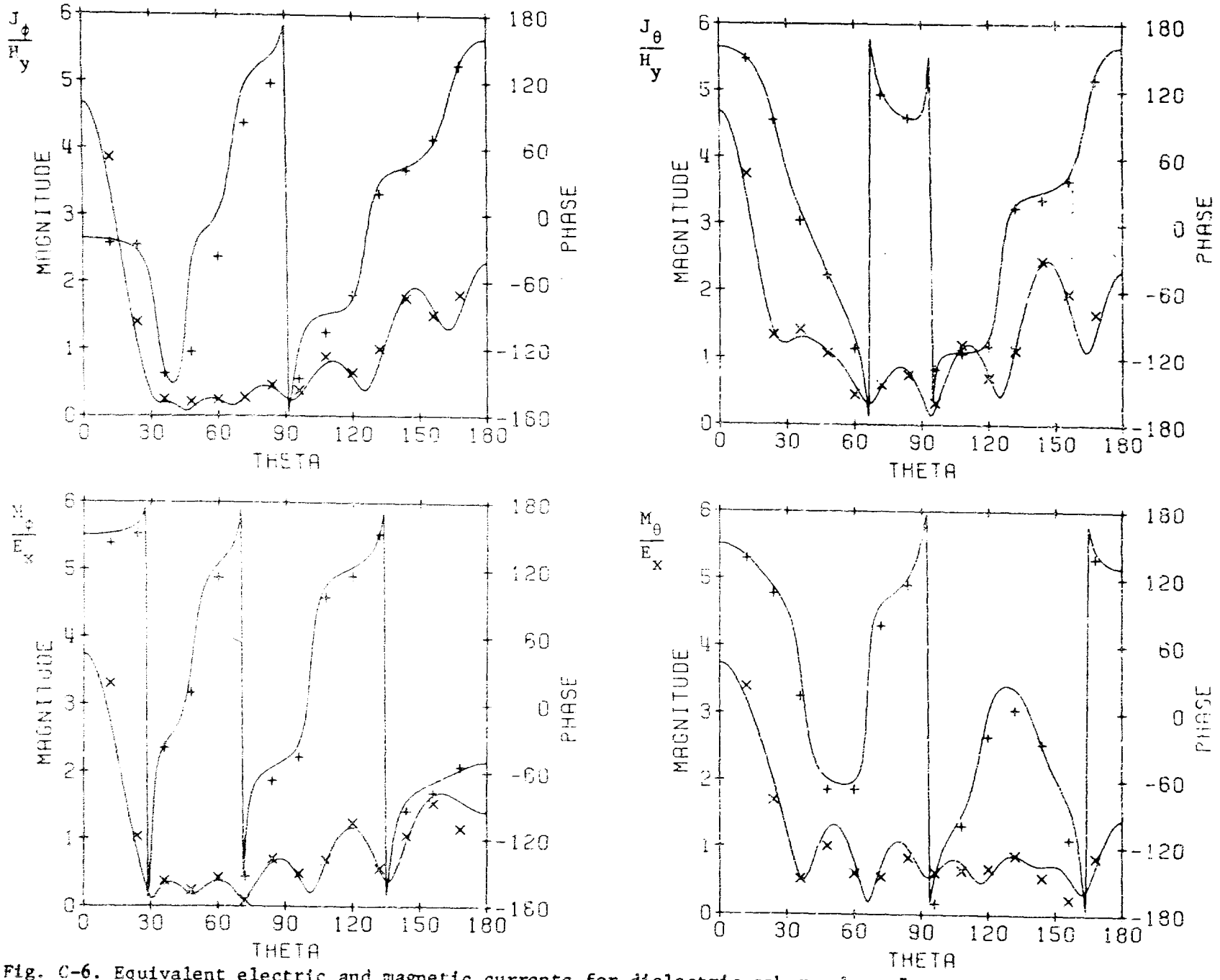

Fig. C-6. Equivalent electric and magnetic currents for dielectric sphere, ka = 5, ϵ_r = 4, Müller solution. Symbols × and + denote magnitude and phase respectively. Solid line denotes exact solution.

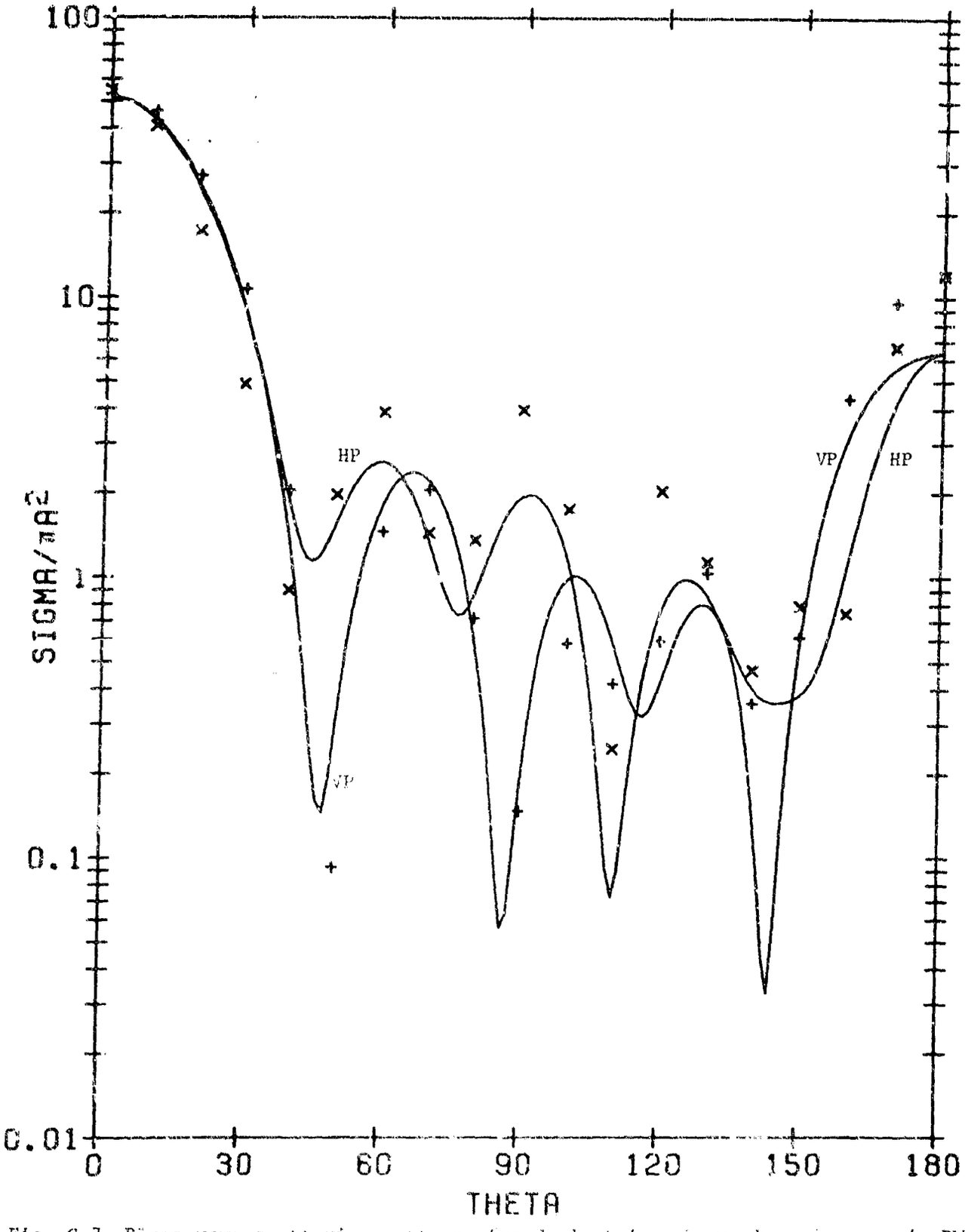

Fig. C-7. Plane wave scattering patterns for dielectric sphere, ka = [illegible] ε_r = 4, PMCHW solution. Symbols · and + denote horizontal polarization and vertical polarization respectively. Solid line denotes exact solution.

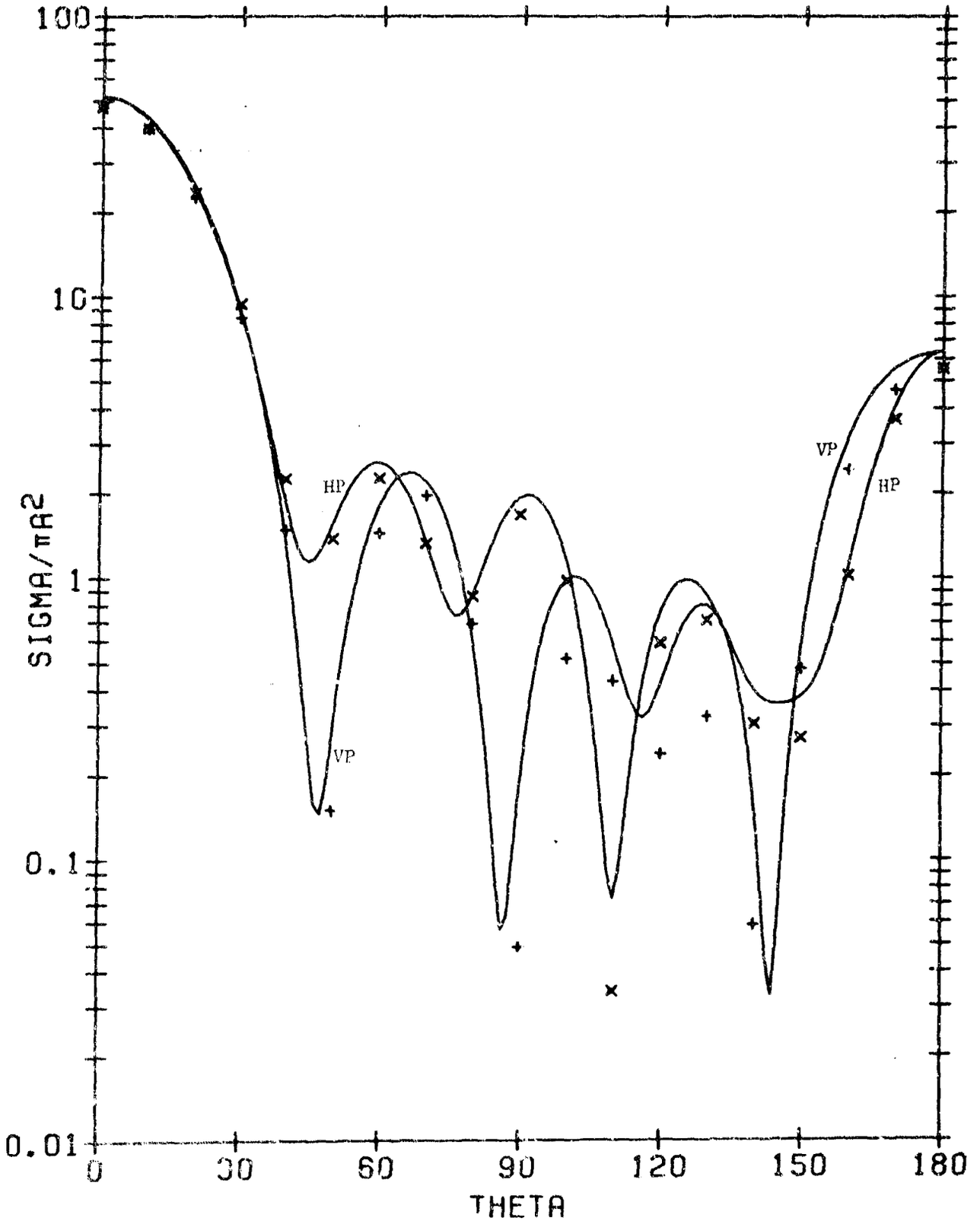

Fig. C-8. Plane wave scattering patterns for dielectric sphere, ka = 5, ϵ_r = 4, Miller solution. Symbols × and + denote horizontal polarization and vertical polarization respectively. Solid line denotes exact solution.

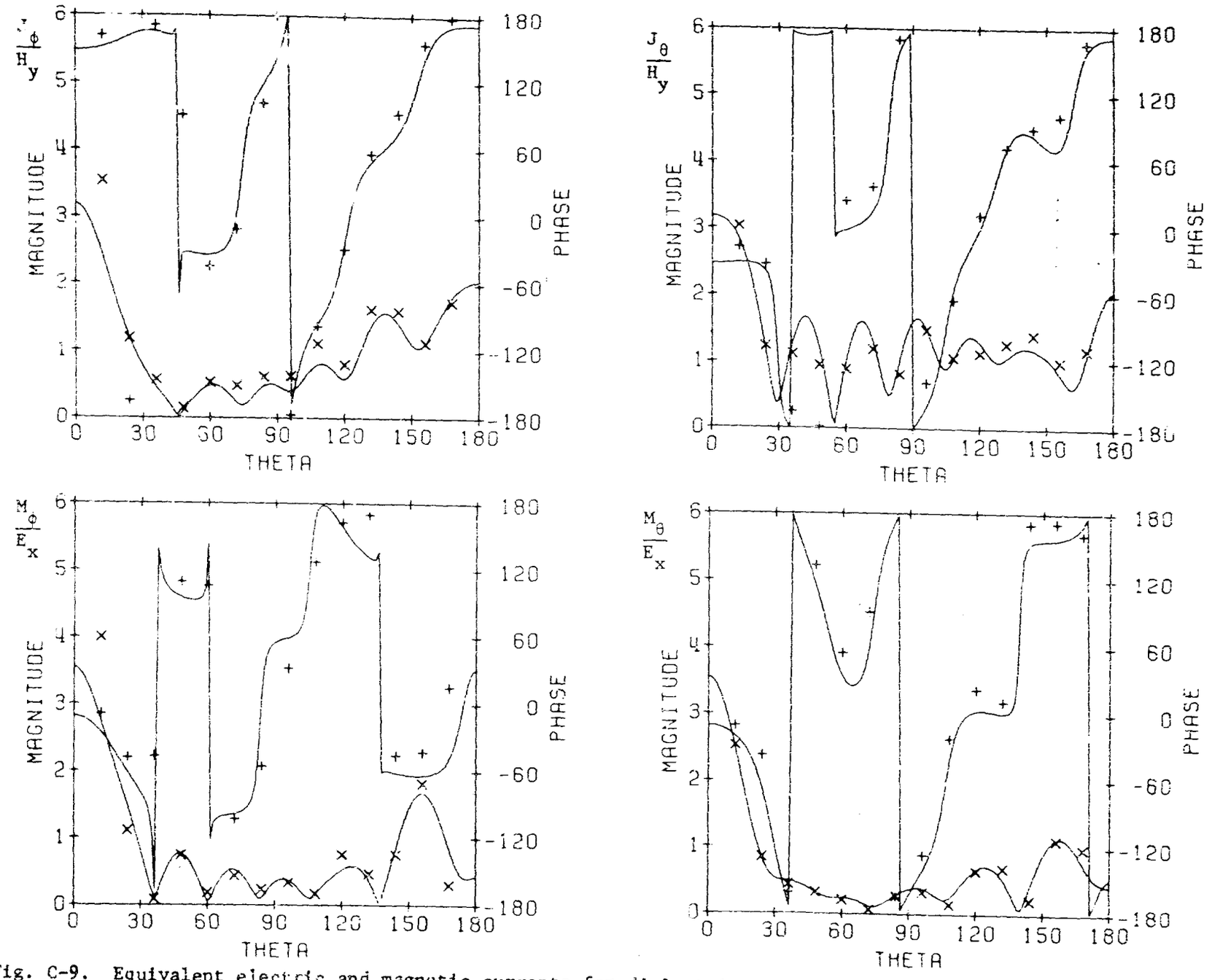

Fig. C-9. Equivalent electric and magnetic currents for dielectric sphere, ka = 6, ε_r = 4, PMCHW solution. Symbols × and + denote magnitude and phase respectively. Solid line denotes exact solution.

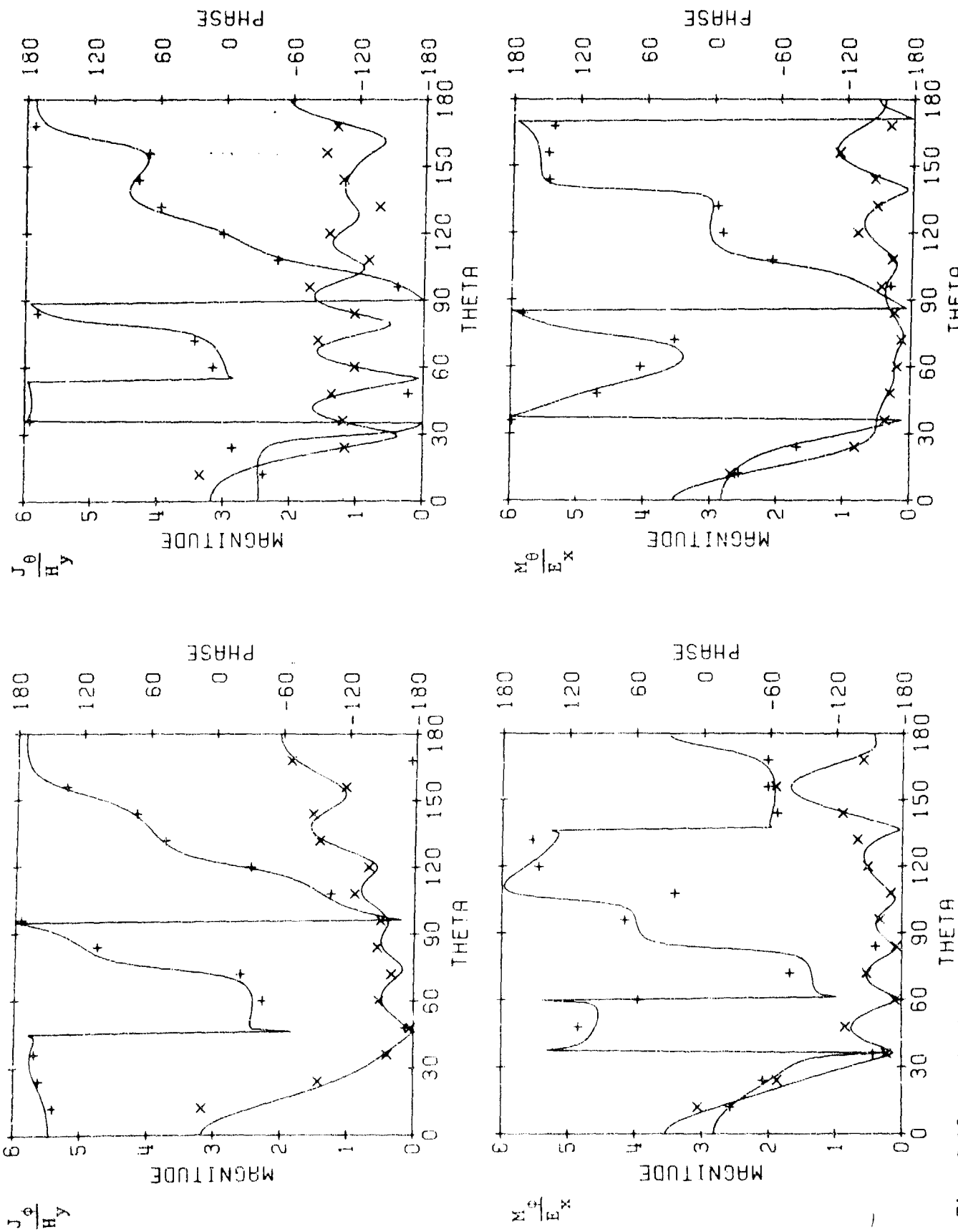

Fig. C-10. Equivalent electric and magnetic currents for dielectric sphere, ka = 6, ε_r = 4, Müller solution. Symbols × and + denote magnitude and phase respectively. Solid line denotes exact solution.

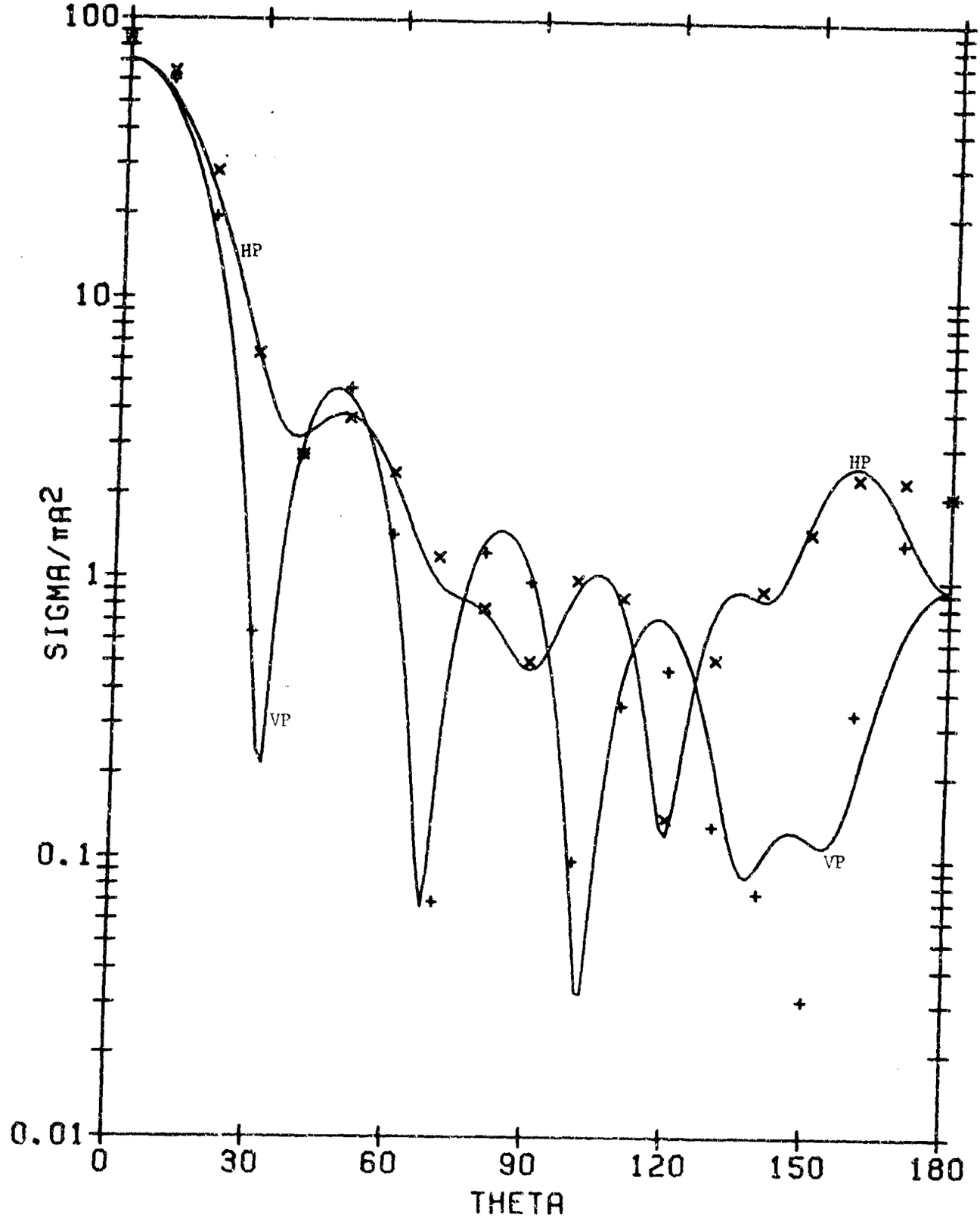

Fig. C-11. Plane wave scattering patterns for dielectric sphere, ka = 6, ϵ_r = 4, PMCHW solution. Symbols × and + denote horizontal polarization and vertical polarization respectively. Solid line denotes exact solution.

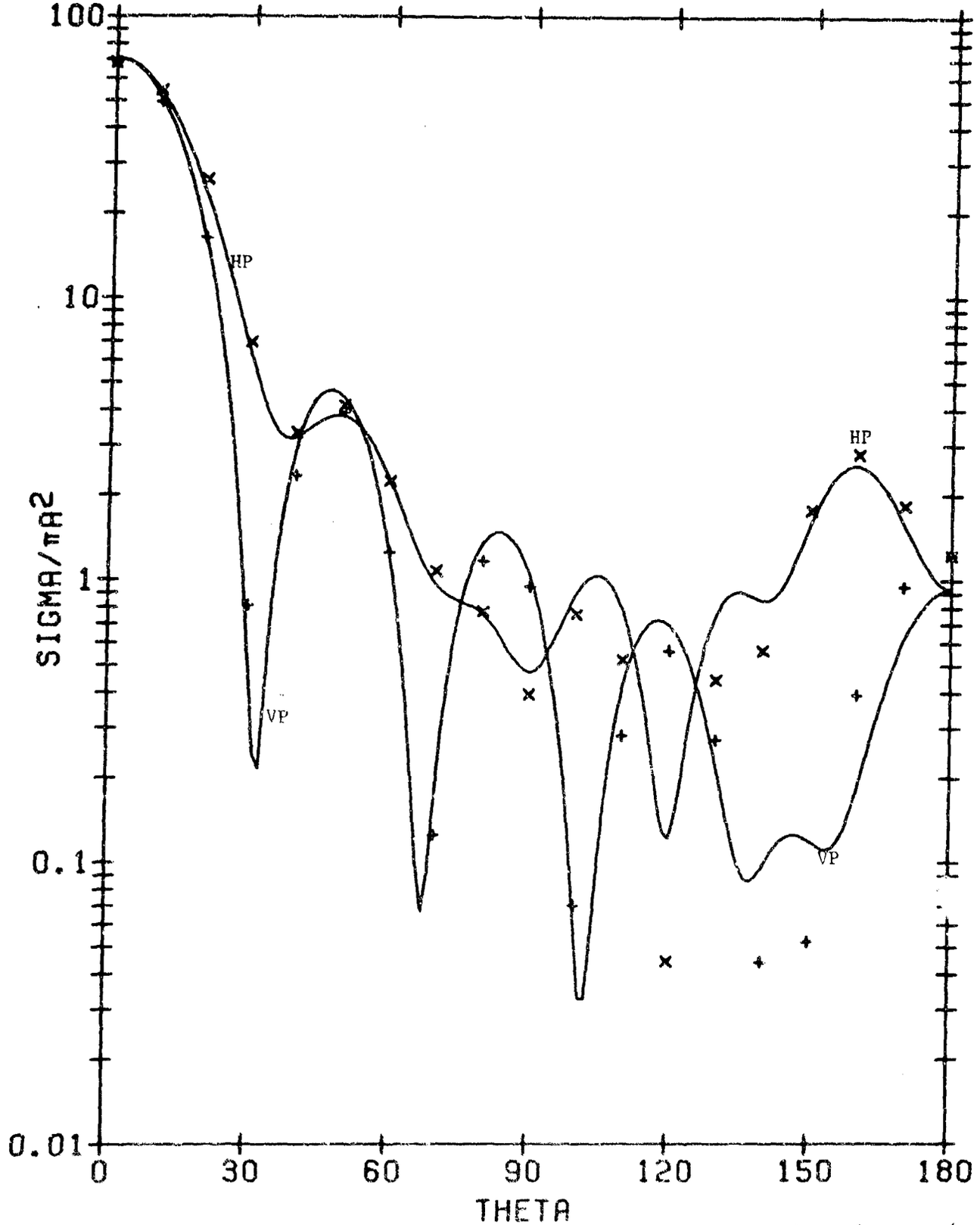

Fig. C-12. Plane wave scattering patterns for dielectric sphere, ka = 6, ϵ_r = 4, Müller solution. Symbols × and + denote horizontal polarization and vertical polarization respectively. Solid line denotes exact solution.

PART TWO

COMPUTER PROGRAM

I. INTRODUCTION

The computer program calculates the equivalent electric and magnetic currents (58) and (59) and the scattering patterns (70) for a loss-free homogeneous dielectric and/or magnetic material body of revolution immersed in an axially incident plane wave. This computer program consists of a main program and the subroutines YZ, PLANE, DECOMP and SOLVE.

Part Two consists of definitions of the input and output for the subroutines YZ, PLANE, DECOMP, and SOLVE, listings of these subroutines, definitions of the input and output for the main program, a verbal flow chart of the main program, and a listing of the main program with sample input and output. The subroutines YZ and PLANE are similar to subroutines of the same name in [10]. The subroutines DECOMP and SOLVE are, except for dimension statements, exactly the same as in [13]. Hence, the insides of the subroutines YZ, PLANE, DECOMP, and SOLVE are not described in detail in Part Two. Because these subroutines are quite complicated, a black box approach is suggested wherein the user is concerned with just the input and output of these subroutines. However, the user is encouraged to delve inside the main program and to make any changes therein that he deems necessary to suit his needs.

II. THE SUBROUTINE YZ

Description:

The subroutine YZ(NN, NP, NPHI, M, MT, RH, ZH, X, A, Y, Z) stores the matrices Y_{nf} and Z_{nf} defined by

$$Y_{nf} = \begin{bmatrix} Y_{nf}^{tt} & Y_{nf}^{t\phi} \\ Y_{nf}^{\phi t} & Y_{nf}^{\phi\phi} \end{bmatrix} \tag{75}$$

$$Z_{nf} = \begin{bmatrix} Z_{nf}^{tt} & Z_{nf}^{t\phi} \\ Z_{nf}^{\phi t} & Z_{nf}^{\phi\phi} \end{bmatrix} \tag{76}$$

by columns in Y and Z respectively. The submatrices on the right-hand sides of (75) and (76) are given by (40) and (41). The first 9 arguments of YZ are input variables. Except for the new input variables M and MT, the subroutine YZ is the same as the old subroutine YZ on pages 17-21 of [10]. If M = - 1 and MT = 2, these subroutines are exactly the same as far as the calculation of Y and Z in terms of the rest of the input variables is concerned.

M = - 1 for field evaluation just inside S and M = + 1 for field evaluation just outside S. M = - 1 if f = e in (75) and M = + 1 if f = d in (75). The value of M is not used in calculating (76) because the tangential components of the electric field operator E_{wf} in (41) are continuous across S. All numerical integrations over t of $f_j(t)$ appearing in (35) and (36) are done by sampling each $f_j(t)$ 2*MT times. The representations of $\rho f_i(t)$ and $\frac{d}{dt}(\rho f_i(t))$ given by (66) and (67) of [9] are replaced by representations which contain 2*MT impulse functions instead of 4 impulse functions. For instance, (66) of [9] is replaced by

$$\rho f_i(t) = \frac{1}{k} \sum_{p=1}^{2*MT} T_{p+(i-1)*2*MT}\, \delta(t-t_{p+(i-1)*MT}), \qquad (77)$$

i=1,2,...N where N will be defined in the paragraph which follows the next paragraph. The T's appearing in (77) will be defined by (78).

Seven of the input variables are the same as in the old subroutine YZ on pages 17-21 of [10]. These variables are defined in terms of variables appearing in [9] by

$$NN = n$$

$$NP = P, \quad \text{page 9}$$

$$NPHI = N_{\phi}, \quad \text{page 13}$$

$$RH(i) = k\bar{\rho}_i, \quad \text{page 9}$$

$$ZH(i) = k\bar{z}_i, \quad \text{page 9}$$

$$X(k) = x_k, \quad \text{page 13}$$

$$A(k) = A_k, \quad \text{page 13}$$

In summary, n denotes the $e^{jn\phi}$ dependence in (35) and (36), $(\bar{\rho}_i, \bar{z}_i)$, i=1,2,...P are coordinates on the generating curve, the k which multiplies $\bar{\rho}_i$ and $\bar{z}_i$ is the propagation constant, and x_k and A_k are the abscissas and weights for the N_ϕ point Gaussian quadrature integration in ϕ. Note that NP-1 should be an integer multiple of MT. If NP-1 is not an integer multiple of MT, the program will ignore RH(m) and ZH(m) for

$$[(NP-1)/MT]*MT+1 < m \leq NP$$

where [(NP-1)/MT] is the largest integer which does not exceed (NP-1)/MT.

Minimum allocations are given by

```
COMPLEX Y(4*N*N), Z(4*N*N)
DIMENSION RH(NP), ZH(NP), X(NPHI), A(NPHI), D(NG)
   PD(NG), TF(2*MT*N), CR(NPHI), C1(NPHI), C2(NPHI),
   C3(NPHI), C4(NPHI)
COMMON RS(NG), ZS(NG), SV(NG), CV(NG), T(2*MT*N)
```

where

$$N = [(NP-1)/MT] - 1$$

$$NG = (N+1)*MT$$

The variables in common make the results of some intermediate calculations done in YZ available to the subroutine PLANE described in Section III of Part Two.

We mention a few portions of YZ which differ from the subroutine listed on pages 18-21 of [10]. Equation (29) of [9] has been generalized to

$$T_{2*MT*(J-1)+I} = \frac{k^2}{\Lambda_1}\left(\sum_{q=1}^{I} d_{MT*(J-1)+q} - \frac{1}{2} d_{MT*(J-1)+I}\right) d_{MT*(J-1)+I} \tag{78}$$

$$T_{2*MT*J-MT+I} = \frac{k}{\Lambda_2}\left(\Lambda_2 - k\sum_{q=I}^{I} d_{MT*J+q} + \frac{k}{2} d_{MT*J+I}\right) d_{MT*J+I} \tag{79}$$

for J = 1,2,...N and I = 1,2,...MT where

$$\Lambda_1 = k \sum_{I=1}^{MT} d_{MT*(J-1)+I} \tag{80}$$

$$\Lambda_2 = k \sum_{I=1}^{MT} d_{MT*J+I} \tag{81}$$

and the d's are given by equation (28) of [9]. Note that Δ_1 is the electrical length of generating curve over which the first half of $f_J(t)$ exists and that Δ_2 is the electrical length of generating curve over which the second half of $f_J(t)$ exists. The generalization of equation (68) of [9] is

$$T'_{2*MT*(J-1)+I} = \frac{kd_{MT*(J-1)+I}}{\Delta_1} \tag{82}$$

$$T'_{2*MT*J-MT+I} = \frac{-kd_{MT*J+I}}{\Delta_2} \tag{83}$$

for J = 1,2,...N, and I = 1,2,...MT where Δ_1 and Δ_2 are given by (80) and (81). Expressions (78) - (83) are calculated in DO loop 68. DO loop 12 accumulates Δ_1 in DEL. DO loop 19 puts (78) in T(2*MT*(J-1)+I) and (82) in TP(2*MT*(J-1)+I). DO loop 15 accumulates Δ_2 in DEL. DO loop 16 puts (79) in T(2*MT*J-MT+I) and (83) in TP(2*MT*J-MT+I).

The subscripts KT, LT, and J1 inside DO loop 32 are obtained as follows. Since the generating curve consists of NG = (N+1)*MT small intervals, it is composed of (N+1) large intervals where the mth large interval consists of the ((m-1)*MT+1)th through the (m*MT)th small intervals. The index I of DO loop 60 denotes the Ith small interval. The Ith small interval is contained in the (I9+1)th large interval where I9 = [(I-1)/MT]. The second half of $f_{I9}(t)$ and the first half of $f_{I9+1}(t)$ are in this large interval. The index K of DO loop 32 denotes $f_{I9+K-1}(t)$. Since T((m-1)*2*MT+1) through T(m*2*MT) is allotted to $f_m(t)$, m=1,2,...,N, $f_m(t)$ is preceded by (m-1) overlaps. For each overlap the subscript of T increases by an amount MT not accounted for by I. Hence, replacing m by I9+K-1, we arrive at the subscript

$$KT = I + (I9+K-2)*MT$$

for T. Here, KT is the field subscript which refers to the testing function. By analogy, the source subscript LT which refers to the expansion function is given by

$$LT = J + (J9+L-2)*MT$$

Retaining $f_{I9+K-1}(t)$ as the testing function, we take the analogously subscripted function $f_{J9+L-1}(t)$ to be the expansion function and arrive at the matrix subscript

$$J1 = (J9+L-2)*N2 + I9+K-1$$

where, as in the program, N2 = 2*N.

DO loop 17 accumulates in R1 the contribution to $(Y_n^{tt})_{J,J}$ of equation (31) of [9] due to the $\frac{\pi}{k^2 d_i \rho_i}$ term in equation (32) of [9]. This contribution is given by

$$R1 = \sum_{I=1}^{2*MT} T_{I+2*MT*(J-1)} * T_{I+2*MT*(J-1)} * PD(I+MT*(J-1))$$

where, as in the program,

$$PD(i) = -M * \left(\frac{\pi}{k^2 d_i \rho_i}\right)$$

Here, the factor -M not included in equation (32) of [9] provides for the choice of field evaluation either outside or inside S.

DO loop 18 accumulates in R1 the contribution to $(Y_n^{tt})_{J-1,J}$ of equation (31) of [9] due to the $\frac{\pi}{d_i \rho_i}$ term in equation (32) of [9]. This contribution is given by

$$R1 = \sum_{I=1}^{MT} T_{I+2*MT*(J-1)-MT} T_{I+2*MT*(J-1)} * PD(I+MT*(J-1)).$$

LISTING OF THE SUBROUTINE YZ

```
SUBROUTINE YZ(NN,NP,NPHI,M,MT,RH,ZH,X,A,Y,Z)
COMPLEX U,Y(784),Z(784),G1,G2,G3,G4,G5,G6,Y1,Y2,Y3,Y4,Z1,Z2,Z3,Z4
DIMENSION RH(161),ZH(161),X(48),A(48),D(160),PD(160),TP(320)
DIMENSION CR(48),C1(48),C2(48),C3(48),C4(48)
COMMON RS(160),ZS(160),SV(160),CV(160),T(320)
PI=3.141593
PIM=-M*PI
N=(NP-1)/MT-1
N2=2*N
NG=(N+1)*MT
NGM=NG-MT
MT2=MT*2
DO 57 I=1,NG
```

```
      I2=I+1
      DR=RH(I2)-RH(I)
      DZ=ZH(I2)-ZH(I)
      D(I)=SQRT(DR*DR+DZ*DZ)
      RS(I)=.5*(RH(I2)+RH(I))
      ZS(I)=.5*(ZH(I2)+ZH(I))
      SV(I)=DR/D(I)
      CV(I)=DZ/D(I)
      PD(I)=PIM/(D(I)*RS(I))
   57 CONTINUE
      J1=0
      J5=0
      DO 68 J=1,N
      DEL=0.
      DO 12 I=1,MT
      J1=J1+1
      DEL=DEL+D(J1)
   12 CONTINUE
      J1=J1-MT
      SN=0.
      DO 19 I=1,MT
      J5=J5+1
      J1=J1+1
      SN=SN+D(J1)
      TP(J5)=D(J1)/DEL
      T(J5)=(SN-.5*D(J1))*TP(J5)
   19 CONTINUE
      DEL=0.
      DO 15 I=1,MT
      J1=J1+1
      DEL=DEL+D(J1)
   15 CONTINUE
      J1=J1-MT
      SN=DEL
      DO 16 I=1,MT
      J5=J5+1
      J1=J1+1
      SN=SN-D(J1)
      TP(J5)=-D(J1)/DEL
      T(J5)=-(SN+.5*D(J1))*TP(J5)
   16 CONTINUE
      J1=J1-MT
   68 CONTINUE
      PI2=.[illegible]*PI
      FN=NN
      DO 25 K=1,NPHI
      PH=PI2*(X(K)+1.)
      PHN=PH*FN
      SN=SI[illegible](.5*PH)
      CR(K)=4.*SN*SN
      R1=PI2*A(K)
      CS=R1*COS(PHN)
      C1(K)=.5*CR(K)*CS
      C2(K)=COS(PH)*C[illegible]
      C2(K)=R1*SIN(PH)*SIN(PHN)
```

```
      C4(K)=CS
   25 CONTINUE
      N2N=N2*N
      N4N=N2N*2
      DO 62 J=1,N4N
      Y(J)=0.
      Z(J)=0.
   62 CONTINUE
      U=(0.,1.)
      DO 59 J=1,NG
      FJ=FN/RS(J)
      L1=1
      L2=2
      IF(J.LE.MT) L1=2
      IF(J.GT.NGM) L2=1
      J9=(J-1)/MT
      JT=J+MT*(J9-2)
      J5=(J9-2)*N2-1
      S1=1.
      DO 60 I=1,J
      I9=(I-1)/MT
      IT=I+MT*(I9-2)
      J6=I9+J5
      FI=FN/RS(I)
      RP=RS(J)-RS(I)
      ZP=ZS(J)-ZS(I)
      R2=RP*RP+ZP*ZP
      IF(I.NE.J) GO TO 41
      S1=.5
      R2=.0625*D(J)*D(J)
   41 R3=RS(I)*RS(J)
      G1=0.
      G2=0.
      G3=0.
      G4=0.
      G5=0.
      G6=0.
      DO 61 K=1,NPHI
      R4=R2+R3*CR(K)
      R5=SQRT(R4)
      Z1=S1/R5*(COS(R5)-U*SIN(R5))
      Y1=Z1*(1.+U*R5)/R4
      G1=C1(K)*Y1+G1
      G2=C2(K)*Y1+G2
      G3=C3(K)*Y1+G3
      G4=C4(K)*Z1+G4
      G5=C2(K)*Z1+G5
      G6=C3(K)*Z1+G6
   61 CONTINUE
      G1=U*G3
      Y1=(RP*CV(J)-ZP*SV(J))*G2-RS(I)*CV(J)*G1
      Y2=(RS(J)*SV(I)*CV(J)-RS(I)*SV(J)*CV(I)-ZP*SV(I)*SV(J))*G3
      Y3=ZP*G3
      Y4=(RP*CV(I)-ZP*SV(I))*G2+RS(J)*CV(I)*G1
      Z1=U*(SV(I)*SV(J)*G5+CV(I)*CV(J)*G4)
      G1=-U*G4
      Z2=-SV(J)*G6
      G2=-FI*G4
      Z3=SV(I)*G6
      G3=FJ*G4
```

```
      Z4=U*(G5-FI*G3)
      K1=1
      K2=2
      IF(I.LE.MT) K1=2
      IF(I.GT.NGM) K2=1
      DO 31 L=L1,L2
      LT=JT+MT*L
      J7=J6+L*N2
      DO 32 K=K1,K2
      KT=IT+MT*K
      TT=T(LT)*T(KT)
      J1=J7+K
      J2=J1+N
      J3=J1+N2N
      J4=J3+N
      Y(J1)=TT*Y1+Y(J1)
      Y(J2)=TT*Y2+Y(J2)
      Y(J3)=TT*Y3+Y(J3)
      Y(J4)=TT*Y4+Y(J4)
      Z(J1)=TT*Z1+TP(LT)*TP(KT)*G1+Z(J1)
      Z(J2)=TT*Z2+TP(LT)*T(KT)*G2+Z(J2)
      Z(J3)=TT*Z3+TP(KT)*T(LT)*G3+Z(J3)
      Z(J4)=TT*Z4+Z(J4)
   32 CONTINUE
   31 CONTINUE
   60 CONTINUE
   59 CONTINUE
      N2P=N2+1
      KD1=1
      J1=0
      J5=0
      DO 11 J=1,N
      R1=0.
      DO 17 I=1,MT2
      J1=J1+1
      J5=J5+1
      R1=R1+T(J1)*T(J1)*PD(J5)
   17 CONTINUE
      J1=J1-MT2
      J5=J5-MT2
      KD2=KD1+N
      KD3=KD1+N2N
      KD4=KD3+N
      G1=Y(KD1)-Y(KD4)
      Y(KD1)=R1+G1
      Y(KD2)=0.
      Y(KD3)=0.
      Y(KD4)=R1-G1
      Z(KD1)=Z(KD1)+Z(KD1)
      Z(KD2)=Z(KD2)-Z(KD3)
      Z(KD3)=-Z(KD2)
      Z(KD4)=Z(KD4)+Z(KD4)
      IF(J-1) 26,27,26
   27 J1=J1+MT2
      J5=J5+MT
      GO TO 22
   26 KU1=KD1-1
      KU2=KD2-1
      KU3=KD3-1
```

```
      KU4=KD4-1
      KL1=KD1-N2
      KL2=KD2-N2
      KL3=KD3-N2
      KL4=KD4-N2
      R1=0.
      DO 18 I=1,MT
      J1=J1+1
      J5=J5+1
      R1=R1+T(J1)*T(J1-MT)*FD(J5)
   18 CONTINUE
      J1=J1+MT
      G1=Y(KU1)-Y(KL4)
      G2=Y(KU4)-Y(KL1)
      Y(KU1)=R1+G1
      Y(KU2)=Y(KU2)-Y(KL2)
      Y(KU3)=Y(KU3)-Y(KL3)
      Y(KU4)=R1+G2
      Y(KL1)=R1-G2
      Y(KL2)=-Y(KL2)
      Y(KL3)=-Y(KU3)
      Y(KL4)=R1-G1
      Z(KU1)=Z(KU1)+Z(KL1)
      Z(KU2)=Z(KU2)-Z(KL3)
      Z(KU3)=Z(KU3)-Z(KL2)
      Z(KU4)=Z(KU4)+Z(KL4)
      Z(KL1)=Z(KU1)
      Z(KL2)=-Z(KU3)
      Z(KL3)=-Z(KU2)
      Z(KL4)=Z(KU4)
   22 KD1=KD1+N2P
   11 CONTINUE
      IF(N.LT.3) RETURN
      J2=N2
      DO 13 I=3,N
      J2=J2+N2
      J1=I-2
      KL1=I
      DO 14 J=1,J1
      KU1=J2+J
      KU2=KU1+N
      KU3=KU1+N2N
      KU4=KU3+N
      KL2=KL1+N
      KL3=KL1+N2N
      KL4=KL3+N
      Y(KL1)=-Y(KU4)
      Y(KL2)=-Y(KU2)
      Y(KL3)=-Y(KU3)
      Y(KL4)=-Y(KU1)
      Z(KL1)=Z(KU1)
      Z(KL2)=-Z(KU3)
      Z(KL3)=-Z(KU2)
      Z(KL4)=Z(KU4)
      KL1=KL1+N2
   14 CONTINUE
   13 CONTINUE
      RETURN
      END
```

III. THE SUBROUTINE PLANE

Description:

The subroutine PLANE(NN, N, MT, NT, THR, R) puts R_{nj}^{pq} of (49) in R(j + (m-1)*N+(L-1)*4*N) where j=1,2,...N, m=1 denotes pq = tθ, m=2 denotes pq = φθ, m=3 denotes pq = tφ, m=4 denotes pq = φφ, and L=1,2,...NT. Here, L denotes the Lth value of the receiver angle θ_r. The first 5 arguments of PLANE are input variables. Except for the new input variable MT, the subroutine PLANE is the same as the old subroutine PLANE on pages 22-26 of [10]. If MT = 2, these subroutines are exactly the same as far as the calculation of R in terms of the rest of the input variables is concerned.

The integration of $f_j(t)$ over t inherent in (49) is approximated by sampling $f_j(t)$ 2*MT times instead of 4 times. The representation of $f_j(t)$ given by (66) of [9] is replaced by (77). NN is the value of n appearing in R_{nj}^{pq}. It is required that NN $\geq$ 0 but this requirement causes no real loss of generality because R_{nj}^{pq} is either even or odd in n. N is the number of expansion functions lying on the generating curve. Specifically, N is the maximum value of i in (77). THR(L) is the Lth value of the receiver angle θ_r where L = 1,2,...NT. The variables RS, ZS, SV, CV, and T appearing in the common statement early in the subroutine PLANE are input variables calculated by calling the subroutine YZ beforehand. The calculated values of these variables depend only on the second, fifth, sixth, and seventh arguments (NP, MT, RH, ZH) of YZ.

Minimum allocations are given by

```
COMPLEX R(4*NT*N)
DIMENSION THR(NT), BJ(M)
COMMON RS(NG), ZS(NG), SV(NG), CV(NG), T(2*MT*N)
```

where

$$NG = (N+1)*M$$

and M is the largest of the values of M calculated by PLANE. The suggested allocation BJ(50) will work if the maximum circumference of the body of revolution is less than 26 wavelengths.

Most of the statements in the subroutine PLANE are the same as or very similar to statements in the old subroutine PLANE listed on pages 25-26 of [10]. The major difference is in the calculation of the subscript (IT+MT*K) for T and the subscript J1 for R. Using reasoning similar to that used to obtain the subscripts KT and J1 in the subroutine YZ, we arrive at

$$(IT + MT*K) = I + (I9 + K-2)*MT$$

$$J1 = I9 + K-1$$

where

$$I9 = [(I-1)/MT]$$

The above J1 is valid only for L=1. If L ≠ 1, then (L-1)*4*N must be added to this J1.

LISTING OF THE SUBROUTINE PLANE

```
      SUBROUTINE PLANE(NN,N,MT,NT,THR,R)
      COMPLEX R(1064),U,U1,U2,R1,R2,R3,R4
      DIMENSION THR(37),BJ(50)
      COMMON RS(160),ZS(160),SV(160),CV(160),T(320)
      NG=(N+1)*MT
      U=(0.,1.)
      U1=3.141593*U**NN
      N4=4*N
      JR=N4*NT
      DO 22 J=1,JR
      R(J)=0.
   22 CONTINUE
      J5=-1
      DO 12 L=1,NT
      CS=COS(THR(L))
      SN=2.*SIN(THR(L))
      DO 13 I=1,NG
      X=.25*RS(I)*SN
      IF(X.LE..5E-7) GO TO 18
      M=2.8*X+13.-2./X
      IF(X.LT..5) M=10.8*ALOG10(X)
      IF(M.GE.(NN+2)) GO TO 19
   18 BJ1=0.
      BJ2=0.
      BJ3=0.
      IF(NN.EQ.1) BJ1=1.
      IF(NN.EQ.0) BJ2=1.
      GO TO 24
   19 BJ(M)=0.
      JM=M-1
      BJ(JM)=1.
```

```
      DO 14 J=3,M
      JM=J M-1
      BJ(JM)=JM/X*BJ(JM+1)-BJ(JM+2)
   14 CONTINUE
      S=0.
      DO 15 J=3,M,2
      S=S+BJ(J)
   15 CONTINUE
      S=BJ(1)+2.*S
      BJ2=BJ(NN+1)/S
      BJ3=BJ(NN+2)/S
      BJ1=-BJ3
      IF(NN.GT.0) BJ1=BJ(NN)/S
   24 ARG=ZS(I)*CS
      U2=U1*(COS(ARG)+U*SIN(ARG))
      R4=(BJ3-BJ1)*U*U2
      R2=(BJ3+BJ1)*U2
      R1=-BJ2*CV(I)*SN*U2+CS*SV(I)*R4
      R3=SV(I)*R2
      R2=-CS*R2
      I9=(I-1)/MT
      IT=I+MT*(I9-2)
      J7=I9+J5
      K1=1
      K2=2
      IF(I9.EQ.0) K1=2
      IF(I9.EQ.N) K2=1
      DO 20 K=K1,K2
      TT=T(IT+MT*K)
      J1=J7+K
      J2=J1+N
      J3=J2+N
      J4=J3+N
      R(J1)=TT*R1+R(J1)
      R(J2)=TT*R2+R(J2)
      R(J3)=TT*R3+R(J3)
      R(J4)=TT*R4+R(J4)
   20 CONTINUE
   13 CONTINUE
      J5=J5+N4
   12 CONTINUE
      RETURN
      END
```

IV. THE SUBROUTINES DECOMP AND SOLVE

Description:

The subroutines DECOMP(N,IPS,UL) and SOLVE(N,IPS,UL,B,X) solve a system of N linear equations in N unknowns. These subroutines will be used in Section V to solve the matrix equation (39). The input to DECOMP consists of N and the N by N matrix of coefficients on the left-hand side of the matrix equation stored by columns in UL. The output from DECOMP is IPS and UL. This output is fed into SOLVE. The rest of the input to SOLVE consists of N and the column of coefficients on the right-hand side of the matrix equation stored in B. SOLVE puts the solution to the matrix equation in X.

Minimum allocations are given by

```
COMPLEX UL(N*N)
DIMENSION SCL(N), IPS(N)
```

in DECOMP and by

```
COMPLEX UL(N*N), B(N), X(N)
DIMENSION IPS(N)
```

in SOLVE.

More detail concerning DECOMP and SOLVE is on pages 46-49 of [13]

LISTING OF THE SUBROUTINES DECOMP AND SOLVE

```
      SUBROUTINE DECOMP(N,IPS,UL)
      COMPLEX UL(3136),PIVOT,EM
      DIMENSION SCL(56),IPS(56)
      DO 5 I=1,N
      IPS(I)=I
      RN=0.
      J1=I
      DO 2 J=1,N
      ULM=ABS(REAL(UL(J1)))+ABS(AIMAG(UL(J1)))
      J1=J1+N
      IF(RN-ULM) 1,2,2
    1 RN=ULM
    2 CONTINUE
      SCL(I)=1./RN
    5 CONTINUE
      NM1=N-1
      K2=0
      DO 17 K=1,NM1
      BIG=0.
      DO 11 I=K,N
      IP=IPS(I)
      IPK=IP+K2
```

```
      SIZE=(ABS(REAL(UL(IPK)))+ABS(AIMAG(UL(IPK))))*SCL(IP)
      IF(SIZE-BIG) 11,11,10
   10 BIG=SIZE
      IPV=I
   11 CONTINUE
      IF(IPV-K) 14,15,14
   14 J=IPS(K)
      IPS(K)=IPS(IPV)
      IPS(IPV)=J
   15 KPP=IPS(K)+K2
      PIVOT=UL(KPP)
      KP1=K+1
      DO 16 I=KP1,N
      KP=KPP
      IP=IPS(I)+K2
      EM=-UL(IP)/PIVOT
   18 UL(IP)=-EM
      DO 16 J=KP1,N
      IP=IP+N
      KP=KP+N
      UL(IP)=UL(IP)+EM*UL(KP)
   16 CONTINUE
      K2=K2+N
   17 CONTINUE
      RETURN
      END
      SUBROUTINE SOLVE(N,IPS,UL,B,X)
      COMPLEX UL(3136),B(56),X(56),SUM
      DIMENSION IPS(56)
      NP1=N+1
      IP=IPS(1)
      X(1)=B(IP)
      DO 2 I=2,N
      IP=IPS(I)
      IPB=IP
      IM1=I-1
      SUM=0.
      DO 1 J=1,IM1
      SUM=SUM+UL(IP)*X(J)
    1 IP=IP+N
    2 X(I)=B(IPB)-SUM
      K2=N*(N-1)
      IP=IPS(N)+K2
      X(N)=X(N)/UL(IP)
      DO 4 IBACK=2,N
      I=NP1-IBACK
      K2=K2-N
      IPI=IPS(I)+K2
      IP1=I+1
      SUM=0.
      IP=IPI
      DO 3 J=IP1,N
      IP=IP+N
    3 SUM=SUM+UL(IP)*X(J)
    4 X(I)=(X(I)-SUM)/UL(IPI)
      RETURN
      END
```

V. THE MAIN PROGRAM

Description:

The main program calculates the electric and magnetic currents (58)-(59) and the normalized scattering cross sections $\frac{\sigma_{\theta\theta}}{\lambda^2}$ and $\frac{\sigma_{\phi\theta}}{\lambda^2}$ (70) for the θ polarized axially incident ($\theta_t = 180°$) plane wave (50)-(51). The main program calls the subroutines YZ, PLANE, DECOMP, and SOLVE. The main program is short and simple. It is a representative application of the theory in Part One of this report.

Input data is read early in the main program according to

```
      READ(1,10) NP, NPHI, MT, NT
10    FORMAT(4I3)
      READ(1,11) BK, UR, ER, ALP, BET
11    FORMAT(5E14.7)
      READ(1,12)(RH(I), I=1, NP)
      READ(1,12)(ZH(I), I=1, NP)
12    FORMAT(10F8.4)
      READ(1,11)(X(K), K=1, NPHI)
      READ(1,11)(A(K), K=1, NPHI)
```

The input variables NP, NPHI, MT, RH, ZH, X, and A are very similar to variables of the same names in the argument list of the subroutine YZ. In summary, (RH(i), ZH(i)), i=1,2,...NP, are the cylindrical coordinates (ρ_i^-, z_i^-) on the generating curve, 2*MT is the number of values of t at which $f_j(t)$ is sampled for the purpose of numerical integration, and X and A are respectively the abscissas and weights for the NPHI point Gaussian quadrature integration in ϕ.

The scattering cross sections are evaluated at receiver angles $\theta_r = (J-1)\pi/(NT-1)$ radians for J=1,2,...NT. BK is the propagation constant k in the external medium. This k appears in (50)-(51). UR and ER are respectively the relative permeability $\frac{\mu_d}{\mu_e}$ and the relative permittivity $\frac{\varepsilon_d}{\varepsilon_e}$ of the body of revolution. Here, μ_d and ε_d are the permeability and permittivity of the (diffracting) body of revolution

and μ_e and ε_e are those of the external medium. ALP and BET are respectively the constants α and β appearing in (39). The PMCHW solution is obtained by setting $\alpha = \beta = 1$. The Müller solution is obtained if α and β are given by (22) and (23).

Minimum allocations are given by

```
COMPLEX YE(4*N*N), ZE(4*N*N), R(4*NT*N),
    B(4*N), YD(4*N*N), ZD(4*N*N), Y(16*N*N),
    C(4*N)
DIMENSION RH(NP), ZH(NP), X(NPHI), A(NPHI),
    THR(NT), RC(N), IPS(4*N)
```

where

$$N = [(NP-1)/MT] - 1$$

Statement 38 puts Y_{1e} defined in accordance with (75) by

$$Y_{1e} = \begin{bmatrix} Y_{1e}^{tt} & Y_{1e}^{t\phi} \\ Y_{1e}^{\phi t} & Y_{1e}^{\phi\phi} \end{bmatrix} \tag{84}$$

in YE and Z_{1e} defined in accordance with (76) by

$$Z_{1e} = \begin{bmatrix} Z_{1e}^{tt} & Z_{1e}^{t\phi} \\ Z_{1e}^{\phi t} & Z_{1e}^{\phi\phi} \end{bmatrix} \tag{85}$$

in ZE. Storage of Y_{1e} and Z_{1e} is by columns.

Statement 39 puts the matrix R_1 defined by

$$R_1 = \begin{bmatrix} \vec{R}_1^{t\theta} & \vec{R}_1^{t\phi} \\ \vec{R}_1^{\phi\theta} & \vec{R}_1^{\phi\phi} \end{bmatrix} \tag{86}$$

in R. The column vectors on the right-hand side of (86) appear in (56). For receiver angle θ_r = THR(J), R_1 of (86) is stored by columns in R((J-1)*4*N+1) through R((J*4*N).

DO loop 22 uses (56) to store the right-hand side of (39) in B. DO loop 22 also puts $2/(k\bar{\rho}_{I*MT+1})$ in RC where $\bar{\rho}_{I*MT+1}$ is the cylindrical coordinate radius evaluated at the peak of the triangle function inherent in $f_I(t)$.

Statement 40 puts Y_{ld} defined by

$$Y_{ld} = \begin{bmatrix} \hat{Y}_{ld}^{tt} & Y_{ld}^{t\phi} \\ Y_{ld}^{\phi t} & \hat{Y}_{ld}^{\phi\phi} \end{bmatrix} \tag{87}$$

in YD and Z_{ld} defined by

$$Z_{ld} = \begin{bmatrix} Z_{ld}^{tt} & Z_{ld}^{t\phi} \\ Z_{ld}^{\phi t} & Z_{ld}^{\phi\phi} \end{bmatrix} \tag{88}$$

in ZD. Storage of Y_{ld} and Z_{ld} is by columns.

Nested DO loops 26 and 27 put the first two columns of submatrices on the left-hand side of (39) in Y. The index J of DO loop 26 denotes the Jth column of the composite square matrix on the left-hand side of (39).

Nested DO loops 28 and 29 put the third and fourth columns of submatrices on the left-hand side of (39) in Y. The index J of DO loop 28 denotes the (2*N+J)th column of the composite square matrix on the left-hand side of (39).

Statements 41 and 42 solve the matrix equation (39) for the composite column vector consisting of $\vec{V}_1^t$, $\vec{V}_1^\phi$, $\vec{I}_1^t$, and $\vec{I}_1^\phi$. This composite column vector is stored in C.

At the peak of the Jth triangle function, the n=1 term of the equivalent electric current (58) reduces to

$$\underset{\sim}{J}^{\theta} = (2/\bar{\rho}_{MT*J+1})\ I_{1J}^{t\theta}\ \underset{\sim}{u}_t \cos\phi + (2j/\bar{\rho}_{MT*J+1})\ I_{1J}^{\phi\theta}\ \underset{\sim}{u}_\phi \sin\phi \tag{89}$$

DO loop 31 prints the real and imaginary parts of

$$U1 = (2/(k\bar{\rho}_{MT*J+1}))I_{1J}^{t\theta}\ ,$$

the real and imaginary parts of

$$U2 = (2j/(k\bar{\rho}_{MT*J+1}))I_{1J}^{\phi\theta}$$

and the magnitudes of U1 and U2. Here, U1 is the t component of the equivalent electric current in the E plane and U2 is the ϕ component of the equivalent electric current in the H plane when the y component of the incident magnetic field is minus one at the origin.

At the peak of the Jth triangle function, the n=1 term of the equivalent magnetic current (59) reduces to

$$\frac{1}{\eta}\underset{\sim}{M}^{\theta} = (2j/\bar{\rho}_{MT*J+1})V_{1J}^{t\theta}\ \underset{\sim}{u}_t \sin\phi + (2/\bar{\rho}_{MT*J+1})V_{1J}^{\phi\theta}\ \underset{\sim}{u}_\phi \cos\phi \tag{90}$$

DO loop 34 prints the real and imaginary parts of

$$B(J) = (2j/(k\bar{\rho}_{MT*J+1}))V_{1J}^{t\theta}$$

and the real and imaginary parts of

$$U2 = (2/(k\bar{\rho}_{MT*J+1}))V_{1J}^{\phi\theta}$$

and the magnitudes of B(J) and U2. Here, B(J) is the t component of the equivalent magnetic current in the H plane and U2 is the ϕ component of the equivalent magnetic current in the E plane when the x component of the incident electric field is minus one at the origin.

Nested DO loops 35 and 36 calculate and print $\frac{\sigma_{\theta\theta}}{\lambda^2}$ and $\frac{\sigma_{\phi\theta}}{\lambda^2}$ of (70). Inner DO loop 36 accumulates the portion

$$\tilde{R}_1^{t\phi\to t\theta} V_1^{t\theta} + \tilde{R}_1^{\phi\phi\to\phi\theta} V_1^{\phi\theta} + \tilde{R}_1^{t\theta\to t\theta} I_1^{t\theta} + \tilde{R}_1^{\phi\theta\to\phi\theta} I_1^{\phi\theta}$$

of (62) in ET and the portion

$$-\tilde{R}_1^{t\theta\to t\theta} V_1^{t\theta} - \tilde{R}_1^{\phi\theta\to\phi\theta} V_1^{\phi\theta} + \tilde{R}_1^{t\phi\to t\theta} I_1^{t\theta} + \tilde{R}_1^{\phi\phi\to\phi\theta} I_1^{\phi\theta}$$

of (63) in EP. The W1 and W2 printed in DO loop 35 are respectively $\frac{\sigma_{\theta\theta}}{\lambda^2}$ and $\frac{\sigma_{\phi\theta}}{\lambda^2}$ for receiver angle θ_r = (J-1)*π/(NT-1) radians.

Suggested modifications of the main program are:

1) Changing the normalization of the scattering patterns. For example, one could replace (70) by (69). All scattering patterns in Part One, Section V are plots of (69).

2) Removing the restriction that the values of the input arguments NP, NPHI, MT, RH, ZH, X, and A of the subroutine YZ be the same in call statements 38 and 40. This modification is indicated by (74).

3) Generalizing from axial plane wave incidence to oblique plane wave incidence.

The above three modifications can be realized without tampering with any of the subroutines YZ, PLANE, DECOMP, and SOLVE.

The sample input and output accompanying the listing of the main program is for the dielectric sphere with ka = 1 and ε_r = 4.

LISTING OF THE MAIN PROGRAM

```
//PSM JOB (XXXX,XXXX,1,2),'MAUTZ,JOE',REGION=200K
// EXEC WATFIV
//GO.SYSIN DD *
$JOB            MAUTZ,TIME=1,PAGES=40
C      SUBRCUTINES YZ, PLANE, DECOMP, AND SOLVE ARE CALLED.
       COMPLEX YE(784),ZE(784),R(1064),B(56),YD(784),ZD(784),Y(3136)
       COMPLEX C(56),U,U1,U2,ET,EP,CONJG
       DIMENSION RH(161),ZH(161),X(48),A(48),THR(37),RC(19),IPS(56)
       READ(1,10) NP,NPHI,MT,NT
   10  FORMAT(4I3)
       READ(1,11) BK,UR,ER,ALP,BET
   11  FORMAT(5E14.7)
       READ(1,12)(RH(I),I=1,NP)
       READ(1,12)(ZH(I),I=1,NP)
   12  FORMAT(10F8.4)
       READ(1,11)(X(K),K=1,NPHI)
       READ(1,11)(A(K),K=1,NPHI)
       WRITE(3,13) NP,NPHI,MT,NT
   13  FORMAT('  NP NPHI MT NT'/(1X,I3,I5,2I3))
       WRITE(3,14) BK,UR,ER,ALP,BET
   14  FORMAT(7X,'BK',12X,'UR',12X,'ER',11X,'ALP',11X,'BET'/(1X,5E14.7))
       WRITE(3,15)(RH(I),I=1,NP)
   15  FORMAT(' RH'/(1X,10F8.4))
       WRITE(3,16)(ZH(I),I=1,NP)
   16  FORMAT(' ZH'/(1X,10F8.4))
       WRITE(3,17)(X(K),K=1,NPHI)
   17  FORMAT(' X'/(1X,5E14.7))
       WRITE(3,18)(A(K),K=1,NPHI)
   18  FORMAT(' A'/(1X,5E14.7))
       DO 19 J=1,NP
       RH(J)=BK*RH(J)
       ZH(J)=BK*ZH(J)
   19  CONTINUE
   38  CALL YZ(1,NP,NPHI,-1,MT,RH,ZH,X,A,YE,ZE)
       WRITE(3,20)(YE(I),I=1,4),(ZE(I),I=1,4)
   20  FORMAT(' SOME ELEMENTS OF YE AND ZE'/(1X,4E14.7))
       PI=3.141593
       DT=PI/(NT-1)
       DO 21 J=1,NT
       THR(J)=(J-1)*DT
   21  CONTINUE
       N=(NP-1)/MT-1
   39  CALL PLANE(1,N,MT,NT,THR,R)
       N2=2*N
       N3=3*N
       N4=4*N
       NTN=(NT-1)*N4
       DO 22 I=1,N
       J3=I+NTN
       B(I)=R(J3)
       B(I+N)=-R(J3+N)
       B(I+N2)=-R(J3+N3)
       B(I+N3)=-R(J3+N2)
       RC(I)=2./RH(MT*I+1)
   22  CONTINUE
       WRITE(3,23)(B(I),I=1,N2)
   23  FORMAT(' HALF OF THE ELEMENTS OF B'/(1X,4E14.7))
       EM=SQRT(UR*ER)
```

```
      DO 24 I=1,NP
      RH(I)=EM*RH(I)
      ZH(I)=EM*ZH(I)
   24 CONTINUE
   40 CALL YZ(1,NP,NPHI,1,MT,RH,ZH,X,A,YD,ZD)
      WRITE(3,25)(YD(I),I=1,4),(ZD(I),I=1,4)
   25 FORMAT(' SOME ELEMENTS OF YD AND ZD'/(1X,4E14.7))
      D=SQRT(UR/ER)
      ALPD=ALP*D
      BETD=BET/D
      JY=0
      J1=0
      DO 26 J=1,N2
      DO 27 I=1,N
      JY=JY+1
      J1=J1+1
      J2=J1+N
      Y(JY)=YE(J2)+ALP*YD(J2)
      Y(JY+N)=-YE(J1)-ALP*YD(J1)
      Y(JY+N2)=ZE(J2)+BETD*ZD(J2)
      Y(JY+N3)=-ZE(J1)-BETD*ZD(J1)
   27 CONTINUE
      JY=JY+N3
      J1=J1+N
   26 CONTINUE
      J1=0
      DO 28 J=1,N2
      DO 29 I=1,N2
      JY=JY+1
      J1=J1+1
      Y(JY)=ZE(J1)+ALPD*ZD(J1)
      Y(JY+N2)=YE(J1)+BET*YD(J1)
   29 CONTINUE
      JY=JY+N2
   28 CONTINUE
   41 CALL DECOMP(N4,IPS,Y)
   42 CALL SOLVE(N4,IPS,Y,B,C)
      WRITE(3,30)
   30 FORMAT('0  REAL JT     IMAG JT     REAL JP     IMAG JP     MAG  JT
     1MAG  JP')
      U=(0.,1.)
      DO 31 J=1,N
      RR=RC(J)
      ET=U*RR
      B(J)=ET*C(J)
      J1=J+N
      B(J1)=RR*C(J1)
      U1=RR*C(J+N2)
      U2=ET*C(J+N3)
      W1=CABS(U1)
      W2=CABS(U2)
      WRITE(3,32) U1,U2,W1,W2
   32 FORMAT(1X,6E11.4)
   31 CONTINUE
      WRITE(3,33)
   33 FORMAT('0  REAL MT     IMAG MT     REAL MP     IMAG MP     MAG  MT
     1MAG  MP')
      DO 34 J=1,N
      U2=B(J+N)
      W1=CABS(B(J))
```

```
      W2=CABS(U2)
      WRITE(3,32) B(J),U2,W1,W2
   34 CONTINUE
      WRITE(3,37)
   37 FORMAT('0  SIGTHETA     SIGPHI')
      CON=.25/PI**3
      JR1=0
      DO 35 J=1,NT
      ET=0.
      EP=0.
      DO 36 I=1,N2
      JC2=I+N2
      JR1=JR1+1
      JR2=JR1+N2
      ET=ET+R(JR2)*C(I)+R(JR1)*C(JC2)
      EP=EP-R(JR1)*C(I)+R(JR2)*C(JC2)
   36 CONTINUE
      JR1=JR1+N2
      W1=CON*ET*CONJG(ET)
      W2=CON*EP*CONJG(EP)
      WRITE(3,32) W1,W2
   35 CONTINUE
      STOP
      END
$DATA
 21 20  2 19
 0.1000000E+01 0.1000000E+01 0.4000000E+01 0.1000000E+01 0.1000000E+01
  0.0000  0.1564  0.3090  0.4540  0.5878  0.7071  0.8090  0.8910  0.9511  0.9877
  1.0000  0.9877  0.9511  0.8910  0.8090  0.7071  0.5878  0.4540  0.3090  0.1564
  0.0000
 -1.0000 -0.9877 -0.9511 -0.8910 -0.8090 -0.7071 -0.5878 -0.4540 -0.3090 -0.1564
  0.0000  0.1564  0.3090  0.4540  0.5878  0.7071  0.8090  0.8910  0.9511  0.9877
  1.0000
-0.9931286E+00-0.9639719E+00-0.9122344E+00-0.8391170E+00-0.7463319E+00
-0.6360537E+00-0.5108670E+00-0.3737061E+00-0.2277859E+00-0.7652652E-01
 0.7652652E-01 0.2277859E+00 0.3737061E+00 0.5108670E+00 0.6360537E+00
 0.7463319E+00 0.8391170E+00 0.9122344E+00 0.9639719E+00 0.9931286E+00
 0.1761401E-01 0.4060143E-01 0.6267205E-01 0.8327674E-01 0.1019301E+00
 0.1181945E+00 0.1316886E+00 0.1420961E+00 0.1491730E+00 0.1527534E+00
 0.1527534E+00 0.1491730E+00 0.1420961E+00 0.1316886E+00 0.1181945E+00
 0.1019301E+00 0.8327674E-01 0.6267205E-01 0.4060143E-01 0.1761401E-01
$STOP
/*
//

PRINTED OUTPUT
 NP NPHI MT NT
 21   20  2 19
      BK              UR              ER              ALP             BET
 0.1000000E+01 0.1000000E+01 0.4000000E+01 0.1000000E+01 0.1000000E+01
RH
  0.0000  0.1564  0.3090  0.4540  0.5878  0.7071  0.8090  0.8910  0.9511  0.9877
  1.0000  0.9877  0.9511  0.8910  0.8090  0.7071  0.5878  0.4540  0.3090  0.1564
  0.0000
ZH
 -1.0000 -0.9877 -0.9511 -0.8910 -0.8090 -0.7071 -0.5878 -0.4540 -0.3090 -0.1564
  0.0000  0.1564  0.3090  0.4540  0.5878  0.7071  0.8090  0.8910  0.9511  0.9877
  1.0000
X
-0.9931286E+00-0.9639719E+00-0.9122344E+00-0.8391170E+00-0.7463319E+00
```

```
-0.6360537E+00-0.5108670E+00-0.3737061E+00-0.2277859E+00-0.7652652E-01
 0.7652652E-01 0.2277859E+00 0.3737061E+00 0.5108670E+00 0.6360537E+00
 0.7463319E+00 0.8391170E+00 0.9122344E+00 0.9639719E+00 0.9931286E+00
A
 0.1761401E-01 0.4060143E-01 0.6267208E-01 0.8327675E-01 0.1019301E+00
 0.1181945E+00 0.1316886E+00 0.1420961E+00 0.1491730E+00 0.1527534E+00
 0.1527534E+00 0.1491730E+00 0.1420961E+00 0.1316886E+00 0.1181945E+00
 0.1019301E+00 0.8327675E-01 0.6267208E-01 0.4060143E-01 0.1761401E-01
SOME ELEMENTS OF YE AND ZE
 0.2431891E+01-0.5483869E-02 0.5072693E+00-0.1154096E-01
 0.1015252E+00-0.2041826E-01 0.9178627E-01-0.3066700E-01
 0.9008127E-01-0.7025097E+01 0.7607359E-01 0.1940044E+01
 0.5597932E-01 0.7892063E+00 0.3345479E-01 0.2816698E+00
HALF OF THE ELEMENTS OF B
-0.5464500E+00-0.7503574E+00-0.5449371E+00-0.5690688E+00
-0.4709502E+00-0.3229641E+00-0.2808148E+00-0.1054077E+00
 0.0000000E+00-0.1778790E-01 0.2808146E+00-0.1054077E+00
 0.4709504E+00-0.3229641E+00 0.5449370E+00-0.5690686E+00
 0.5464502E+00-0.7503576E+00 0.7951685E+00-0.5814634E+00
 0.7044444E+00-0.6853659E+00 0.5376098E+00-0.8194968E+00
 0.2939058E+00-0.9327149E+00-0.0000000E+00-0.9769601E+00
-0.2939057E+00-0.9327147E+00-0.5376099E+00-0.8194970E+00
-0.7044442E+00-0.6853657E+00-0.7951688E+00-0.5814636E+00
SOME ELEMENTS OF YD AND ZD
-0.2290969E+01-0.3768066E-01-0.3189305E+00-0.7057631E-01
 0.9599513E-01-0.1088477E+00 0.4942125E-01-0.1374637E+00
 0.3428959E+00-0.2902117E+01 0.2818084E+00 0.1262741E+01
 0.2082631E+00 0.5027283E+00 0.1465860E+00 0.1911734E+00

  REAL JT     IMAG JT     REAL JP     IMAG JP     MAG  JT     MAG  JP
-0.6398E+00-0.1395E+01 0.6170E+00 0.1415E+01 0.1535E+01 0.1543E+01
-0.8349E+00-0.1227E+01 0.8652E+00 0.1174E+01 0.1484E+01 0.1459E+01
-0.1025E+01-0.9274E+00 0.7285E+00 0.9655E+00 0.1382E+01 0.1210E+01
-0.1127E+01-0.4861E+00 0.6632E+00 0.6917E+00 0.1228E+01 0.8582E+00
-0.1094E+01 0.5150E-01 0.4185E+00 0.6316E+00 0.1096E+01 0.7576E+00
-0.8731E+00 0.5874E+00 0.1349E+00 0.7185E+00 0.1052E+01 0.7311E+00
-0.5410E+00 0.1026E+01 0.1116E+00 0.1011E+01 0.1160E+01 0.1017E+01
-0.1626E+00 0.1320E+01-0.9319E-01 0.1256E+01 0.1330E+01 0.1260E+01
 0.1722E+00 0.1479E+01 0.2244E+00 0.1496E+01 0.1489E+01 0.1513E+01

  REAL MT     IMAG MT     REAL MP     IMAG MP     MAG  MT     MAG  MP
-0.1064E+00-0.6806E+00-0.8434E-01-0.6963E+00 0.6889E+00 0.7014E+00
-0.2323E+00-0.5834E+00-0.2176E+00-0.5837E+00 0.6279E+00 0.6230E+00
-0.3712E+00-0.4190E+00-0.1639E+00-0.5138E+00 0.5598E+00 0.5393E+00
-0.4731E+00-0.1809E+00-0.1442E+00-0.4209E+00 0.5065E+00 0.4449E+00
-0.5072E+00 0.1093E+00-0.4617E-01-0.4199E+00 0.5188E+00 0.4224E+00
-0.4451E+00 0.3992E+00 0.5351E-01-0.4940E+00 0.5979E+00 0.4969E+00
-0.3171E+00 0.6397E+00 0.7018E-01-0.6418E+00 0.7140E+00 0.6457E+00
-0.1556E+00 0.8002E+00 0.1272E+00-0.7901E+00 0.8152E+00 0.8003E+00
-0.1304E-01 0.8852E+00-0.1307E-01-0.8971E+00 0.8853E+00 0.8972E+00

  SIGTHETA     SIGPHI
 0.1535E+00 0.1535E+00
 0.1488E+00 0.1523E+00
 0.1355E+00 0.1489E+00
 0.1153E+00 0.1433E+00
 0.9112E-01 0.1360E+00
 0.6592E-01 0.1272E+00
 0.4260E-01 0.1176E+00
 0.2343E-01 0.1074E+00
```

0.9801E-02 0.9722E-01
0.2164E-02 0.8741E-01
0.1589E-03 0.7831E-01
0.2810E-02 0.7015E-01
0.8790E-02 0.6308E-01
0.1666E-01 0.5717E-01
0.2504E-01 0.5241E-01
0.3278E-01 0.4879E-01
0.3895E-01 0.4625E-01
0.4290E-01 0.4475E-01
0.4426E-01 0.4426E-01

REFERENCES

[1] A. J. Poggio and E. K. Miller, "Integral Equation Solutions of Three Dimensional Scattering Problems," Chap. 4 of Computer Techniques for Electromagnetics, edited by R. Mittra, Pergamon Press, 1973, Equation (4.17).

[2] Yu Chang and R. F. Harrington, "A Surface Formulation for Characteristic Modes of Material Bodies," Report TR-74-7, Department of Electrical and Computer Engineering, Syracuse University, Syracuse, NY, October 1974.

[3] T. K. Wu, "Electromagnetic Scattering from Arbitrarily-Shaped Lossy Dielectric Bodies," Ph.D. Dissertation, University of Mississippi, 1976.

[4] C. Müller, Foundations of the Mathematical Theory of Electromagnetic Waves, Springer-Verlag, 1969, p. 301, Equations (40)-(41). (There are some sign errors in these equations.)

[5] V. V. Solodukhov and E. N. Vasil'ev, "Diffraction of a Plane Electromagnetic Wave by a Dielectric Cylinder of Arbitrary Cross Section," Soviet Physics - Technical Physics, vol. 15, No. 1, July 1970, pp. 32-36.

[6] N. Morita, "Analysis of Scattering by a Dielectric Rectangular Cylinder by Means of Integral Equation Formulation," Electronics and Communications in Japan, vol. 57-B, No. 10, October 1974, pp. 72-80.

[7] E. N. Vasil'ev and L. B. Materikova, "Excitation of Dielectric Bodies of Revolution," Soviet Physics - Technical Physics, vol. 10, No. 10, April 1966, pp. 1401-1406.

[8] R. F. Harrington, Field Computation by Moment Methods, Macmillan Co., New York, 1968.

[9] J. R. Mautz and R. F. Harrington, "H-Field, E-Field, and Combined Field Solutions for Bodies of Revolution," Interim Technical Report RADC-TR-77-109, Rome Air Development Center, Griffiss Air Force Base, New York, March 1977.

[10] J. R. Mautz and R. F. Harrington, "Computer Programs for H-Field, E-Field, and Combined Field Solutions for Bodies of Revolution," Interim Technical Report RADC-TR-77-215, Rome Air Development Center, Griffiss Air Force Base, New York, June 1977.

[11] R. F. Harrington, Time-Harmonic Electromagnetic Fields, McGraw-Hill Book Co., 1961. Section 6-9.

[12] P. Barber and C. Yeh, "Scattering of Electromagnetic Waves by Arbitrarily Shaped Dielectric Bodies," Applied Optics, vol. 14, No. 12, December 1975, pp. 2864-2872.

[13] J. R. Mautz and R. F. Harrington, "Transmission from a Rectangular Waveguide into Half Space Through a Rectangular Aperture," Interim Technical Report RADC-TR-76-264, Rome Air Development Center, Griffiss Air Force Base, New York, August 1976.